THEORETICAL STUDIES OF MECHANISMS

OF EPOXY CURING SYSTEMS

by

My-Phuong Pham

A dissertation submitted to the faculty of
The University of Utah
in partial fulfillment of the requirements for the degree of

Doctor of Philosophy

Department of Chemistry

The University of Utah

May 2011

The University of Utah Graduate School

STATEMENT OF DISSERTATION APPROVAL

The dissertation of   **My-Phuong Pham**

has been approved by the following supervisory committee members:

Thanh N. Truong	, Chair	**07/20/2009** Date Approved
Feng Liu	, Member	**07/20/2009** Date Approved
Richard D. Ernst	, Member	**07/20/2009** Date Approved
Jack P. Simons	, Member	**07/20/2009** Date Approved
Valeria Molinero	, Member	**07/20/2009** Date Approved

and by   **Henry S. White**   , Chair of

the Department of   **Chemistry**

and by Charles A. Wight, Dean of The Graduate School.

ABSTRACT

The epoxy resin market is faced with an ever increasing demand for a "designer" range of properties for the epoxy end-use products. Therefore, it is necessary to obtain a complete mechanism and accurate kinetic model that has predictive capabilities. This dissertation addresses the issue in two sections.

The first section is an analysis of systematic theoretical studies on the mechanisms of four main curing reactions, epoxy-amine, epoxy-phenol, epoxy-acid and epoxy-anhydride, at the molecular-level using B3LYP density functional theory. The strength of these mechanistic models is their ability to extrapolate to different reactions that use a particular epoxy resin, a particular curing agent and/or a particular catalyst. The examination of all possible reaction pathways for each curing system can allow us to predict the most preferable pathway in the system and can enable the development of a more accurate kinetic model for the system. In addition, it provides insight into the role of tertiary amines in catalyzing the curing reaction.

The second section involves the development of a new kinetic model for the epoxy-amine curing system guided by quantum chemistry calculations. This accurate kinetic model for an epoxy-amine curing system has the potential to be applied to other curing systems, solving successfully an industrial issue by quantum chemistry calculation.

TABLE OF CONTENTS

.

ACKNOWLEDGMENTS

My five-year journey in the United States, especially at University of Utah, was a huge learning process I could not have done alone. It was supported by the help of many people whom I would like to deeply acknowledge.

First, I would especially like to express my appreciation and gratitude to my graduate advisor Prof. Thanh N. Truong for all of his help and guidance. I have learned much from his patience, his knowledge, and his experience combined with his excellent teaching skills as well as his easy-going nature.

I would like to express my sincere appreciation to my committee members, Prof. Jack S. Simons, Prof. Scott L. Anderson, Prof. Richard D. Ernst, Prof. Feng Liu and Prof. Valeria Molinero for their involvement and encouragement. I also appreciate the help I have received from many faculty and staff in the chemistry department and from the Center for High Performance Computing, who invested so much time in providing excellent teaching and assistance. The Vietnamese Ministry of Education and Training (MOET) is acknowledged for their graduate fellowship support. I would like to thank the Dow Chemical Company for the partial financial support.

Many thanks to all of my past and present colleagues in my group who, by their friendship and professional help, have made my graduate study an enjoyable and worthwhile experience. I want to particularly thank Dr. Quang Nguyen, for our friendship, encouragement and support ever since we were in undergraduate school, Dr. Nguyen Pham for her contribution to Chapter 5, Dr. Hongzhi Zhang for letting me take part in some

CHAPTER 1

INTRODUCTION

1.1   General introduction

Epoxy-based polymer materials have diverse applications such as metal can coatings, automotive primers, printed circuit boards, semiconductor encapsulants, adhesives, aerospace composite materials, and even as building materials for rotor blades of wind turbines.[1-3] These amorphous materials have a set of unique properties that are not commonly found in other plastic materials, such as excellent mechanical strength, outstanding chemical, moisture and corrosion resistance, good thermal, adhesive, and electrical properties; dimensional stability (i.e., low shrinkage upon curing) and a lack of volatile emissions.[1, 4-6]

Most industrial applications of epoxy resins are in thermosetting, a process in which an epoxy resin reacts with a curing cross-link agent known as a hardener. The largest class of hardeners (50%) utilizes primary and secondary amines. The second largest class of hardeners involves carboxylic acids and anhydrides, which make up about 36% of the class. The remaining segment of the class is phenols and related substances (cf. Figure 1.1).[7] In order to achieve the desired properties, careful selection of an epoxy resin, the proper curing agent, and the right epoxy/agent curing proportions in a formulation process must be made. Sometimes additional agents such as catalysts, accelerators, fillers, solvents, diluents, plasticizers, and tougheners are required to
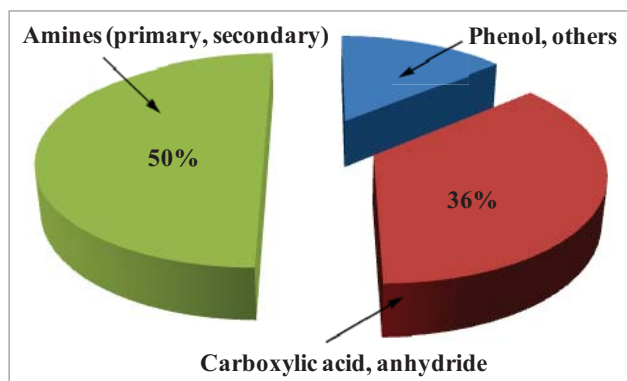
Figure 1.1. Total curing agent volume used in U.S. market (2001 data).

facilitate the curing process or to improve the final properties of the products.

The epoxy resin market is faced with an ever increasing demand for a "designer" range of properties of epoxy resin end-products. For example, as electronic equipment gets smaller, there is higher demand on the thermo-stability and electro-conductivity of the coating materials, a greater economic pressure for efficiency, and a larger focus on the environmental impact requirements. Meanwhile, the known formulation process, in both mechanism and kinetic models, is not fully understood and lacks predictive and functional-design capabilities.

1.2 Overview on the mechanism and kinetic models of epoxy curing reactions

1.2.1 Mechanism of epoxy-amine curing

Due to their extensive use, much work has been done on amines. The general curing reaction occurs via a nucleophilic attack of the amine nitrogen on the terminal carbon of the epoxy function. The mechanism has been accepted to be a S_N2-type II and thus the reaction rate obeys second-order kinetics (Scheme 2.1).[7, 8]

In this mechanism, a primary amine (PA) can react twice with two epoxy group
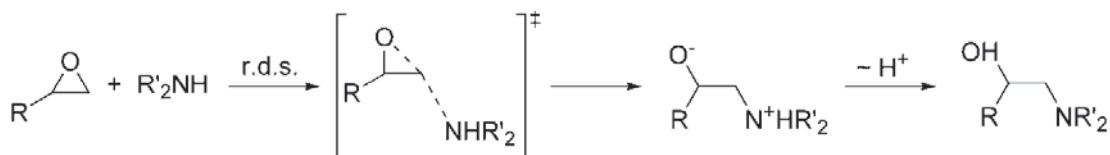
Scheme 2.1. General mechanism for epoxy-amine curing. The first step is assumed to be the rate determining step and the proton transfer is fast compared to the nucleophilic attack.

while a secondary amine (SA) can react only once.[9] The reaction was known to be catalyzed by hydroxyl groups[10, 11] or by catalytic impurities.[12] Mijovic and coworkers suggested a possible concerted mechanism which involves three types of acyclic hydrogen bond complexes with reactant amine molecules, i.e., epoxy-amine, epoxy-hydroxyl and amine-hydroxyl, but considered only epoxy-amine complexes for epoxy-amine kinetics.[13] Meanwhile, only the epoxy-hydroxyl complexes were used in the recent Riccardi's,[14] Blanco's[15] and Mounif's[16] models. In other curing systems such as the curing of epoxy by phenol and the curing of epoxy by acid, the hydrogen bond complex of either epoxy-acid or epoxy-phenol is not considered. Thus, mechanisms of different kinds of epoxy curing reactions are similarly incomplete.

Models of possible hydrogen bond complexes with amines have been used,[13] refined or slightly altered or extended to the present time, especially Horie's model[9] for epoxy-amine curing reactions. Other approaches were also employed to evaluate the reaction mechanism, particularly using kinetic modeling combined with experimental measurements.[15-18] In such cases, a kinetic model was used involving a set of elementary reactions whose rate parameters were determined by fitting with experimental data from rate equation thermometric measurements conducted with the aid of differential scanning calorimetry (DSC).[19, 20] Elucidation of the epoxy-amine reaction mechanism using this approach has a number of limitations. The approach cannot provide any information at the molecular-level

on the mechanism of individual elementary reactions. For example, it cannot address the possibility of cyclic transition states involving an epoxy and two amine molecules, described in a review by Rozenberg.[21] Cyclic and acyclic transition states of the same stoichiometry cannot be distinguished by thermometric measurements although their reaction pathways for this specific reaction differ considerably; the amine addition via a cyclic transition state is believed to be a concerted one-step process, whereas the acyclic pathway is a step-wise process that occurs via an intermediate. It is a well-accepted fact that the cyclic hydrogen bond complex often stabilizes the transition state and thus it is considered to be a more favorable pathway[22-24] This speculation was proven in recent studies to be incorrect; i.e., the cyclic TS pathway is energetically less favorable compared to the acyclic TS pathway by quantum calculation.[8]

1.2.2 Mechanism of epoxy-carboxylic acid/anhydride curing

Despite being the second most important class of curing agents, not much is known in molecular detail about the mechanism of reactions using carboxylic acids and anhydrides. Steinmann found from C^{13}-NMR and HPLC data that reaction between epoxy and a carboxylic acid not only yields the usual main products of α-hydroxy-ester and β-hydroxy-ester but also gives an abnormal β-hydroxy-ester.[25] This indicates the mechanism for reaction with carboxylic acids is more complex than currently known.

Reactions between epoxy and anhydrides often require a tertiary amine (R_3N) Lewis base as the catalyst. Previous studies mutually agreed the mechanism is an anionic one. However, Fischer suggested R_3N opens anhydride first to form a zwitterion which can then undergo reaction with the epoxy.[26] Okaya, Takana and Yuki, on the other hand, suggested R_3N creates a zwitterion with epoxy first before reacting with the anhydride.[27] Two

additional mechanisms were also proposed based on initiation by tertiary amine with the participation of (1) a preexisting proton donor and (2) a proton donor formed during the reaction.[7] All of these suggestions indicate only that the reaction mechanism is not fully understood.

1.2.3   Mechanism of epoxy-phenol curing

Similarly, the role of tertiary amines as catalysts for curing by phenols is not understood clearly. Shechter and Wynstra proposed a mechanism in which the epoxy is opened by a tertiary amine catalyst first to form a zwitterion which then reacts with phenols.[28] Sorokin et al. declared that a tertiary amine creates a complex with phenols and then this complex cures the epoxy.[29]

1.2.4   Kinetic model of epoxy-amine curing

Since the mechanisms for epoxy curing reactions are not fully understood, current kinetic models used to approximate mechanisms are empirical or semiempirical and rely on experimental thermometric measurements of the overall process. Such models cannot specifically guarantee the completeness of the mechanism and can hide the non-completeness of the mechanism because rate constants were used as adjustable parameters. For instance, a recent study by Blanco et al.[15] proposed a mechanistic model that involved the uncatalyzed reaction between epoxy and amine and the catalyzed reaction by a hydroxyl group, but did not consider the self-promoted reaction by other amines. The authors justified the accuracy of the model based on its ability to fit data from differential scanning calorimetry experiments for a given set of reaction conditions. Such an approach is far from being predictive because it cannot be extended to other reaction conditions. Furthermore, since rate parameters are being used as fitting parameters, there is no guarantee that these

parameters are physical. For example, in Blanco et al.'s kinetic model, the activation energy for the complex formation step between epoxy and an alcohol group is 58.2 kJ/mol.[15] This is significantly higher than the well-accepted physical range for this step of 1-5 kJ/mol confirmed by the first-principles quantum chemistry calculation.

1.3 Research objectives

Compared with traditional theory and experimentation, computational molecular science can be accepted as the 'third' pillar of scientific research, providing reliable information on the mechanism, thermodynamic and kinetic parameters needed for meso- and macro-scaled modeling of the chemical process.[30] Quantum chemistry calculations performed recently successfully proved that in the overall mechanism of epoxy-amine curing reactions, the acyclic transition states are more preferred energetically than cyclic transition states, which is completely opposite with previous speculation for such S_N2 type II processes like curing reactions. Thus, first-principles quantum chemistry calculations can be applied to achieve a fundamental understanding of the mechanisms of curing reactions as well as the catalytic and accelerative role of Lewis bases and acids. These results are continually used to develop and validate the mechanistic model for the epoxy cured by different curing agents. The purpose of this research is to create mechanisms and kinetic models that have predictive and functional-design capabilities for epoxy curing reactions. These mechanisms and kinetic models can answer what the mechanical properties of the resulting polymer will be by using a particular curing agent, a particular epoxy resin, or by changing the reaction conditions.

Curing reactions classified by four main curing agents (amines, phenols and carboxylic acids and anhydrides) were examined. Three steps are required to develop a kinetic model for a given curing reaction: (1) perform first-principles quantum chemistry

calculations to explore all possible reaction pathways to construct the mechanistic model; (2) calculate thermodynamic properties and rate constants for each reaction pathway using conventional statistical mechanics methods to provide necessary parameters for the mechanism model; and finally (3) carry out kinetic simulations and directly compare the results to DSC experimental data.

The results are divided into two parts. The first part, involving step 1 for all four classes of curing reactions, is presented in Chapters 2, 3, 4 and 5, and concerns the understanding of mechanisms at the molecular level and catalytic roles of tertiary amines in the curing reactions. In Chapter 2, the substituent effects on the reactivity of primary/secondary amine curing agents are examined. Chapter 3 presents the catalytic role of tertiary amines based on the study of epoxy-phenol mechanisms. Chapters 4 and 5 show the overall mechanism of the second class of curing agents, carboxylic acids and anhydrides. The second part presents steps 2 and 3 specifically for epoxy-amine curing reactions (Chapter 6).

CHAPTER 2

SUBSTITUENT EFFECTS ON THE REACTIVITY

OF EPOXY-AMINE CURING REACTION

2.1 Introduction

Amine compounds are among the earliest and most broadly used epoxy curing agents.[7] Primary amines and secondary amines are highly reactive with epoxies. Depending on the substituents, these amines are generally divided into three main groups: aliphatic, cycloaliphatic and aromatic amines. Among these groups, aromatic amines typically produce cured resins having the highest chemical and thermal resistance properties; however, they require long cure cycles at high temperature (~150 ^{0}C). Cycloaliphatic amines produce products having thermal resistance and toughness superior to those from aliphatic amines but they are more expensive than aliphatic amines.[7] Due to its importance of substituent effects on the reactivity, the epoxy-amine curing process has been the subject of many studies [8, 9, 13, 31-36]; however, several issues are still not fully understood.[7, 8, 36]

It is well accepted that epoxy curing by an amine follows the S_N2 type II mechanism as shown in the Scheme 2.1.

In this mechanism, the hydrogen atom of the amine group does not react directly with an epoxy group but rather the nucleophilic nitrogen atom attacks a carbon atom of the epoxy ring, and then the hydrogen atom from the amine eventually transfers to the epoxy oxygen atom to form OH. Therefore, a primary amine (PA) can react twice with two epoxy groups
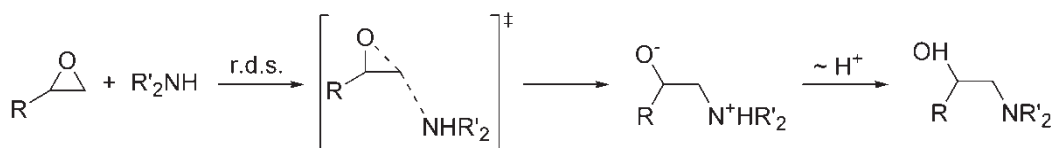
Scheme 2.1. The general mechanism of an epoxy- amine curing reaction.[8] (r.d.s. stands for rate determining step).

while a secondary amine (SA) can react only once. A tertiary amine, which has no active hydrogens, thus does not react with the epoxy group. However, it generally acts as a catalyst to accelerate other curing reactions by stabilizing the transition state.[7]

From their stoichiometric numbers, if the reactivity in a curing process by PA and SA are the same then the ratio of the reaction rates of the SA to the PA processes is 0.5.[31] The mechanism suggests that the reactivity of this reaction depends on the nucleophilicity of the amine. A secondary amine, having higher basicity, is usually more nucleophilic than a primary amine.[37] Therefore, a secondary amine would react faster than a primary amine. This is in contradiction to the observed slower rate of the SA processes.[31, 33, 36] Previous studies suggested that steric effects are the major factor contributing to the deviation of the reaction rate ratio (SA/PA) in most systems from 0.5.[31, 36] In addition, Mijovic and co-workers[35] found that the reactivity ratio of PA/epoxy and SA/epoxy reactions depends on the amine structure, but is independent of the temperature. Although the ratio is generally reported to be temperature independent,[9, 32, 33, 38] some authors found that the reactivity ratio increases with the curing temperature.[39, 40] Since the initial stage of polymerization is in a liquid phase, wherein fluid increases in viscosity prior to gellation and hardening,[41] condensed phase effects may be of importance. Our previous study found that condensed phase effects lower the activation energy of the curing reaction and became more profound with an increase in solvent polarity.[8] Furthermore, the study suggested that condensed phase

effects may be the key factors for slower rates of reaction with secondary amines; however, systematic examinations of more sterically varied structures of SA reactions or different types of amines were not done.

The objective of this study is to provide insight into the origin of the substituent effects on the relative SA/PA ratio by systematically investigating the effects of the amine structures on the reactivity of their reactions with an epoxy in both gas and condensed phases using Density Functional Theory (DFT).

2.2   Computational details

2.2.1   Physical models

Since the commercial epoxies and amine curing agents are typically large and have complicated structures, it is necessary to choose physical models that can represent key functionalities of these species but are small enough to be computationally feasible. The methyl glycidyl ether (E) was chosen to be a model for bisphenol A diglycidyl ether (BADGE)[7] and ring hydrogenated bisphenol A diglycidyl ether (H_{12}-BADGE). Table 2.1 shows these commercial epoxies and their corresponding computational models.

Commercial amine curing agents can be classified as aliphatic, cycloaliphatic, or aromatic. For example, the common commercial polyamine curing agents diethylenetriamine (DETA) and triethylenetetramine (TETA) are aliphatic, bis(4-aminocyclohexyl)methane (PACM) and isophorone diamine (IPDA) are cycloaliphatic, and 4,4'-diamino-diphenylmethane (DDM) and 4,4'-diamino-diphenyl sulfone (4,4'-DDS) are aromatic as shown in Table 2.2 along with their physical models.[7] These model amines also consist of both primary and secondary amines. In particular, methylamine (MA) and dimethylamine (DMA) were used for aliphatic amines,

Table 2.1. Some common commercial epoxy structures and overview on model complexes.
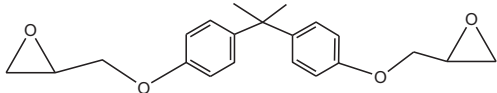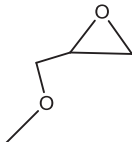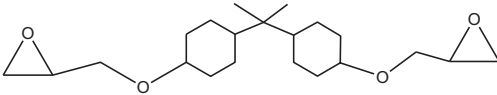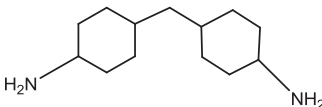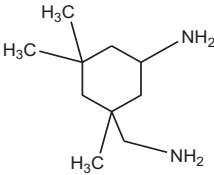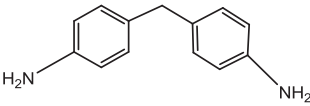
Common commercial epoxies		Model epoxy	
Formula	Abbreviation	Formula	Abbreviation
	BADGE		E
	H$_{12}$-BADGE		

Table 2.2 Some structures of commercial amines.
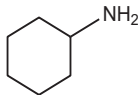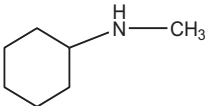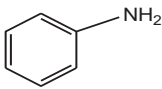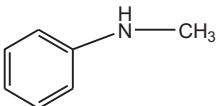
Amines	Commercial amines	
	Formula	Abbreviation
Aliphatic	NH$_2$CH$_2$CH$_2$NHCH$_2$CH$_2$NH$_2$	DETA
	NH$_2$CH$_2$CH$_2$NHCH$_2$CH$_2$NHCH$_2$ CH$_2$NH$_2$	TETA
Cycloaliphatic		PACM
		IPDA
Aromatic		DDM

cyclohexylamine (CHA) and cyclohexylmethylamine (CHMA) for cycloaliphatic amines, and aniline (AA) and methylaniline (MAA) for primary and secondary aromatic amines, respectively (see Table 2.3). Propan-2-ol was used to model an alcohol (-OH) group of an external alcohol accelerator or a product hydroxyl group.

2.2.2 Computational models

All electronic structure calculations were carried out using the Gaussian 03 program package.[42] A hybrid nonlocal density functional theory B3LYP level of theory[43] with the 6-31G(d, p) basis set was used for locating all stationary points, namely reactants, transition states, intermediates, and products. Stationary points were characterized by normal mode analyses. To confirm the transition state for each reaction pathway, the minimum energy paths (MEPs) from the transition state to both the reactants and products were calculated using the Gonzalez-Schlegel steepest descent path method[44, 45] in the mass weight Cartesian coordinates with the step size of 0.01 $(amu)^{1/2}$ Bohr. To calculate the condensed effects,

Table 2.3 Overview on model complexes of amine curing agents

| Amines | Model amines | | | |
| | Primary Amines (PA) | | Secondary Amines (SA) | |
	Formula	Abbreviation	Formula	Abbreviation
Aliphatic	$H_2N{-}CH_3$	MA	$H_3C{\diagdown}N(H){-}CH_3$	DMA
Cycloaliphatic	(cyclohexyl)$-NH_2$	CHA	(cyclohexyl)$-N(H){-}CH_3$	CHMA
Aromatic	(phenyl)$-NH_2$	AA	(phenyl)$-N(H){-}CH_3$	MAA

single-point energy calculations at the optimized structures of all stationary points were done using the polarizable continuum model (PCM)[46] with a dielectric constant equal to 5 to represent the polarity of the polymer matrix. Note that the dielectric constant is about 4 for biopolymers and 3 for the final thermoset.

2.3 Results

In the discussion below, we first present substituent effects on different aspects of the epoxy-amine curing reaction then discuss comparisons between the present results and experimental observations to serve as a validation of the calculated data.

2.3.1 Substituent effects on reaction pathways

In our previous study,[8] amine curing reaction can found to proceed by three different reaction pathways, namely: 1) an isolated pathway, wherein the epoxy reacts with the curing amine molecule alone; 2) a self-promoted pathway wherein the reaction involves two amine molecules, one acting as a curing agent and the other stabilizing the transition state; and 3) an alcohol-accelerated pathway wherein an alcohol group stabilizes the transition state. These pathways are shown in Figure 2.1. Subscripts i, s, and a designate isolated, self-promoted and alcohol-accelerated pathways, respectively. Geometries of the transition states (TS), classical barrier heights ($\Delta V^{\neq}$), zero-point energy corrected barriers $\Delta V_a^{\neq G}$ (vibrationally adiabatic ground-state barrier heights) which are activation energies at 0 K of each pathway for three different classes of amines are given in Tables 2.4-6.

As the reaction proceeds from the reactant to product, the C1-O1 bond of the epoxy ring is broken and the new C1-N1 bond is formed (see Figure 2.1). The bond lengths of these two "active" bonds at the TS provide information on how close the TS to the reactant
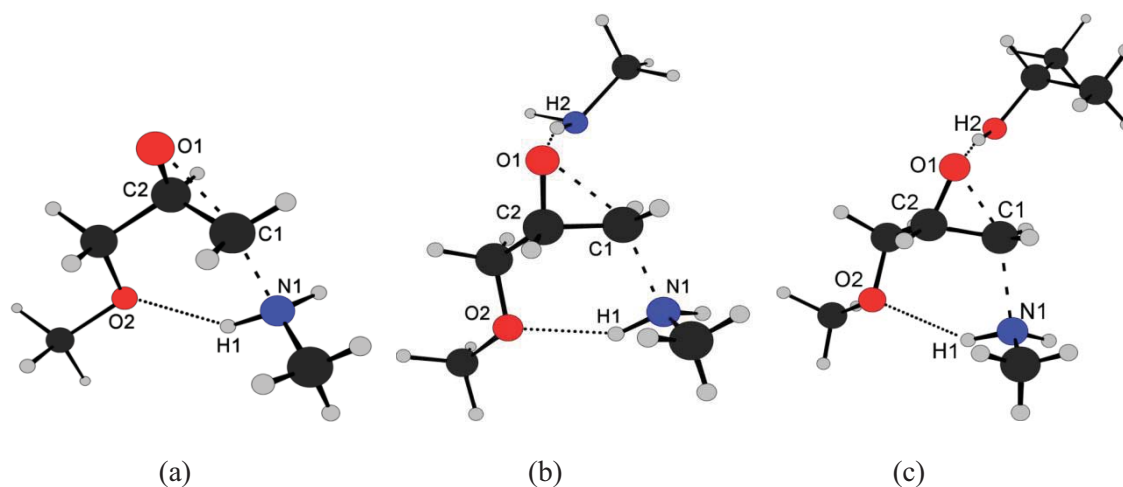
Figure 2.1. Structures of the acyclic transition states for (a) the isolated (**TS$_i$**), (b) self-promoted (**TS$_s$**) by an addition amine and (c) alcohol-accelerated pathways (**TS$_a$**) of the methylamine curing reaction.

Table 2.4 Imaginary Frequencies ($v^{\neq}$), Selected Optimized Geometrical Parameters of the Transition States along the Acyclic TS Routes, Classical Barrier Heights ($\Delta V_{gas}^{\neq}$, $\Delta V_{sol}^{\neq}$), and Zero-point Energy Corrected Barriers ($\Delta V_{a\_gas}^{\neq G}$) of the Isolated pathway (**i**) of Epoxy and Methylamine (MA), Dimethylamine (DMA), Cyclohexylamine (CHA), Cyclohexylmethylamine (CHMA), Aniline (AA) and Methylaniline (MAA) Reactions respectively.

Parameters	MA$_i$	DMA$_i$	CHA$_i$	CHMA$_i$	AA$_i$	MAA$_i$
$v^{\neq}$ (i.cm^{-1})	374.9	376.1	367.5	362.4	330.2	342.5
d(N1-C1) (Å)	1.858	1.884	1.868	1.882	1.778	1.801
d(H1-O2) (Å)	1.931	1.953	1.932	1.946	1.848	1.876
d(C1-O1) (Å)	2.054	2.037	2.065	2.061	2.129	2.114
d(C2-O1) (Å)	1.347	1.349	1.344	1.345	1.337	1.338
d(C1-C2) (Å)	1.495	1.493	1.501	1.501	1.512	1.513
$\angle$(O1-C2-C1) (deg)	92.4	91.4	92.9	92.7	96.5	95.6
$\angle$(C2-C1-N1) (deg)	113.8	114.5	115.3	115.9	113.8	115.4
$\Delta V_{gas}^{\neq}$ (kJ/mol)	101.70	97.25	107.07	105.35	121.89	119.87
$\Delta V_{a\_gas}^{\neq G}$ (kJ/mol)	109.60	101.77	111.66	109.98	126.62	124.30
$\Delta V_{sol}^{\neq}$ (kJ/mol)	70.12	72.54	75.76	78.87	90.81	96.09

Table 2.5 Imaginary Frequencies $(\nu^{\neq})$, Selected Optimized Geometrical Parameters of the Transition States along the Acyclic TS Routes, Classical Barrier Heights ($\Delta V_{gas}^{\neq}$, $\Delta V_{sol}^{\neq}$), and Zero-point Energy Corrected Barriers ($\Delta V_{a\_gas}^{\neq G}$) of the Self-promoted pathway (**s**) of Epoxy and Methylamine (MA), Dimethylamine (DMA), Cyclohexylamine (CHA), Cyclohexylmethylamine (CHMA), Aniline (AA) and Methylaniline (MAA) Reactions respectively.

Parameters	MA$_s$	DMA$_s$	CHA$_s$	CHMA$_s$	AA$_s$	MAA$_s$
$\nu^{\neq}$ (i.cm^{-1})	388.8	384.8	381.5	373.7	370.0	377.2
d(N1-C1) (Å)	1.951	1.980	1.969	1.997	1.914	1.941
d(H1-O2) (Å)	1.973	2.006	1.994	2.008	1.919	1.957
d(H2-O1) (Å)	1.955	1.957	1.964	1.974	1.848	1.838
d(C1-O1) (Å)	1.994	1.973	1.999	1.990	2.043	2.025
d(C2-O1) (Å)	1.367	1.370	1.366	1.367	1.366	1.369
d(C1-C2) (Å)	1.482	1.480	1.484	1.483	2.043	1.487
$\angle$(O1-C2-C1) (deg)	88.7	87.6	89.0	88.4	91.3	90.3
$\angle$(C2-C1-N1) (deg)	111.6	112.2	112.8	113.3	112.8	113.7
$\Delta V_{gas}^{\neq}$ (kJ/mol)	76.10	72.84	81.55	79.35	84.72	83.69
$\Delta V_{a\_gas}^{\neq G}$ (kJ/mol)	85.10	78.90	87.42	84.96	91.82	89.88
$\Delta V_{sol}^{\neq}$ (kJ/mol)	61.63	64.00	66.50	71.99	73.93	78.83

Table 2.6. Imaginary Frequencies $(\nu^{\neq})$, Selected Optimized Geometrical Parameters of the Transition States along the Acyclic TS Routes, Classical Barrier Heights ($\Delta V_{gas}^{\neq}$, $\Delta V_{sol}^{\neq}$), and Zero-point Energy Corrected Barriers ($\Delta V_{a\_gas}^{\neq G}$) of the Propan-2-ol-accelerated pathway (**a**) of Epoxy and Methylamine (MA), Dimethylamine (DMA), Cyclohexylamine (CHA), Cyclohexylmethylamine (CHMA), Aniline (AA) and Methylaniline (MAA) Reactions respectively.

Parameters	MA$_a$	DMA$_a$	CHA$_a$	CHMA$_a$	AA$_a$	MAA$_a$
$\nu^{\neq}$ (i.cm^{-1})	394.5	397.5	392.6	389.1	374.0	380.5
d(N1-C1) (Å)	2.002	2.025	2.011	2.032	1.930	1.948
d(H1-O2) (Å)	1.994	2.011	1.993	2.007	1.909	1.937
d(H2-O1) (Å)	1.712	1.712	1.710	1.714	1.688	1.686
d(C1-O1) (Å)	1.951	1.934	1.963	1.955	2.026	2.016
d(C2-O1) (Å)	1.380	1.382	1.378	1.379	1.373	1.375
d(C1-C2) (Å)	1.476	1.475	1.479	1.479	1.488	1.486
$\angle$(O1-C2-C1) (deg)	86.1	85.2	86.7	86.3	90.1	89.4
$\angle$(C2-C1-N1) (deg)	110.7	111.1	111.5	112.3	112.2	113.2
$\Delta V_{gas}^{\neq}$ (kJ/mol)	61.60	58.32	66.73	65.28	78.09	77.36
$\Delta V_{a\_gas}^{\neq G}$ (kJ/mol)	70.50	64.28	73.58	71.60	85.31	84.22
$\Delta V_{sol}^{\neq}$ (kJ/mol)	50.83	53.87	55.37	58.91	68.75	74.74

(entrance) channel or to the product (exit) channel. For instance, the shortening of the C1-O1 and the lengthening of the C1-N1 bond indicate that the TS has moved closer to the reactant channel. For all amines considered in this study, the transition state of the alcohol-accelerated pathway $\textbf{TS}_\textbf{a}$ is closest to the reactant (entrance) channel, while the isolated pathway $\textbf{TS}_\textbf{i}$ is the farthest (i.e., closest to the product channel). For example, for reaction with aniline, the breakening C1-O1 bond decreases from 2.129, 2.043, to 2.026 Å while the forming C1-N1 bond increases from 1.778, 1.914, to 1.930 Å in the isolated, self-promoted, and alcohol-accelerated pathways, respectively.

Corresponding with the increase in the reactant-like characteristics from $\textbf{TS}_\textbf{i}$, $\textbf{TS}_\textbf{s}$ to $\textbf{TS}_\textbf{a}$, the classical barrier height decreases from the isolated, self-promoted to alcohol-accelerated pathway. For example, for reaction with aniline the classical barrier is 121.89 kJ/mol for the isolated pathway, 84.72 kJ/mol for self-promoted and 78.09 kJ/mol for the propan-2-ol-accelerated pathway. This trend is consistent with the Hammond postulate, which states that more reactant-like characteristics of the transition state structure would lead to a smaller classical barrier. Such trend is observed for all types of amines and is consistent with those in the Ehlers et al. study.[8]

For epoxies that have an ether group such as those considered here, the transition state structure can be stabilized by two hydrogen bonds. One is between hydrogen amine H1 and the ether oxygen O2. The other is between the epoxide oxygen O1 with the hydrogen (i.e., H2) either of an amine as in the self-promoted $\textbf{TS}_\textbf{s}$, or of an alcohol as in the alcohol-accelerated $\textbf{TS}_\textbf{a}$ transition states. The second hydrogen bond H2-O1 is the determining factor in differentiating the relative importance of each pathway since the first hydrogen bond exists in all pathways. The H2-O1 hydrogen bond is stronger in $\textbf{TS}_\textbf{a}$ as compared to

TS$_s$ as indicated by its shorter bond distances. In particular, for reaction with aniline the H2-O1 hydrogen bond distance is 1.848 Å in AA$_s$ and 1.688 Å in AA$_a$ corresponding to the classical barrier heights of 84.72 and 78.09 kJ/mol, respectively.

2.3.2   Substituent effects on the reactivity of curing agents

Since the alcohol-accelerated pathway is the lowest energy pathway, it should have the largest dependence on the substituent effects. For this reason, the discussion on the substituent effects here is based only on the results for the alcohol-accelerated pathway. Potential energy information of this pathway for reactions with different classes of amines is given in Table 2.5. When compared to aliphatic amines, transition state structures for curing by cycloaliphatic amines have both active C1-O1 and N1-O1 bonds longer. This leads to an increase in the classical energy barriers by about 6 kJ/mol. Since aliphatic and cycloaliphatic amines exhibit similar electronic donating properties, the higher barriers in the latter are due mostly to larger steric effects.

Since both aromatic and cycloaliphatic amines considered here are similar in size and thus are expected to have similar steric effects, comparisons of the transition state properties of these two amines would yield the relative importance of the electronic effects. Curing by aromatic amines leads to more product-like TS geometries when compared to those from cycloaliphatic amines. This is indicated by the elongation of the breaking C1-O1 bond and the shortening of the forming N1-O1 bond by more than 0.05 Å. In consistent with the Hammond postulate, this leads to higher barrier by about 12 kJ/mol. This can be explained by the decrease in the nucleophilicity of the amine group due to the electron withdrawing property of the phenyl substituent in aromatic amines. Furthermore, in comparison to the steric effects above, electronic effects are noticeably larger. The electronic effects suggest

the higher pK_b amines (the weaker bases) will have lower nucleophilicities and thus would generate higher barriers. For comparison, the pK_b values are 3.36 for MA, 3.27 for DMA, 3.3 for CHA 3.3, 3.1 for CHMA, 9.4 for AA and 9.16 for MAA.[37] The significantly larger pK_b values for aromatic amines are consistent with their larger barrier heights compared to those of aliphatic amines. This is also consistent with the experimental observation that curing of aliphatic amines can be done at room temperature while the others require higher temperatures.[7] Note that pK_b's for the aliphatic and cycloaliphatic amines considered here are similar, so in such case steric effects are dominant in the observed differences in the barrier heights between cycloaliphatic and aliphatic amines.[47]

When a methyl group replaces a hydrogen atom in the primary amines considered here, the corresponding TS geometries of all pathways for all reactions are shifted toward the reactant channel, i.e., they become more reactant-like. In particular, in alcohol-accelerated pathways, there are decreases in the C1-O1 bond lengths by 0.01-0.02 Å and increases in the C1-N1 bond lengths by 0.01-0.02 Å in all cases. This leads to lower classical barrier heights for curing by SA compared to those of PA by less than 5 kJ/mol in the three classes of amines (Table 2.5). Larger effects are observed for aliphatic amines as compared to those for aromatic amines. For example, methyl substitution lowers the barrier by 3.28 kJ/mol in the alcohol-accelerated pathways for aliphatic amines, 1.45 kJ/mol in cycloaliphatic amines, and 0.73 kJ/mol in aromatic amines. Similar to the discussion of the electronic effects above, the nucleophilicities of the amines can be used to explain the lowering of barrier heights for SA compared to PA processes. For all three classes of amines, the pK_b's of SA's are smaller than those of PA's, namely, DMA (3.27) as compared to MA (3.36), CHMA (3.1) to CMA

(3.3) and MAA (9.16) to AA (9.4). The results suggest that SA cures faster than PA since it has a lower activation barrier. This, however, contradicts experimental observations.[31, 33, 36]

2.3.3   Condensed phase effects

In this study, condensed phase effects due to a polymer matrix in the curing process are modeled by the PCM dielectric continuum model with a dielectric constant of 5. Figure 2.2 plots barrier heights for reactions with all three classes of amines in both the gas and condensed phases. Solvent effects lower the barrier heights in all pathways and all reactions considered here. On the average, they decrease the barriers by 28 kJ/mol in isolated pathways (Table 2.3), 10 kJ/mol in self-promoted pathways (Table 2.4) and 7 kJ/mol in alcohol-accelerated pathways (Table 2.5). Since the alcohol-accelerated pathway is dominant, solvent effects along this pathway would be most crucial to the overall dynamics of the reaction.

On average, the decreases of the energy barriers are approximately equal in all reactions of three classes of amine curing agents, i.e., 15.66 kJ/mol for aliphatic amines, 16.32 kJ/mol for cycloaliphatic amines and 13.74 kJ/mol for aromatic amines. Consequently, the relative reactivity of these amine classes remain the same, i.e., aliphatic $\geq$ cycloaliphatic > aromatic.

Unlike the results in the gas phase, in condensed phases the barrier heights of reactions with SA's are higher than those of corresponding PA's. On average, for reactions considered here in all three pathways, solvent effects lower the barrier by 18 kJ/mol for PA and 12 kJ/mol for SA processes. Specifically for the dominant alcohol-accelerated pathways, solvent effects on the average lower the barrier by 10 kJ/mol for PA and 4 kJ/mol for SA reactions. The much larger solvent effects for PAs lead to the barriers for reactions
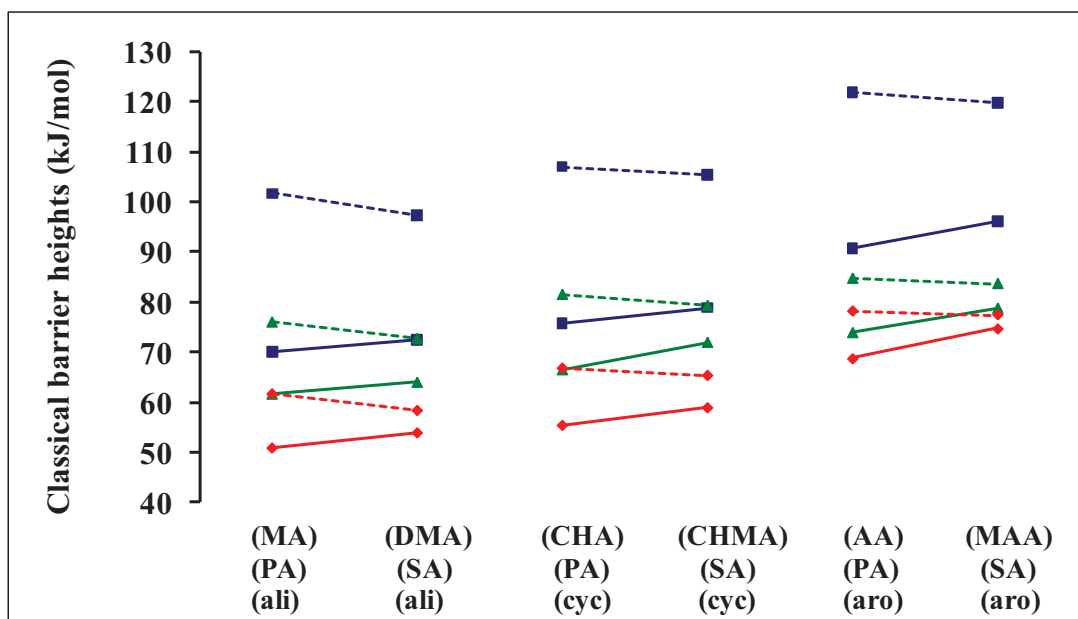
Figure 2.2. Classical barrier heights (kJ·mol^{-1}) in both gas (dash lines) and condensed phases (solid lines) of the Isolated (■), Self-promoted (▲) and Alcohol-catalyzed (♦) pathways of Epoxy and Methylamine (MA), Dimethylamine (DMA), Cyclohexylamine (CHA), Cyclohexylmethylamine (CHMA), Aniline (AA) and Methylaniline (MAA) reactions respectively from left to right, primary amine (PA) and secondary amine (SA), or aliphatic (ali), cycloaliphatic (cyc), and aromatic (aro) amines. * Propan-2-ol is used as an alcohol accelerator.

with a SA being larger than those of a PA and thus yield dramatic changes in the relative rates of SA and PA processes as indicated by the ratio of the SA/PA rate constants, from being larger than 0.5 to being smaller than 0.5. For example, the classical barrier heights of **AA$_a$** and **MAA$_a$** in the condensed phase are 68.75 kJ/mol and 74.74 kJ/mol as compared to 78.09 and 77.36 kJ/mol in the gas phase, respectively (Table 2.6).

2.4 Discussion

The competing reactions of epoxies with secondary amine (k_2) and primary amine groups (k_1) were examined by different experimental methods and the ratio of the rate constants, k_2/k_1, were usually smaller than 0.5. In the Johncock et al. HPLC study,[48]

reactions of 3-trifluoromethylaniline with epichlorohydrin, and aniline with phenyl glycidyl ether and with some N-alkyl-N-glycidylanilines, the observed ratios were in the range of 0.14 to 0.24. Wang and Gillham[39] determined the ratio k_2/k_1 to be in the range of 0.16-0.33 for the trimethylene glycol di-p-aminobenzoate/diglycidyl ether of the bisphenol A system using FTIR spectroscopy. In the Liu et al. study,[31] these ratios were within 0.17-0.5 for epoxy and aromatic diamine resin systems. As discussed above, solvent effects are the key factor to cause these ratios to be less than 0.5, and thus are responsible for bringing theory into agreement with experimental observations.

The order of the calculated classical barrier values of three classes of amines (aliphatic < cycloaliphatic < aromatic amines) also agrees well with experimental data. Kamon et al.[47] used differential scanning calorimetry (DSC) to study the curing reaction of BADGE epoxy resin with diethylenetriamine (DETA, an aliphatic amine), para-amino cyclohexyl methane (PACM, a cycloaliphatic amine) and 4,4'-diamino-diphenylmethane (DDM, an aromatic amine). These amines are commercial curing agents as shown in Table 2.2. The observed activation energies for curing are 67.36, 66.53 and 74.40 kJ/mol for DETA, PACM and DDM, respectively. These can be compared with the zero point energy corrected barriers in the condensed phase: 59.73, 62.22 and 75.97 kJ/mol for the model amines (methylamine, cyclomethylhexylamine, and aniline). Zero point energy corrections were approximated by the gas phase values in this case. In addition, our results for reactions of epoxy resin with aliphatic amines have similar activation energies (59.73 – 65.23 kJ/mol) with those in the range of 54.39 – 58.57 kJ/mol used in the Horie et al. kinetic model.[9]

2.5 Conclusions

In this study, substituent effects of epoxy curing reactions with three different classes of amine, namely aliphatic, cycloaliphatic, and aromatic amines were examined using quantum chemistry density functional theory. Both gas and condensed phase results reflect reactivities as expected for SN_2 type II process, and correlating with the amine nucleophilicity as indicated by its pK_b, and specifically following the order: aliphatic $\geq$ cycloaliphatic > aromatic.

Comparing the curing reactivities of aliphatic and cycloaliphatic amines that have similar pK_b values but different sizes and shapes provides an estimate on the importance of the steric effects in increasing the curing activation energy by about 5 kJ·mol^{-1} on the average. Similarly, an increase in pK_b of a curing agent leads to an increase in the activation energy when comparing reactivities of cycloaliphatic and aromatic amines that have similar sizes and shapes. In particular, changing from aliphatic to aromatic amines yields an increase of the activation energy by about 13 kJ/mol. Substituent effects are modelled by the relative rate of curing reaction with primary and secondary amines. However, solvent effects lower the activation energy in all three classes of amines by about 15 kJ·mol^{-1} from the gas phase.

Differences in steric and electronic effects lead to lower activation energies for curing with secondary amines comparing to primary amines. Solvent effects lower the activation energy by 10 kJ/mol for PA and 4 kJ/mol for SA along the dominant alcohol-accelerated pathway. This difference is responsible for the larger activation energy for the reactions of a SA as compared to that of a PA, and for bringing theory into agreement with experimental observation.

CHAPTER 3

MECHANISMS OF THE EPOXY-PHENOL CURING REACTIONS

3.1   Introduction

The majority of industrial applications of epoxy resins involve thermosettings, in which epoxy resins react with crosslinking agents known as hardeners. The two most popular hardening classes are comprised of primary/secondary amines (50%) and carboxylic acid/anhydrides (36%). Phenols and other substances constitute the remaining classes.[7] Thermosetting with amines exhibits toxicity and deterioration of electrical properties at high temperature and humidity, while carboxylic acids or anhydrides require high-energy consumptions resulting from prolonged curings at high temperature.[49]   Meanwhile, thermosetting by phenols leads to excellent insulating characteristics, good adhesive properties, outstanding chemical resistance, retention of properties under severe operating conditions, low moisture adsorption, and no reaction by-products.[1, 6] Thus, it has been used increasingly in the electronic industry as encapsulating and packing materials.[5, 6, 49]

Epoxy-phenol curing reactions can be carried out at moderate temperatures (150-200^0C) in the presence of catalysts such as quaternary ammonium salts, tertiary amines, and/or metal alkoxides.[7, 28, 29, 50, 51] Among these catalysts, tertiary amines are often used.[7, 52-58] Using epoxy (denoted as E), phenol (denoted as PhOH), and tertiary amine catalyst (denoted as NR_3), three possible hydrogen bonding complexes, namely epoxy-phenol, phenol-tertiary amine and phenol-phenol can be formed. Possible outcomes of epoxy-phenol

curing reactions, which are either uncatalyzed or catalyzed, are illustrated in Table 3.1. The former involves two pathways, an isolated pathway ($\mathbf{R_i}$) wherein the epoxy reacts with phenol alone, and a self-promoted pathway ($\mathbf{R_p}$) in which an additional phenol molecule forms a hydrogen bonding complex with the epoxy moiety to stabilize the transition state (TS). For catalyzed reactions, a tertiary amine can participate in two different actions. First, it can open the epoxy ring to create a zwitterion and then the epoxy zwitterion can react with a phenol curing agent similar to the uncatalyzed reactions, whether via the isolated or self-promoted pathways. The role of the NR_3 catalyst can thus be used to name these reactions, distinguishing them from uncatalyzed reactions. They are described as the isolated ring opening by tertiary amine catalyzed pathway ($\mathbf{R_{i,ro}^c}$) and the self-promoted ring opening by tertiary amine catalyzed pathway ($\mathbf{R_{p,ro}^c}$) in Table 3.1. Second, a tertiary amine can form a hydrogen-bonding complex with a phenol curing agent first, which then reacts with the epoxy ring in a similar pathway as for the uncatalyzed reactions. The reactions are named as an isolated hydrogen bonding catalyzed pathway ($\mathbf{R_{i,hb}^c}$) and a self-promoted hydrogen bonding catalyzed pathway ($\mathbf{R_{p,hb}^c}$).

The uncatalyzed reaction (cf. Scheme 3.1), that was not confirmed to be either isolated ($\mathbf{R_i}$) or self-promoted ($\mathbf{R_p}$), was found to be sluggish at 200^0C and to proceed at a reasonable rate only at higher temperatures.[5, 28, 49] In catalyzed reactions (Table 3.1), pathway ($\mathbf{R_{i,ro}^c}$) was first suggested by Shechter and Wynstra[28] in 1956 (cf. Scheme 3.2).

Sorokin and Shode's experimental study proposed a pathway that occurred via a trimolecular transition state[29] (Scheme 3.3) and was mostly applied to examine the effect of reactant ratio[49] as well as the effects of different kinds of catalysts.[5, 49, 59, 60] Such a

Table 3.1. Possible reactions of epoxy- phenol curing system.

Uncatalyzed reaction

Isolated pathway

$(\mathbf{R_i})$ $E + PhOH \longrightarrow [TS_i]^{\neq} \longrightarrow P_i$

Self-promoted pathway

$(\mathbf{R_p})$ $E...HOPh + PhOH \longrightarrow [TS_p]^{\neq} \longrightarrow P_p$

Catalyzed reaction

Isolated ring-opening by tertiary amine catalyzed pathway

$(\mathbf{R_{i,ro}^c})$
$\begin{cases} E + NR_3 \longrightarrow [TS_{i,ro}^{c1}]^{\neq} \longrightarrow P_{i,ro}^{c1} \\[2mm] P_{p,ro}^{c1} + PhOH \longrightarrow [TS_{p,ro}^{c2}]^{\neq} \longrightarrow P_{i,ro}^{c2} \end{cases}$

Self-promoted ring-opening by tertiary amine catalyzed pathway

$(\mathbf{R_{p,ro}^c})$
$\begin{cases} E...HOPh + NR_3 \longrightarrow [TS_{p,ro}^{c1}]^{\neq} \longrightarrow P_{p,ro}^{c1} \\[2mm] P_{p,ro}^{c1} + PhOH \longrightarrow [TS_{p,ro}^{c2}]^{\neq} \longrightarrow P_{p,ro}^{c2} \end{cases}$

Isolated hydrogen bonding catalyzed pathway

$(\mathbf{R_{i,hb}^c})$
$\begin{cases} PhOH + NR_3 \longrightarrow PhOH...NR_3 \\[2mm] E + PhOH...NR_3 \longrightarrow [TS_{i,hb}^c]^{\neq} \longrightarrow P_{i,hb}^c \end{cases}$

Self-promoted hydrogen bonding catalyzed pathway

$(\mathbf{R_{p,hb}^c})$
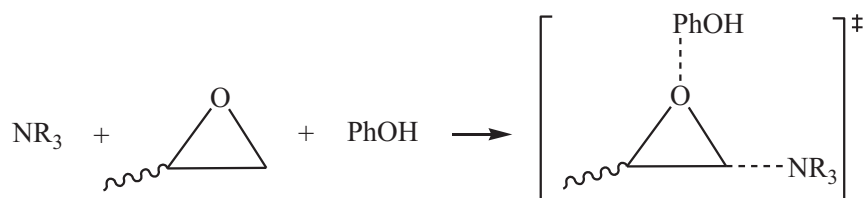$\begin{cases} PhOH + NR_3 \longrightarrow PhOH...NR_3 \\[2mm] E...HOPh + PhOH...NR_3 \longrightarrow [TS_{p,hb}^c]^{\neq} \longrightarrow P_{p,hb}^c \end{cases}$
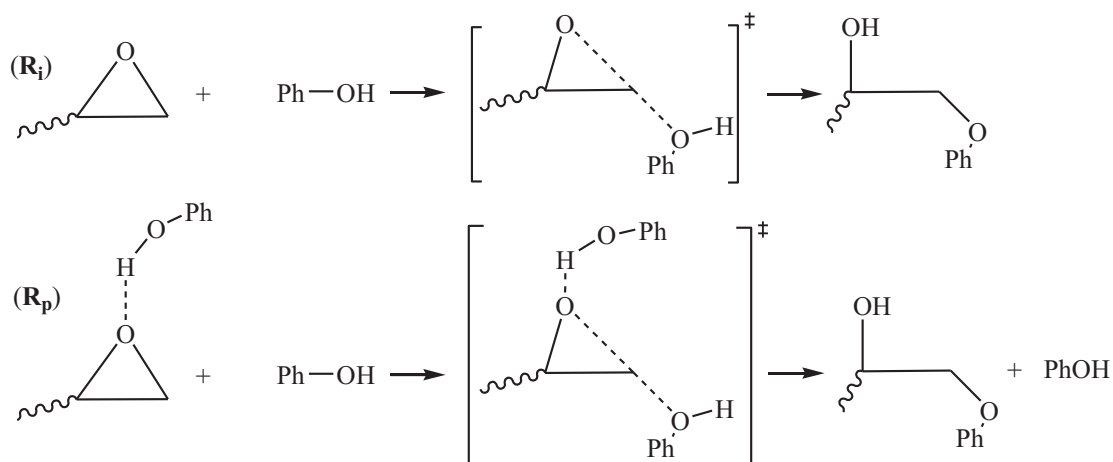
Scheme 3.1. Uncatalyzed reactions in the epoxy-phenol curing.
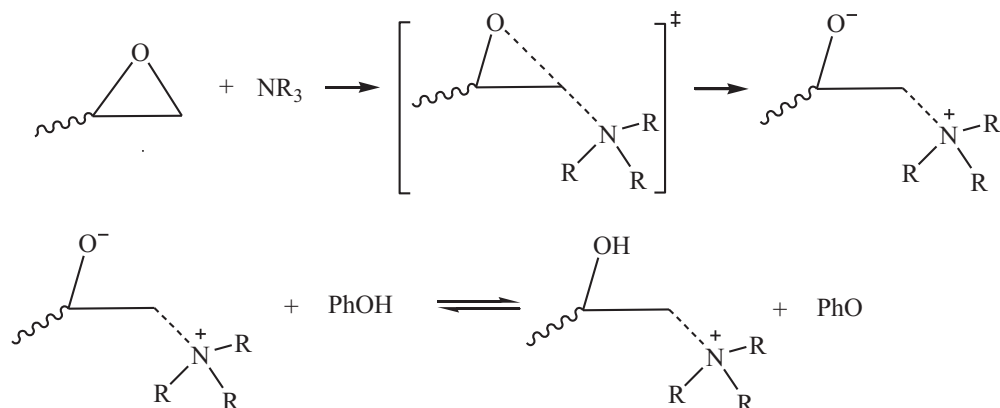
Scheme 3.2. Shechter and Wynstra's pathways ($\mathbf{R}_{i,ro}^{c}$).

Scheme 3.3. Catalyzed reaction via a trimolecular TS.

trimolecular transition state structure has not been confirmed as either acyclic or cyclic along the ($\mathbf{R}_{p,ro}^{c}$) pathway. Along with the pathway ($\mathbf{R}_{p,ro}^{c}$), the pathway ($\mathbf{R}_{i,hb}^{c}$) was suggested via a cyclic transition state (Scheme 3.4).

The data for one or more of the reactions in Table 3.1 were included in the kinetic modeling of the phenol curing system by fitting to experimental data using Differential Scanning Calorimetery (DSC). Although the fittings between the kinetic models and experimental data were usually reported to be reasonable,[5, 59-61] such models cannot be extrapolated for other phenol curing systems nor can they prove that the mechanism is complete.

To the best of our knowledge, there has not been any theoretical study on the mechanism of the epoxy-phenol curing system. From the above discussion, previously

$$R_3N \ + \ PhOH \longrightarrow R_3NH^+\text{---}OPh^-$$

$$R_3NH^+\text{---}OPh^- \ + \ \text{(epoxide)} \longrightarrow \text{(epoxide with } R_3NH^+\text{---}OPh^- \text{)}$$
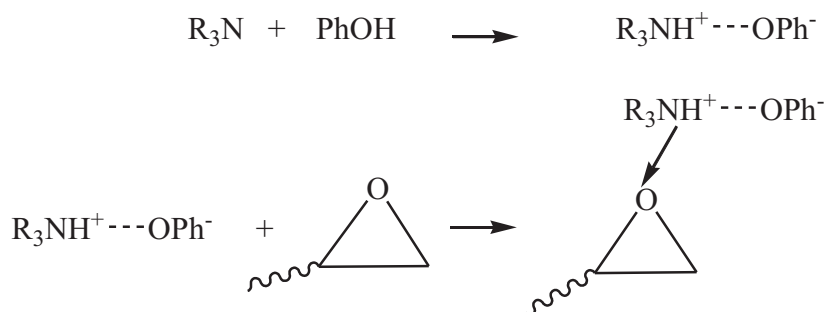
Scheme 3.4. Catalyzed pathway via a hydrogen bond complex forming ($\mathbf{R}^c_{i,hb}$).

proposed mechanisms involve competitive pathways and are not mutually exclusive as originally suggested. In addition, the roles of the tertiary amine catalysts in either opening the epoxy ring or forming a hydrogen bond complex with a phenol curing agent have not been confirmed. For instance, the pathway ($\mathbf{R}^c_{p,hb}$), which may be the dominant pathway because the TS is stabilized by two hydrogen bonds, has not been suggested.

The main objective of this study is to perform systematic theoretical studies on the mechanism of these epoxy-phenol curing reactions at the molecular-level using B3LYP density functional theory. Examination of all possible reaction pathways of an epoxy-phenol curing system at the same level of theory enables the development of a more accurate kinetic model for the system. In addition, it would also provide insight into the roles of tertiary amines in catalyzing the curing reaction.

3.2 Computational details

3.2.1 Physical models

Bisphenol A diglycidyl ether (BADGE) is the basis of the liquid epoxy resin, and the phenol curing agents can be phenol-, cresol-, or bisphenol A terminated epoxy resin hardeners.[7] These commercial epoxies and phenol curing agents have large and complicated structures. Therefore, it is necessary to choose physical models that can represent these

commercial reactants, yet are small enough to be computationally feasible. Some commercial epoxy and curing agent structures along with their models are presented in Table 3.2. Similarly, trimethylamine ($(CH_3)_3N$) is the model for catalytic tertiary amines such as triethylamine (TEA) and benzyl dimethyl amine (BDMA).

3.2.2   Computational models

All electronic structure calculations were carried out using the Gaussian 03 program package.[42]   A hybrid nonlocal density functional theory (DFT), particularly Becke's gradient-corrected exchange-correlation density functionals B3LYP[43] with the 6-31G(d, p) basis set was used to locate all stationary points. These are reactants, transition states, intermediates, and products. Normal mode analyses were done at the same level. To confirm the transition state for each reaction pathway, the minimum energy paths (MEPs) from the transition state to both the reactants and products were calculated using the Gonzalez-Schlegel steepest descent path method[44, 45] in mass weight cartesian coordinates with the step size of 0.01 $(amu)^{1/2}$ Bohr.

Single point solvation calculations were performed on the optimized DFT geometries using a polarizable continuum model (PCM)[46, 62] with a dielectric constant of 4.9 that is close to the dielectric constant of phenol ($\varepsilon=4.6$) to mimic the reactions in the solutions. It has been shown that the solvation free energies obtained from single point PCM calculations with the gas phase geometries from DFT calculations are in reasonable agreement with the values from full geometry optimizations.[63, 64] All solvation calculations used the simple united atom topological model (UAO).

Table 3.2. Some common commercial epoxy and curing agent and tertiary amine catalyst structures and overview on the model complexes.

Common commercial epoxies, phenol and catalysts		Model systems	
Formula	Abbreviation	Formula	Abbreviation
	BADGE		**E**
	H12-BADGE		
	BPA		
			PhOH
	TEA		
	BDMA		
			TMA

3.3   Results

The hydrogen bond precursor complex is presented first, followed by an examination of all pathways in Scheme 3.1 in both the gas and condensed phases. Geometries of the transition states (TS) and their zero-point energy corrected barriers $\Delta V_a^{\neq G}$ are used to compare the reactivities of all pathways. Zero point energy corrected barriers in the condensed phase are approximated as reaction activation energies E_a. Zero point energy corrections were approximated by the gas phase values in this case. The classical barrier in the gas phase ($\Delta V^{\neq}$), the zero-point energy (*ZPE*), and the zero-point corrected enthalpy of reaction (ΔH) are also presented in Table 3.3.

Table 3.3. Energetic values (kJ/mol) of possible reactions in Table 1.
(* is symbol for the enthalpy of reaction ΔH)

Pathways		ΔV	ZPE	$\Delta V_a^{\neq G}$	ΔV_{sol}	E_a
	C1	-64	9	-54	-51	-41
	C2	-54	8	-46	-37	-30
	C3	-60	8	-52	-48	-40
$\mathbf{R_i}$	TS_i	148	-5	143	161	156
$\mathbf{R_p}$	TS_p	98	3	101	92	95
	P_p	88*	4*	92*	77*	82*
$\mathbf{R_{i,ro}^c}$	$TS_{i,ro}^{c1}$	115	7	122	108	115
$\mathbf{R_{p,ro}^c}$	$TS_{p,ro}^{c1}$	62	5	67	51	57
	$P_{p,ro}^{c1}$	-13*	16*	2*	-8*	7*
	$TS_{p,ro}^{c2}$	13	-1	12	52	51
	$P_{p,ro}^{c2}$	-135*	2*	-133*	-84*	-82*
$\mathbf{R_{i,hb}^c}$	$TS_{i,hb}^c$	171	2	173	131	133
$\mathbf{R_{p,hb}^c}$	$TS_{p,hb}^c$	108	-7	101	102	95
	$P_{p,hb}^c$	19*	17*	36*	5*	22*

3.3.1 Hydrogen bonding precursor complexes

Complexes 1-3 (cf. Figure 3.1) show possible reactant complexes between the phenol groups, the amine functional groups and the epoxy oxygen. Table 3.4 illustrates that the order of strong hydrogen bond interaction is C1 < C2 < C3 and the OH…N hydrogen bond of C3 is strongest because nitrogen is a better hydrogen acceptor (Lewis base) than oxygen. Therefore, the complexes C2 and C3 can participate in the curing reactions together with epoxy, phenol and tertiary amine.

3.3.2 Uncatalyzed reactions

Uncatalyzed reactions include isolated ($\mathbf{R_i}$) and self-promoted ($\mathbf{R_p}$) pathways. Each pathway is examined for both cyclic and acyclic TS routes. As the reaction proceeds from
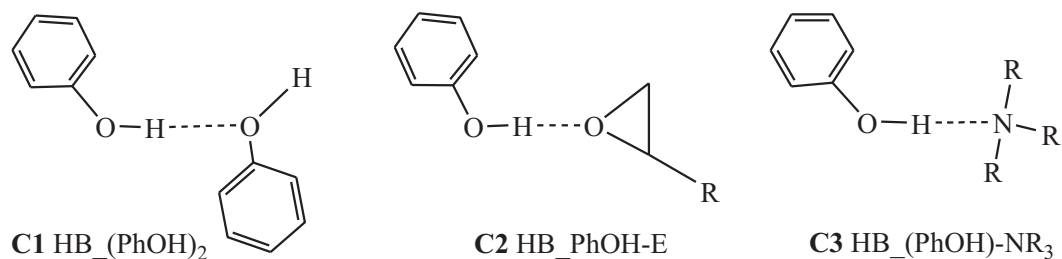
C1 HB_(PhOH)$_2$ **C2** HB_PhOH-E   **C3** HB_(PhOH)-NR$_3$

Figure 3.1. Hydrogen bond complexes

Table 3.4. Bond distance and the binding energy of hydrogen complexes

	C1 HB_(PhOH)$_2$	**C2** HB_PhOH-E	**C3** HB_PhOH-NR$_3$
d(OH-O) (Å)	1.903	1.837	
d(OH-N) (Å)			1.818
ΔE_{bind} (kJ/mol)	-54	-46	-52

the reactant to product, the C2-O1 bond of the epoxy ring is broken and a new C2-O2 bond is formed. The transition states are presented in Figures 3.2 and 3.3 and Table 3.5. Note that all hydrogen atoms not involved in the reactions are deleted in all figures for clarity and the dashed lines illustrate the forming and breaking of bonds. In the isolated pathway ($\mathbf{R_i}$), the epoxy-phenol curing in the cyclic TS route is preferred because of its lower energy barrier as compared to the acyclic TS route. In the self-promoted pathway ($\mathbf{R_p}$), the acyclic TS route is preferred due to the advantage of its lowered energy barrier compared with the cyclic TS route. Comparing $\mathrm{TS_p}$ to $\mathrm{TS_i}$, the hydrogen bond of the phenol-epoxy complex accounts for a lowering of the energy barrier by 42 kJ/mol, and $\mathrm{TS_p}$ can be considered as a reference for the following catalyzed reactions.

3.3.3 Catalyzed reactions

The tertiary amine catalyst can assume different roles: 1) Opening the epoxy ring to form a zwitterion first, after which the zwitterion attaches to a phenol and 2) Forming a hydrogen bond complex with a phenol curing agent that stabilizes the TS.
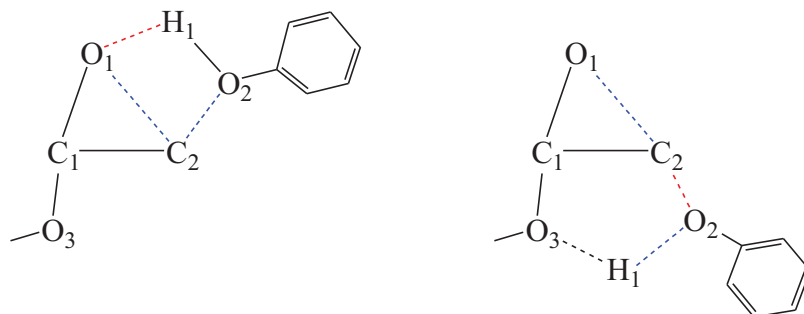
Figure 3.2. The cyclic (left) and acyclic (right) TS in isolated pathway (TS_i).
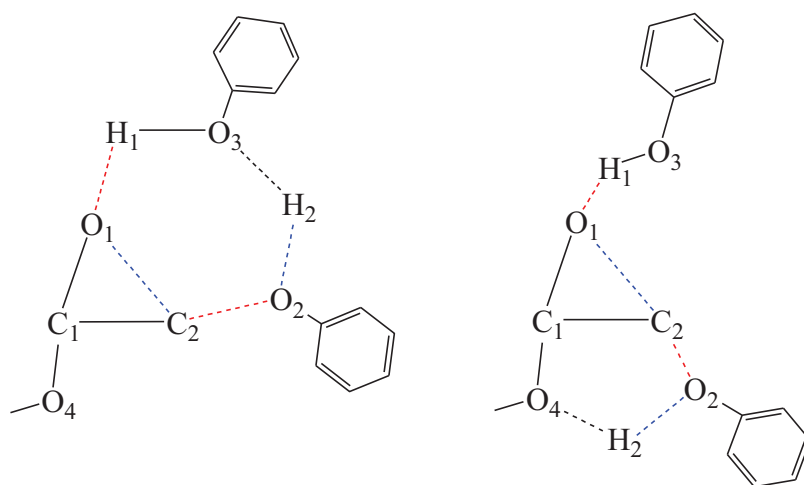

Figure 3.3. The cyclic (left) and acyclic (right) TS in the self-promoted pathway (TS_p).

Table 3.5. Parameter of the TS geometries in uncatalyzed reactions. (* is denoted for selected transition state)

Parameters	TS_i		TS_p	
Route	cyc	acyc	cyc	Acyc
$v^{\neq}$ (i.cm^{-1})	636	531	486	224
d(H1-O1) (Å)	1.375		1.323	1.492
d(O1-C2) (Å)	2.104	2.272	2.168	2.204
d(O1-C1) (Å)	1.398	1.319	1.392	1.361
d(C1-C2) (Å)	1.471	1.540	1.470	1.515
d(C2-O2) (Å)	2.274	1.587	2.263	1.677
d(O2-H2) (Å)		1.173	1.011	1.038
$\angle$ (O1-C1-C2) (deg)	94.38	104.93	98.48	99.96
$\angle$ (C1-C2-O2) (deg)	100.53	110.79	84.89	110.34
$\Delta V_a^{\neq G}$ (kJ/mol)	143*	169	141*	101

3.3.3.1 Ring opening by tertiary amine catalyzed pathway

Pathways ($R_{i,ro}^{c}$) and ($R_{p,ro}^{c}$) in Table 3.1 are considered here. Since these pathways

are different from each other by a hydrogen bond complex of an epoxy and a phenol

molecule, they are an isolated ring opening by tertiary amine catalyzed pathway ($R_{i,ro}^{c}$) and a

self-promoted ring opening by tertiary amine pathway ($R_{p,ro}^{c}$). Since each pathway proceeds

via two steps, the numbers 1 and 2 were added to the transition states' names.

The first steps of pathways ($R_{i,ro}^{c}$) and ($R_{p,ro}^{c}$) are examined and compared in both

front-side and backside attachments. The transition state geometries and their parameters for

the isolated ring opening by the tertiary amine pathway ($TS_{i,ro}^{c1}$) are illustrated in Figure 3.4

and Table 3.6. Those of the self-promoted ring opening by tertiary amine pathway ($TS_{p,ro}^{c1}$)

are in Figure 3.5 and Table 3.6.

In either $TS_{i,ro}^{c1}$ or $TS_{p,ro}^{c1}$, the backside attachment is preferred vs. the front-side

attachment because of a lower energy barrier and consequently, the backside energy barrier

is chosen to compare to step one of each pathway. Comparing $TS_{i,ro}^{c1}$ to $TS_{p,ro}^{c1}$ (see Table

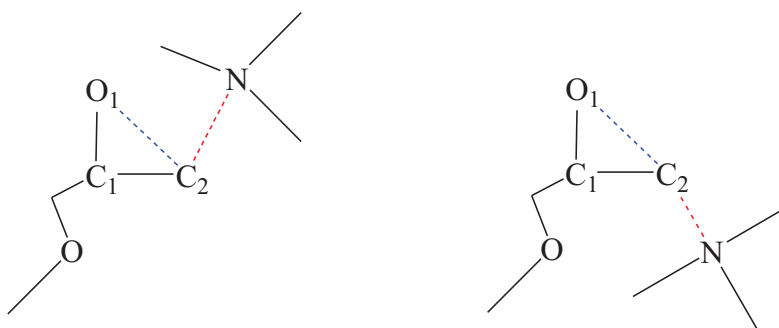3.6), the hydrogen bond between the phenol promoter and the epoxy lowers the energy

Figure 3.4. Front-side (left) and backside (right) attachments in the $TS_{i,ro}^{c1}$.

Table 3.6. Parameter of TS geometries in the ring opening by tertiary amine catalyzed pathways. * The reference point is the product of the first step in the pathway ($\mathbf{R}^c_{p,ro}$).

| Parameters	$TS^{c1}_{i,ro}$		$TS^{c1}_{p,ro}$		$TS^{c2}_{p,ro}$
Route	front	Back	front	back	
$v^{\neq}$ (i.cm^{-1})	362	266	369	382	442
d(H1-O1) (Å)			1.599	1.607	0.983
d(O1-C2) (Å)	2.079	2.109	2.041	1.934	2.437
d(C2-N) (Å)	2.190	1.778	2.260	2.028	2.057
d(O1-C1) (Å)	1.383	1.338	1.400	1.386	1.406
d(C1-C2) (Å)	1.470	1.529	1.467	1.483	1.518
d(C2-O2) (Å)					2.104
d(H2-O2) (Å)					1.521
d(H2-O3) (Å)					1.025
d(O3-H1) (Å)					1.817
$\angle$(O1-C1-C2) (deg)	93.48	94.47	90.73	84.70	112.84
$\angle$(C1-C2-N) (deg)	119.53	123.96	122.85	118.55	102.52
$\angle$(O1-C1-C2-N) (deg)				179	96
$\angle$(O1-C1-C2-N) (deg)					-82
$\Delta V^{\neq G}_a$ (kJ/mol)	188	122	150	67	12*
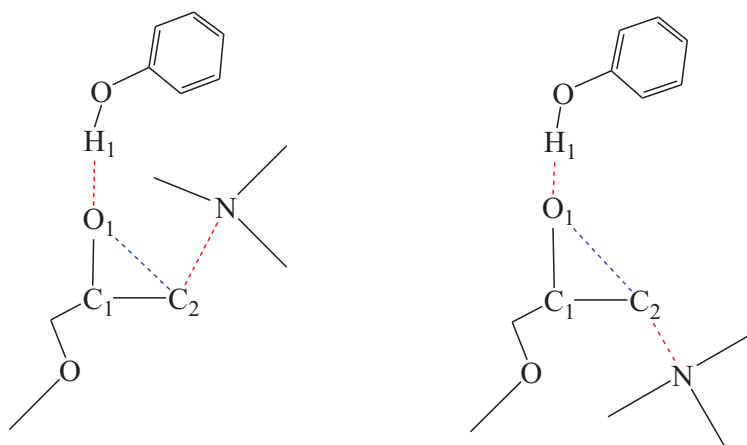
Figure 3.5. Front-side (left) and backside (right) attachments in the $TS^{c1}_{p,ro}$.

barrier by 55 kJ/mol, leading us to pursue further study of the second step of the self-promoted ring-opening by a tertiary amine pathway. Step 1 of the self-promoted ring-opening by the tertiary amine catalyzed pathway is followed by the formation of a six-centered cyclic transition state structure, in which a synchronized transfer of an electron pair takes place as shown in Figure 3.6 ($TS_{p,ro}^{c2}$). A strong hydrogen bond O1-H1 can be formed by a hydrogen atom transfer either from a phenol promoter or from a phenol curing agent to the epoxide oxygen. The required energy for such a hydrogen transfer can be ignored relative to the zwitterion's creation in step 1, ($TS_{p,ro}^{c1}$). This hydrogen transfer might happen before the attachment of the phenol curing agent into an epoxy which is indicated by an imaginary frequency of -442 cm^{-1}.

In the zwitterion formation ($TS_{p,ro}^{c1}$), the nitrogen atom of the tertiary amine is in the plane of the epoxy ring ($\angle$ (O1-C1-C2-N) = 179^0) but in the six-centered cyclic formation ($TS_{p,ro}^{c2}$), it is at a right angle to the epoxide plane ($\angle$ (O1-C1-C2-N) = 96^0) (see Table 3.6). Phenol attaches to the epoxy ring on the opposite side of the tertiary amine at the epoxide atom C2 ($\angle$ (O1-C1-C2-O3) = -82^0) and this attachment requires less energy than the first step (12 kJ/mol compared to 67 kJ/mol). This leads to a conclusion that after the epoxy ring
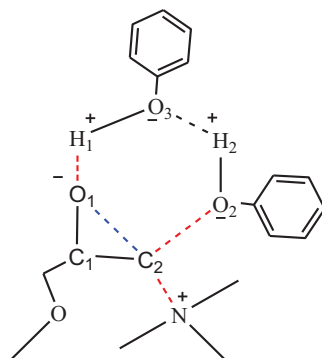

Figure 3.6. The transition state geometry ($TS_{p,ro}^{c2}$) of step 2 in the pathway $\mathbf{R_{p,ro}^c}$.

is opened by a tertiary amine, the phenol does not attach to the epoxy via either a *cis-* or *trans*-ring but on the opposite side with the tertiary amine in the epoxide plane.

3.3.3.2 Hydrogen bonded catalyzed pathways

The role of the tertiary amine in this case is to form a hydrogen bond complex with a phenol curing agent. This step is followed by the attachment of this complex to the epoxy ring of either the alone epoxy in $\mathbf{R}_{i,hb}^{c}$ or to the epoxy-phenol complex in $\mathbf{R}_{p,hb}^{c}$. Since the reaction rate of the second step is too slow compared with that of the first step, the second step is considered to be the rate-determining step. The transition state geometries and their parameters are presented in Figure 3.7 and Table 3.7. Note that due to the lower energy barrier of the acyclic TS route and the backside attachment in the previous pathways, only the acyclic TS is examined for this study.

The bond lengths of two "active" bonds, the breaking O1-C2 bond and the forming C2-O2 bond, at the TS, provide information on how close the TS is to the reactant (entrance) channel or to the product (exit) channel. Comparing the two TS's of hydrogen bonding catalyzed pathways, the shortening of the O1-C2 and the lengthening of the C2-O2 bond distances indicate that the $TS_{p,hb}^{c}$ is moved closer to the reactant channel than $TS_{i,hb}^{c}$. The decrease of 62 kJ/mol in the energy barrier when $TS_{p,hb}^{c}$ is compared to $TS_{i,hb}^{c}$ is consistent with the Hammond postulate, which states that more reactant-like characteristics of the transition state structure would lead to a smaller energy barrier. It confirms the role of the stabilization of a hydrogen bond complex between a phenol promoter and an epoxy reactant as seen in previous pathways.
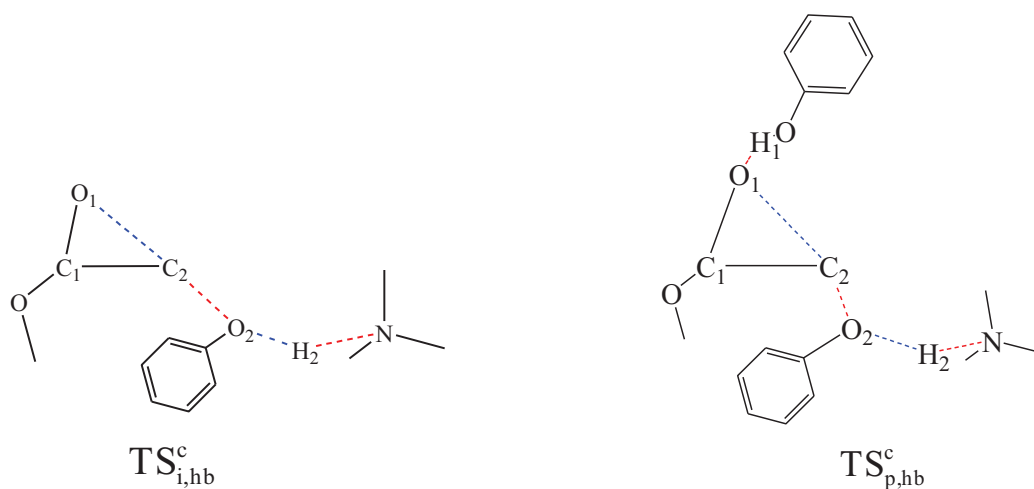
$$TS_{i,hb}^c \qquad\qquad TS_{p,hb}^c$$

Figure 3.7. Transition state geometries of hydrogen bond catalyzed pathways.

Table 3.7. Parameter of TS geometries in hydrogen bonding catalyzed pathways ($\mathbf{R}_{i,hb}^c$ and $\mathbf{R}_{p,hb}^c$).

Parameter	$TS_{i,hb}^c$	$TS_{p,hb}^c$
$v^{\neq}$ ($i.$cm^{-1})	244	651
d(H1-O1) (Å)		1.545
d(O1-C2) (Å)	2.115	1.992
d(C2-O2) (Å)	1.695	1.846
d(O2-H2) (Å)	1.481	1.210
d(H2-N) (Å)	1.104	1.277
d(O1-C1) (Å)	1.340	1.388
d(C1-C2) (Å)	1.515	1.488
$\angle$ (O1-C1-C2) (deg)	95.39	87.60
$\angle$ (C1-C2-O2) (deg)	122.28	120.82
$\Delta V_a^{\neq G}$ (kJ/mol)	173	101

3.4 Discussion

Both energetic values in the gas and the condensed phases of the pathways are presented in Table 3.3. The potential energy diagram of this reaction in the gas phase is presented in Figure 3.8. It will be assumed that the reference point is a point in which the epoxy, phenol and tertiary amine are separated infinitely. Since phenol cures epoxy by heat, both energy barriers and heat consumption are examined for the comparison on the reactivity of each reaction pathway.

Energy barriers are first examined and they follow the following order: $TS_{i,hb}^c$ (173 kJ/mol)$> TS_i$ (143 kJ/mol)$> TS_{i,ro}^{cl}$ (122 kJ/mol)$> TS_p = TS_{p,hb}^c$ (101 kJ/mol)$> TS_{p,ro}^{cl}$ (67 kJ/mol). This trend is divided into two groups: 1) A group that contains the stabilization of the hydrogen bonding between a phenol promoter and epoxy ($TS_{i,hb}^c$, TS_i, $TS_{i,ro}^{cl}$) and 2) A group that does not contain that stabilization (TS_p, $TS_{p,hb}^c$, $TS_{p,ro}^{cl}$). The first group obtains a higher energy barrier than the second by 56 kJ/mol on average.

A comparison of energy barriers between two corresponding pathways whose transition states are different in the hydrogen bonding complex of epoxy and a phenol promoter yields similar results. The transition states containing such hydrogen bonding always render a lower energy barrier than the others. For instance, a lowering of 42 kJ/mol of the energy barrier is obtained when TS_p is compared to TS_i, 55 kJ/mol for a comparison of $TS_{p,ro}^{cl}$ and $TS_{i,ro}^{cl}$, and 62 kJ/mol for $TS_{p,hb}^c$ and $TS_{i,hb}^c$ (see Table 3.7). This leads to the speculation that phenol always plays a dual role as a curing agent and as an accelerator by forming a hydrogen bond complex with epoxy to stabilize the transition state. A similar comparison is applied for two corresponding pathways that differ by a tertiary amine
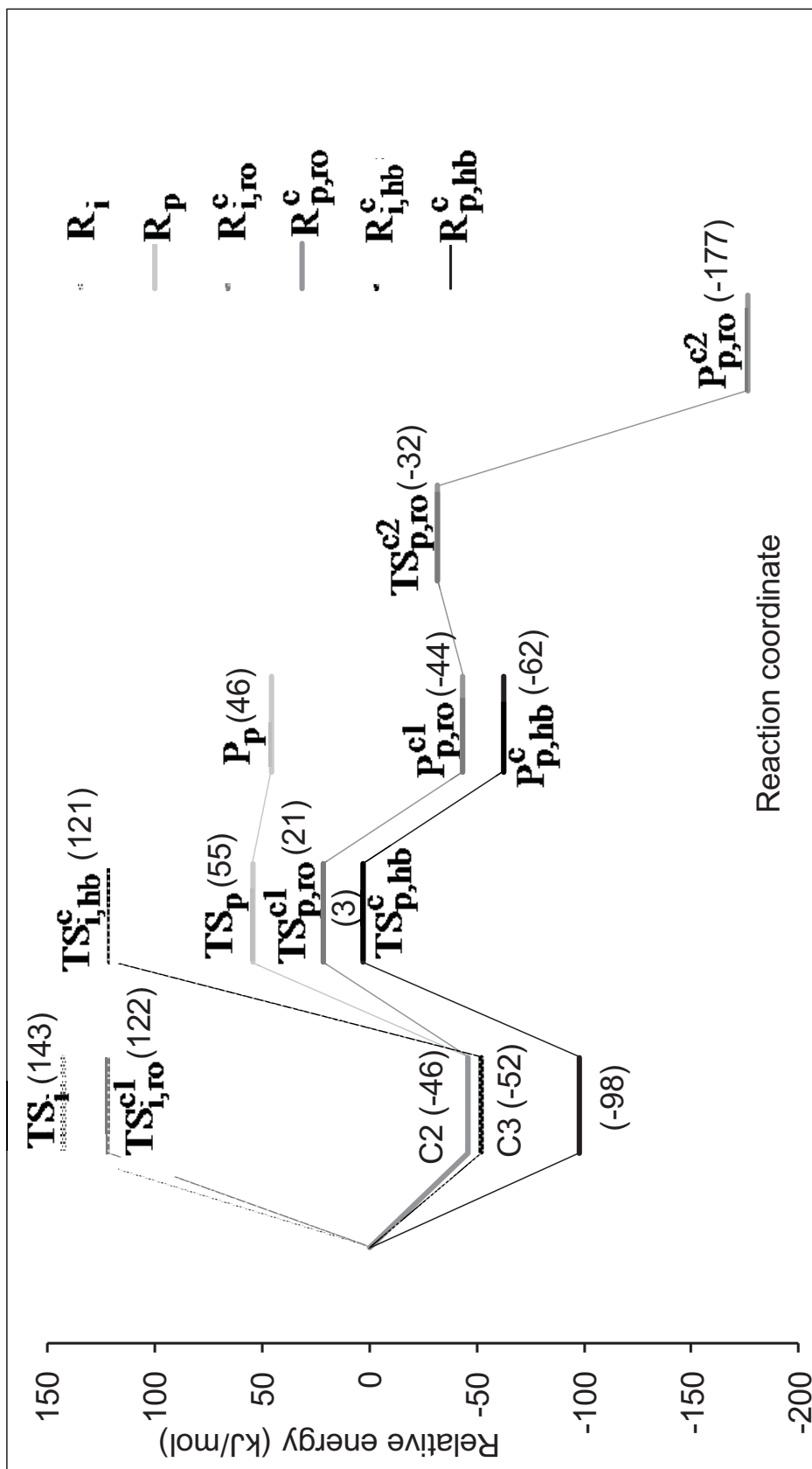
Figure 3.8. Potential energy for epoxy-phenol curing in the gas phase.

molecule. As a tertiary amine participates in the reaction as an epoxide opener, its catalytic property is indicated by the decrease in energy barriers, e.g., TS_i > $TS_{i,ro}^{cl}$ (group 1) and TS_p > $TS_{p,ro}^{cl}$ (group 2). However, as a tertiary amine forms a hydrogen bonded complex with the phenol curing agent, the opposite result is achieved. In the first group, $TS_{i,hb}^c$ yields a higher energy barrier than TS_i by 30 kJ/mol and in the second group, $TS_{p,hb}^c$ and TS_p have the same energy barriers. Meanwhile, the hydrogen bond formation between a phenol curing agent and the NR_3 catalyst is supposed to strengthen the nucleophilicity of the phenol curing agent, leading to a decrease in the energy barrier.
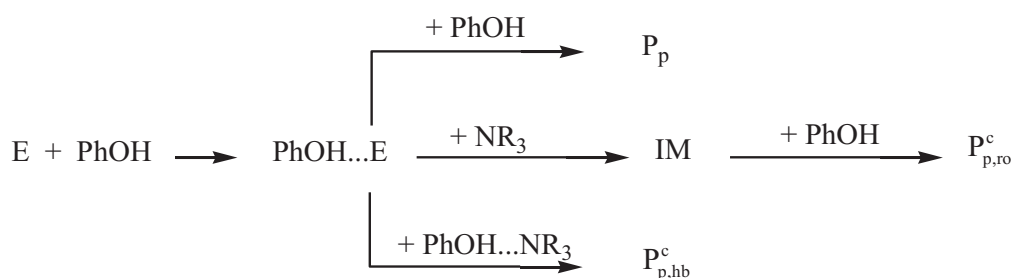
In some pathways, the hydrogen bonding complex C2 and/or C3 participates and releases heat in the curing process. This leads to the order of energy consumption as follows: $\mathbf{R_i}$ (143 kJ/mol) > $\mathbf{R_{i,ro}^c}$ (122 kJ/mol) > $\mathbf{R_{i,hb}^c}$ (121 kJ/mol) > $\mathbf{R_p}$ (55 kJ/mol) > $\mathbf{R_{p,ro}^c}$ (21 kJ/mol) > $\mathbf{R_{p,hb}^c}$ (3 kJ/mol). This trend of energy consumption agrees well with the trend of the energy barriers: Pathways in which transition states are stabilized by hydrogen bonding of the epoxy and phenol promoter yield lower energy consumptions than the others by over 102 kJ/mol on average.

$\mathbf{R_{p,hb}^c}$ is the most dominant process in curing epoxy-phenol because it has the smallest heat consumption. Heat consumption of $\mathbf{R_i}$, $\mathbf{R_{i,ro}^c}$ and $\mathbf{R_{i,hb}^c}$ is over forty times higher than the smallest heat consumption. Therefore, those pathways might not exist in the curing between epoxy and phenol. It also means that epoxy-phenol curing is always promoted by phenol curing agents. This is supported by Batog and coworkers' review[65] that most experimental epoxy-phenol curing reactions occur completely if the ratio of epoxy: phenol functions (E:PhOH) is larger than 1.

Hydroxyl products can accelerate curing by hydrogen bonding with epoxy as a phenol curing agents. Due to the steric effects, those products might not combine with epoxy by hydrogen bonding or they require very high-energy consumption to react with epoxy. Thus, this process can be ignored in the epoxy-phenol curing reactions.

There exist three pathways in the epoxy-phenol curing reaction. They are 1) Self promoted, 2) Ring-opening by tertiary amine catalyzed pathway and 3) Hydrogen bonding catalyzed pathway presented in both gas and condensed phases in Scheme 3.5 and Figure 3.9. The reactivity comparison is opposite with the order of heat consumption. That is self-promoted < ring-opening by tertiary amine < hydrogen bonding catalyzed pathway in both phases.

The hydrogen bonded complexes and transition states are not effectively solvated because the net charge is more distributed in the molecule complex (see Table 3.7). Although energy barriers for each pathway decrease, the potential energy is shifted up in solution. This indicates reasonably that the reaction is favored in the gas phase relative to the condensed phase, or that it requires more heat consumption in the condensed phase. The products are less stable in the condensed phase than in the gas phase; however, the reaction remains endothermic. Among all reactants, transition states and products, $TS_{p,ro}^{c2}$ is most solvated, resulting in the increase of the energy barrier in the condensed phase by

$$E + PhOH \longrightarrow PhOH...E \xrightarrow{+ NR_3} IM \xrightarrow{+ PhOH} P_{p,ro}^c$$

with branches:
$$PhOH...E \xrightarrow{+ PhOH} P_p$$
$$PhOH...E \xrightarrow{+ PhOH...NR_3} P_{p,hb}^c$$

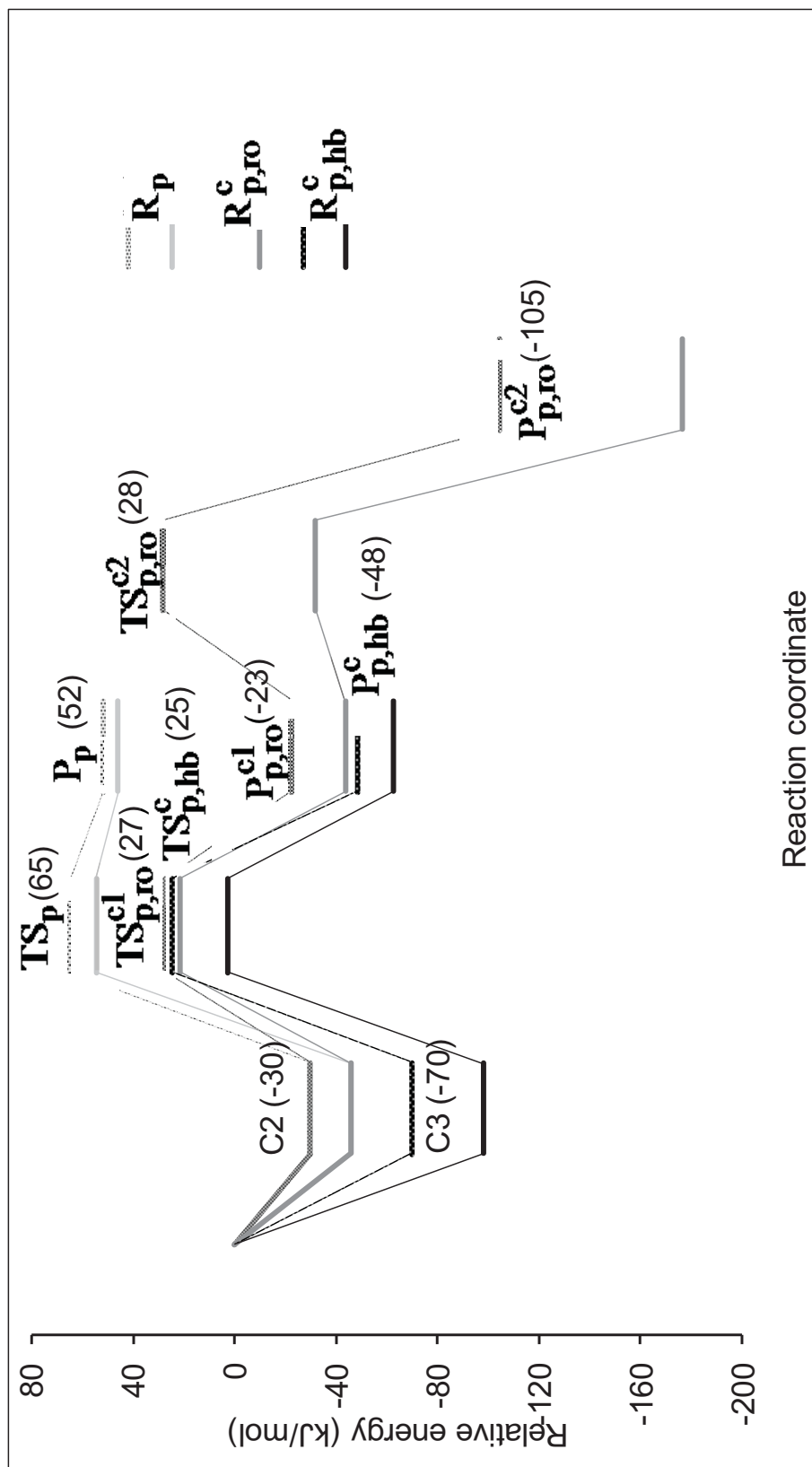**Scheme 3.5**. General mechanism of epoxy-phenol curing reaction.

Figure 3.9. Potential energy for epoxy- phenol curing reaction both in the gas phase (solid lines) and in the condensed phase (dashed lines). Energetic values are in the condensed phase.

29 kJ/mol compared to that in the gas phase (Table 3.7 and Figure 3.9). This demonstrates the weak distribution of the net charge and the synchronized transfer of an electron pair in the six-membered ring (see Figure 3.6).

The tertiary amine participates in two catalytic roles: 1) It leads to the easy attachment of phenol on the epoxy when during zwitterion formation, resulting in a lower energy barrier by 33 kJ/mol and 2) It forms a hydrogen bonded complex with a phenol curing agent without a lower energy barrier but with a lower heat of consumption by 52 kJ/mol. When the reaction is catalyzed by a tertiary amine that forms a zwitterion with the epoxy, its barrier energy is lowered compared to the uncatalyzed reaction, resulting in an increase in the curing rate. That means the tertiary amine's first role as a ring opener is dominant to its second role as a strengthener for a curing agent when the curing rate is considered. However, the opposite result is obtained when the heat of consumption as well as the stabilization are considered. This is achieved by the smallest energy consumption and the most stabilization of the hydrogen bonding catalyzed reaction.

Although tertiary amines were known to be good catalysts for epoxy-phenol curing, resulting in their common usage in industry,[7] the experimental activation energies of a tertiary amine catalyzed epoxy-phenol curing might not be found. Therefore, they can be approximated by epoxy-phenol curing with other catalysts such as trialkyl and/or triaryl nucleophiles of group V_a elements and miscellaneous catalysts, e.g., tetramethylammonium hydroxide.[51] In addition, tertiary amines can react with the curing agents to form salt catalysts. The activation energies of the biphenyl epoxy and phenol novolac resin system using triphenylphosphine (TPP) as a catalyst[5] are 60-70 kJ/mol and the corresponding value for the diglycidyl ether of bisphenol A (DGEBA) and phenol novolac catalyzed by N-

benzylpyrazinium hexafluoroantimonate (BPH) is 75 kJ/mol.[49] In our study, the curing of diglycidyl ether and phenol with a trimethylamine catalyst has an activation energy of 95 kJ/mol. Thus, all these activation energies are within an order of magnitude, which validates the reliability of our mechanistic model of the epoxy-phenol curing reactions.

3.5   Conclusions

In this study, possible pathways in the epoxy-phenol curing reaction were examined using the quantum chemistry density functional theory. Both gas phase and condensed phase results suggest that phenol has dual roles as hardener and as self-promoter. In the second role, phenol combines with epoxies by a hydrogen bond that stabilizes the transition states, leading to a lower energy barrier by 56 kJ/mol and to decrease heat consumption by 102 kJ/mol on average.

Tertiary amines assume two catalytic roles. The first role is to lower the energy barrier of the reaction by opening the epoxy ring to form a zwitterion before a phenol attaches to an epoxy in 33 kJ/mol. The second is to stabilize the transition state by hydrogen bonding with a phenol curing agent as well as to strengthen the nucleophilicity of the phenol curing agent, which does not lead to the decrease in the energy barrier but yields a smaller heat of consumption. Due to the smallest heat of consumption as well as the most stabilization in the self-promoted hydrogen bonding catalyzed reaction, tertiary amines are supposed to be promoters of phenol curing by forming a hydrogen bond complex.

As epoxy-amine curing,[8] epoxy-phenol curing belongs to the S_N2-type II process, and the acyclic TS pathway is preferred relative to the cyclic TS pathway. The mechanism of this curing is presented in Scheme 3.5 and follows an order: self promoted < ring opening by tertiary amine < hydrogen bonding catalyzed. Without the catalyst, phenol cures epoxy

slowly because of a high energy barrier of about 101 kJ/mol. With the assistance of a catalyst, the energy barrier and heat consumption decrease, leading to a faster curing that agrees well with experimental observation.

The resulting mechanism of epoxy-phenol curing performs predictive and functional-design capabilities. Its reactants, transition states, and products can be used as model for other systems by changing substituents on the epoxy, phenols, and even catalysts.

CHAPTER 4

MECHANISMS OF THE EPOXY-CARBOXYLIC

ACID CURING REACTIONS

4.1   Introduction

Carboxylic acids comprise in the second most popular hardening class for curing epoxy resins. They have been used increasingly in powder coatings, accounting for the highest tonnage of epoxy curing agents in the U.S. industry. This is due to their relatively low price, widespread availability as raw materials, and good flexibility and weatherability.[7]

The process of this crosslinking can be described as in Scheme 4.1: the first product is a β-hydroxypropyl ester, which reacts with a second mole of carboxylic acid to yield a diester. The hydroxyl ester can also undergo polymerization by reaction of its secondary hydroxyl group with an epoxy group.[7, 66]
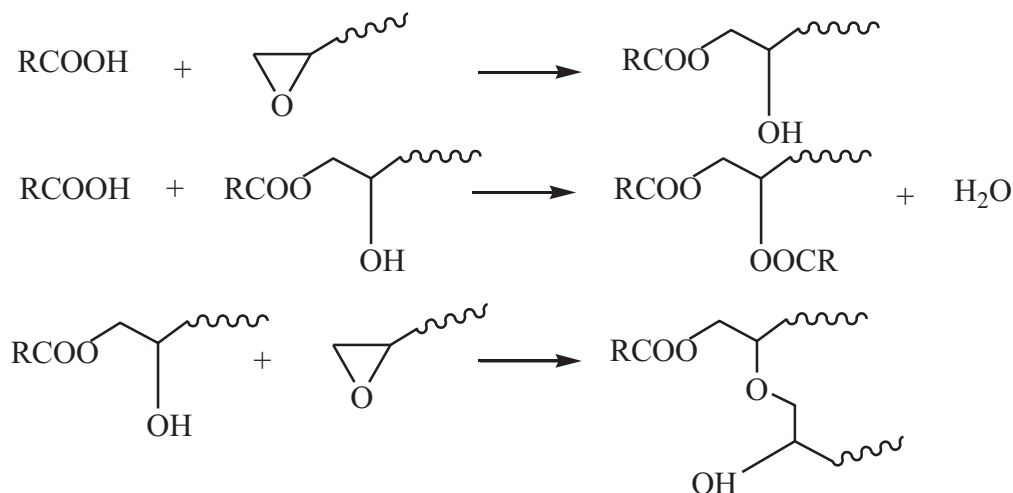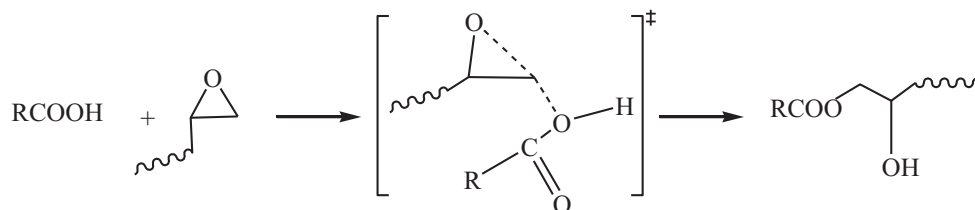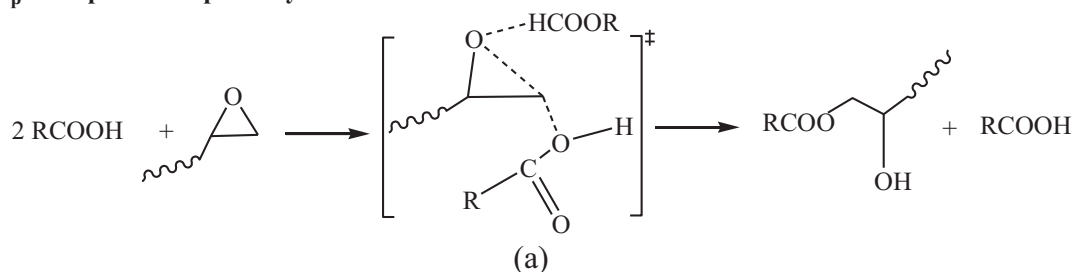

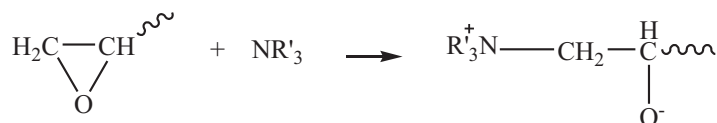**Scheme 4.1.** Process of the crosslinking of epoxy- carboxylic acid.

This process is significant only when the temperature is around 200^0C or is aided by catalysts such as tertiary amines between 80^0C to 120^0C in a lower energy consumption reaction.[66]

All possible reactions for the crosslinking of epoxy-acid units can be illustrated in Scheme 4.2 which is divided into three groups: 1) a group of hydrogen bond formations, 2) a group of uncatalyzed reactions (Scheme 4.2a) and 3) a group of catalyzed reactions (Scheme 4.2b). In the first group, three hydrogen complexes, acid-acid, acid-epoxy and acid-tertiary amine can exist and both acid-epoxy and acid-tertiary amine complexes can participate synchronously in the curing. In the second group, several authors[28, 66-68] suggested that epoxy and acid could react without a catalyst (isolated pathway $\mathbf{R}_i$). Rokaszewski[69] suggested that curing happens automatically, initiated by hydrogen donation by an acid or a hydroxyl product as presented in the self-promoted pathway $\mathbf{R}_p$.
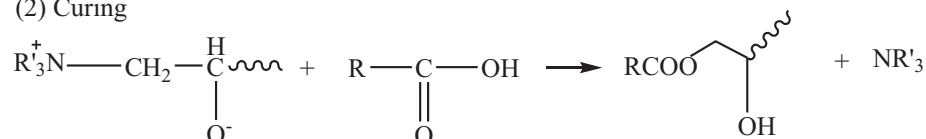
In Scheme 4.2b, the catalyzed reactions are currently known to proceed through only two pathways. The first is $\mathbf{R}_{i,ro}^c$, as suggested by Shechter and Wynstra,[28, 66] In this pathway, a tertiary amine catalyst and an epoxy were proposed to participate in the formation of a zwitterion and then this zwitterion reacted with an acid to form a product, similar to the isolated pathway. Thus, this pathway is distinguished from the isolated pathway by adding the role of the tertiary amine into its name, i.e., the isolated ring-opening of tertiary amine catalyzed pathway. In the second, $\mathbf{R}_{i,hb}^c$, proposed by Sorokin and Gershanova,[66, 70] the amine catalyst was assumed to form a complex with an acid, and then the complex reacts with an epoxy to form a product. Similar to the reaction in the Shechter and Wynstra's study, the reaction is named as the isolated hydrogen bonding catalyzed pathway.

R$_i$: Isolated pathway

RCOOH + (epoxide) → [transition state] → RCOO~~~ with OH

R$_p$: Self-promoted pathway

2 RCOOH + (epoxide) → [transition state with HCOOR] → RCOO~~~ with OH + RCOOH

(a)

R$_{i,ro}^c$: Isolated ring opening of tertiary amine catalyzed pathway

(1) Epoxy ring opening

H_2C—CH + NR'$_3$ → R'$_3$N$^+$—CH$_2$—C with O$^-$

(2) Curing

R'$_3$N$^+$—CH$_2$—C(O$^-$) + R—C(=O)—OH → RCOO~~~ with OH + NR'$_3$

R$_{p,ro}^c$: Self-promoted ring opening of tertiary amine catalyzed pathway

(1) Epoxy ring opening

H_2C—CH (RCOOH) + NR'$_3$ → R'$_3$N$^+$—CH$_2$—CH— with RCOOH----O$^-$

(2) Curing

R'$_3$N$^+$—CH$_2$—CH— (RCOOH----O$^-$) + R—C(=O)—OH → RCOO~~~ with OH + NR'$_3$ + RCOOH
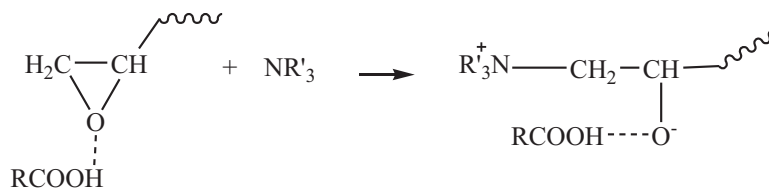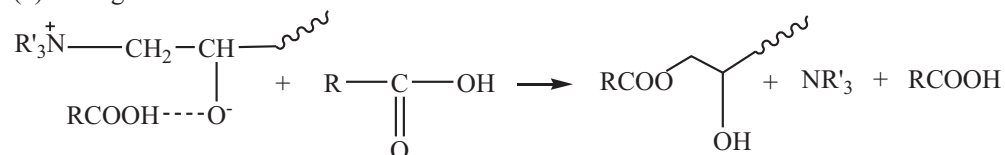
Scheme 4.2. Possible reactions in the epoxy- carboxylic acid curing system.
(a) Uncatalyzed reactions in the epoxy- carboxylic acid curing system.
(b) Catalyzed reactions in the epoxy- carboxylic acid curing system.

$\mathbf{R_{i,hb}^c}$: **Isolated hydrogen bonding catalyzed pathway**
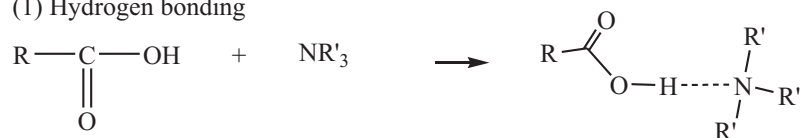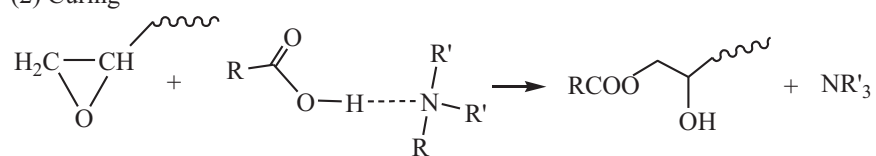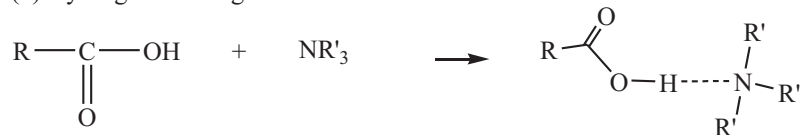
(1) Hydrogen bonding

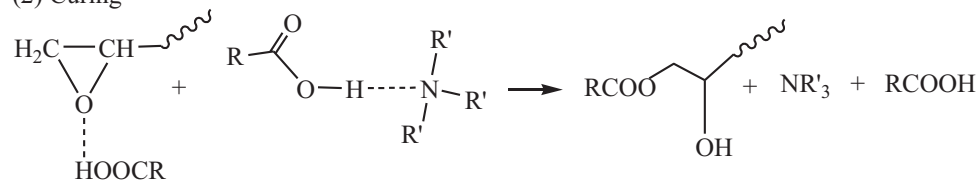(2) Curing

$\mathbf{R_{p,hb}^c}$: **Self-promoted hydrogen bonding catalyzed pathway**

(1) Hydrogen bonding

(2) Curing

(b)

Scheme 4.2 – continued.

To the best of our knowledge, the currently accepted mechanism for the tertiary amine catalyzed epoxy-acid curing reaction does not mention to at least two pathways. The first is $\mathbf{R_{p,ro}^c}$, a reaction of an epoxy-acid complex and a tertiary amine to form a zwitterions. This zwitterion reacts with an acid in a similar fashion as in the isolated ring opening of tertiary amine catalyzed pathway. This is called the self-promoted ring opening of tertiary amine catalyzed pathway. The second is $\mathbf{R_{p,hb}^c}$, a reaction of epoxy-acid complex and acid-tertiary amine complex and it can be named as a self-promoted hydrogen bonding catalyzed pathway. These reactions might be dominant pathways because they achieve stabilization of the transition state (TS) by hydrogen bonds between the epoxy and acid, leading to a lower energy consumption or an acceleration to products as proved in the epoxy-amine and epoxy-phenol curing. In addition, a suggested frontal approach in $\mathbf{R_i}$ [71] and $\mathbf{R_{i,hb}^c}$ [68, 70] would lead to a high energy barrier compared to the well-known backside approach of the typical S_N2 reaction as mentioned in the epoxy-amine[8] or epoxy-phenol curing systems.

In the review of Madec and Maréchal[66] in 1985, there were over 295 cited studies on uncatalyzed, base-catalyzed, and miscellaneous-catalyzed epoxy-carboxy esterifications and polyesterifications having an emphasis on the kinetics and mechanisms of polyesterification. One or more of the reactions in Scheme 4.2 were included in kinetic modelings of the acid curing systems by fitting to experimental data using Differential Scanning Calorimetery (DSC) that could not distinguish between the production of α and β esters. Note that only one α and β esters of such reactions is needed to be included in the mechanism model. Although the fittings between the kinetic models and the experimental data were usually reported to be reasonable, such models cannot be extrapolated for other acid curing systems nor prove that the mechanism is complete. For instance, results of the curing reactions of

acetic acid with some epoxies catalyzed by different tertiary amines[66, 72-76] cannot be extended for use in other reactions having either different epoxies or different tertiary amine catalysts.

The main objective of this study is to perform a systematically theoretical study on the mechanism of these epoxy-acid curing reactions at the molecular-level using B3LYP density functional theory. Examination of all possible reaction pathways of an epoxy-acid curing system at the same level of theory enables the development of a more accurate kinetic model for the system.

4.2   Computational details

4.2.1   Physical models

In industry, large molecules are utilized that are unfeasible for computation. In this study, smaller representative molecules are used. Methyl glycidyl ether was chosen to be a model for commercial epoxies, acetic acid was chosen for carboxylic acids, and trimethylamine was chosen for tertiary amine catalysts.

4.2.2   Computational models

All electronic structure calculations were carried out using the Gaussian 03 program package.[42] A hybrid nonlocal density functional theory B3LYP level of theory[43] with the 6-31G(d, p) basis set was used for locating all stationary points, namely reactants, transition states, intermediates, and products. Stationary points were characterized by normal mode analyses. To confirm the transition state for each reaction pathway, the minimum energy path (MEP) from the transition state to both the reactants and products was calculated using the Gonzales-Schlegel steepest descent path method[44, 45] in mass weight Cartesian

coordinates with the step size of 0.01 $(\text{amu})^{1/2}$ Bohr.

Single point solvation calculations were performed with Gaussian 09[77] on the optimized DFT geometries using a polarizable continuum model (PCM)[46, 62] with the acetic acid solvent ($\varepsilon = 6.25$) to mimic the reactions in solutions. It has been shown that the solvation free energies obtained from single point PCM calculations on the gas phase geometries from DFT calculations are in reasonable agreement with the values from full geometry optimization.[63, 64] All solvation calculations used the UFF (Universal Force Field) radii model, which places a sphere around each solute atom, with the radii scaled by a factor of 1.1 parameters.

4.3 Results

All possible reactions in Scheme 4.2 were studied respectively in the gas and the condensed phases. Hydrogen bond complex formations are examined first and followed by the examination of uncatalyzed and catalyzed reactions in the epoxy-acid curing reactions. Then, the comparison of those reactions and the validation with experimental values are performed. Geometries of the transition states (TS) and their zero-point energy corrected barriers $\Delta V_a^{\neq G}$ are used for the comparison of reactivity. Activation energies E_a that are approximated by the barriers in the condensed phase, corrected by the zero point energy calculated in the gas phase, are used to compare with experimental values. The classical barrier in the gas phase ($\Delta V^{\neq}$), the zero-point energy (ZPE), and the enthalpy of reaction (ΔH) at 0 K are presented in Table 4.1.

Table 4.1. Energetic values (kJ/mol) for all possible pathways in Scheme 4.2 of the epoxy-acid curing reaction at 0 K. (Enthalpy of reaction is reported for products)

Pathways	Compounds	ΔV	ZPE	$\Delta V_a^{\neq G}$	ΔV_{sol}	E_a
	C1	-42	5	-37	-33	-29
	C2	-47	6	-41	-37	-32
	C3	-58	6	-52	-53	-47
$\mathbf{R_i}$	TS_i	135	-10	125	139	130
$\mathbf{R_p}$	TS_p	119	-5	114	117	112
	P_p	71	11	82	63	74
$\mathbf{R_{i,ro}^c}$	$TS_{i,ro}^{c1}$	115	6	122	76	83
$\mathbf{R_{p,ro}^c}$	$TS_{p,ro}^{c1}$	55	3	58	45	48
	$P_{p,ro}^{c1}$	-22	19	-4	-53	-35
	$TS_{p,ro}^{c2}$	71	-7	64	86	79
	$P_{p,ro}^{c2}$	-76	-3	-79	-39	-43
$\mathbf{R_{i,hb}^c}$	$TS_{i,hb}^c$	162	4	166	123	127
$\mathbf{R_{p,hb}^c}$	$TS_{p,hb}^c$	90	0	90	79	79
	$P_{p,hb}^c$	25	12	37	-40	-29

4.3.1 Hydrogen bonding precursor complexes

Complexes C1-C3 (cf. Figure 4.1) show possible reactant complexes between the acid groups, the amine catalyst functional groups and the epoxy oxygen. Note that all hydrogen atoms not involved in the reactions are deleted in all figures for clarity and the dashed lines illustrate the forming and breaking of bonds. Table 4.2 demonstrates that the order of strong hydrogen bond interaction is C1 < C2 < C3 which is consistent with the decrease of the binding energies. The OH…N hydrogen bond of C3 is strongest because nitrogen is a better hydrogen acceptor (Lewis base) than oxygen. So the complexes C2 and C3 can participate in the curing reactions together with epoxy, acid and tertiary amine.
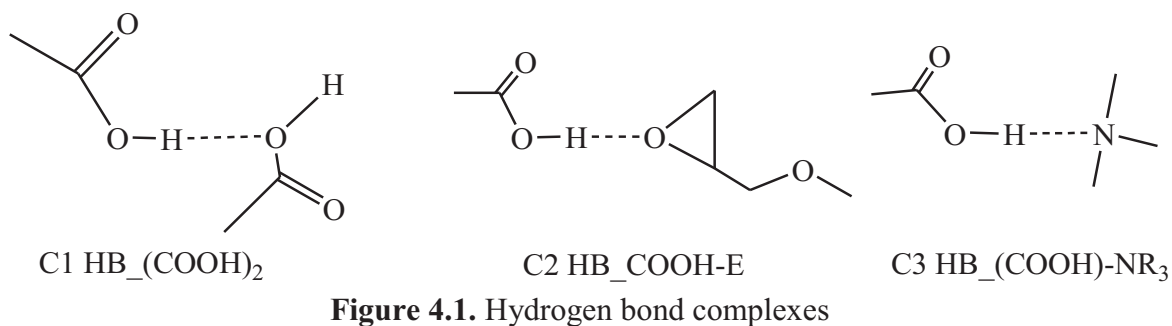
Figure 4.1. Hydrogen bond complexes

Table 4.2. Bond distance and the binding energy of hydrogen complexes. (Binding energy ΔE_{bind} is calculated in the gas phase).

Parameters	C1	C2	C3
d(OH-O) ($\AA$)	1.86, 1.92	1.76	
d(OH-N) ($\AA$)			1.69
ΔE_{bind} (kJ.mol^{-1})	-37	-41	-52

4.3.2 Uncatalyzed reactions (Scheme 4.2a)

Transition states of $\mathbf{R_i}$ (Figure 4.2) and $\mathbf{R_p}$ (Figure 4.3) are examined in both acyclic and cyclic routes. In the process from reactant to product via the acyclic TS, the C2-O1 bond of the epoxy ring is broken and the new C2-O2 bond is formed whereas in the process via the cyclic TS, C2-O2 bond is broken and H1-O1 is formed. These bond lengths, barrier energies, and other parameters of the transition state structures are represented in Table 4.3.

In $\mathbf{R_i}$, the cyclic TS is characterized by a lower energy barrier than the acyclic TS by 73 kJ/mol, and thus is considered as the TS for this pathway. This agrees well with Klebanov et al.'s suggestion[71] that the TS of epoxy-acid curing reaction would have a six-member ring structure where the OH group of acid forms a hydrogen bond with the oxygen atom of the epoxy and the C=O group attacks the methylene group of the epoxy from the front side.
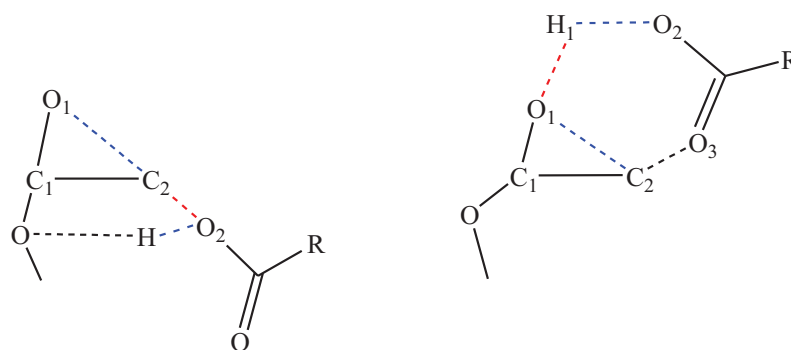
Figure 4.2. Acyclic (left) and cyclic (right) transition states of R_i.
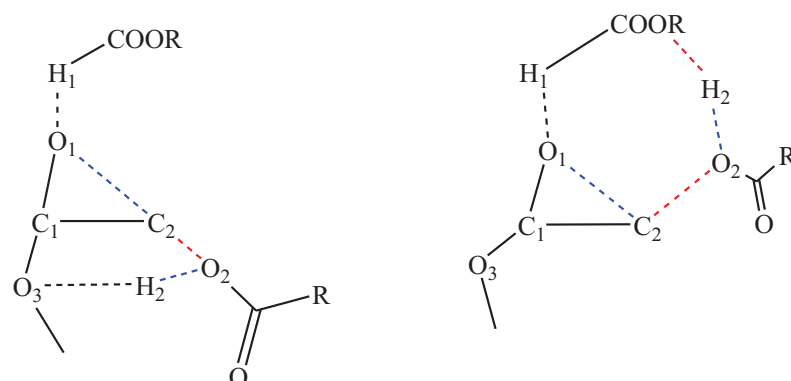
Figure 4.3. Acyclic (left) and cyclic (right) transition states of R_p.

Table 4.3. Parameters of transition state geometries of R_i and R_p.

Parameters	TS_i		TS_p	
Route	Acyc	Cyc	Acyc	Cyc
$v^{\neq}$ ($i.cm^{-1}$)	445	830	508	514
d(H1-O1) (Å)		1.210	1.143	1.036
d(H1-O2) (Å)		1.191		
d(O1- C2) (Å)	2.206	2.026	2.071	2.016
d(C2-O3) (Å)		2.277		
d(C2-O2) (Å)	1.665		1.866	3.342
d(O1- C1) (Å)	1.327	1.411	1.397	1.434
d(C1-C2) (Å)	1.521	1.462	1.490	1.461
d(H2-O2) (Å)			1.018	0.999
$\angle$ (O1-C1-C2) (deg)	101.31	89.7	91.6	88.31
$\angle$ (C1-C2-O3/O2) (deg)	109.91	119.2	107.2	130.33
$\Delta V_a^{\neq G}$ (kJ/mol)	198	125	114	165

In $\mathbf{R_p}$, the acyclic TS dominates the cyclic six-member ring TS in the lower energy barrier, conflicting with the speculation that suggested a *cis*-opening of the epoxy ring [66-68] but agreeing well with the suggestion of a *trans*-opening TS.[66, 78, 79] In addition, it agrees with the recent result in the epoxy-amine curing reaction that stated the acyclic TS is preferred vs the cyclic TS because of the former's smaller energy barrier.[8] Due to the hydrogen donation by the acid to an epoxy ring, the energy barrier of $\mathbf{R_p}$ is lower than that of $\mathbf{R_i}$ by 11 kJ/mol (see Table 4.3). In addition, the sufficient amount of acid as well as the easy binding of an epoxy and an acid account for the existence of the self-promoted pathway, and thus the isolated pathway may serve as a reference for the self promoted pathway as it does not take part in the curing reaction.

4.3.3 Catalyzed reactions (Scheme 4.2b)

4.3.3.1 Ring opening of tertiary amine catalyzed pathways

Pathways $\mathbf{R^c_{i,ro}}$ and $\mathbf{R^c_{p,ro}}$ in Scheme 4.2b are considered here. Since each pathway proceeds via two steps, the numbers 1 and 2 were added to both transition states and products' names. The transition states of step 1 in each pathway ($TS^{c1}_{i,ro}$ and $TS^{c1}_{p,ro}$) are examined, represented in Figures 4.4 and 4.5 respectively. Step 2 is then examined only for the dominant pathway in the comparison of energy barriers of reactions in step 1.

In either $TS^{c1}_{i,ro}$ or $TS^{c1}_{p,ro}$, the backside attachment is preferred as compared to the front-side attachment because of the lower energy barrier and consequently, its energy barrier is chosen as a reference to compare which TS is dominant in the first step of each pathway. Comparing $TS^{c1}_{i,ro}$ to $TS^{c1}_{p,ro}$ (see Table 4.4), the hydrogen bond between an acid
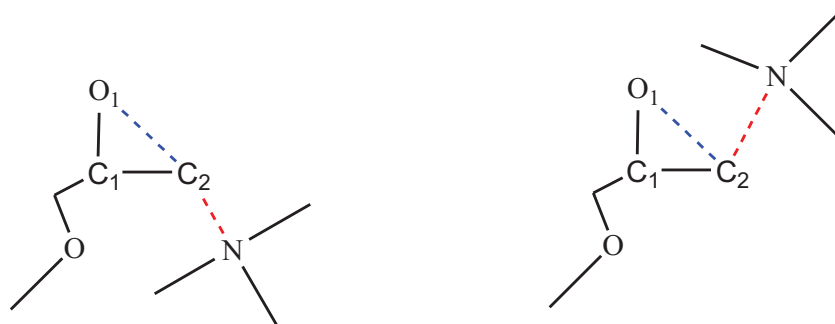
Figure 4.4. Back-side (left) and front-side (right) $TS^{cl}_{i,ro}$.
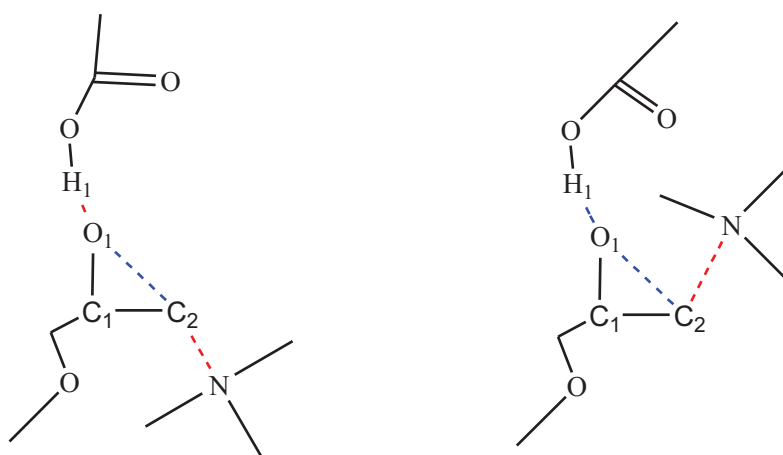
Figure 4.5. Back-side (left) and front-side (right) $TS^{cl}_{p,ro}$.

Table 4.4. Parameters of $TS^{cl}_{i,ro}$ and $TS^{cl}_{p,ro}$.

Parameters	$TS^{cl}_{i,ro}$		$TS^{cl}_{p,ro}$	
Side attachment	front	back*	back*	front
$v^{\neq}$ (i.cm^{-1})	362	266	397	389
d(N-C2) (Å)	2.190	1.778	2.061	2.265
d(C2-O1) (Å)	2.079	2.109	1.908	2.021
d(H1-O1) (Å)			1.479	1.533
d(C1-O1) (Å)	1.383	1.338	1.393	1.398
d(C1-C2) (Å)	1.470	1.529	1.479	1.467
$\angle$ (O1-C1-C2) (deg)	93.48	94.5	83.2	89.72
$\angle$ (C1-C2-N) (deg)	119.53	124.0	117.34	123.88
$\angle$ (C2-N-O1) (deg)	47.36			45.01
$\Delta V^{\neq G}_a$ (kJ/mol)	188	122	58	156

(* is noted for the represented TS)

promoter and an epoxy lowers the energy barriers by 64 kJ/mol, leading to further study of

the second step of the $\mathbf{R}_{p,ro}^c$ pathway.

In the second step of $\mathbf{R}_{p,ro}^c$, the formation of a six-centered cyclic transition state

structure ($TS_{p,ro}^{c2}$), in which a synchronized transfer of an electron pair takes place is shown

in Figure 4.6. The attachment of an acid curing agent to the epoxy is indicated by an

imaginary frequency of -422 cm^{-1} for the vibration of the C2-O2 bond. A strong hydrogen

bond O1-H1 in $TS_{p,ro}^{c2}$ can be formed by a hydrogen atom transfer either from the acid

promoter or from the acid curing agent to the epoxide oxygen. The required energy for such

a hydrogen transfer can be ignored relative to the zwitterion's formation in step 1 ($TS_{p,ro}^{c1}$).

This hydrogen transfer might happen before the attack of the acid into the methylene carbon

on the epoxy ring.

4.3.3.2   Hydrogen bonding catalyzed pathways

Two last pathways ($\mathbf{R}_{i,hb}^c$ and $\mathbf{R}_{p,hb}^c$) in Scheme 4.2b are examined, in which the

tertiary amine creates a hydrogen bond complex with an acid curing agent. It might lead to

the strengthening of the nucleophilic attachment into the epoxy ring. Although they are two

step reactions, the hydrogen bonding step is fast compared to the curing step. So, the

transition state in the curing step is focused in this study.

Due to the significantly lower energy barriers of the acyclic transition states

compared with the cyclic transition states in the $\mathbf{R}_p$ and of the backside TS compared with

the front-side TS of the first step in the $\mathbf{R}_{i,ro}^c$ and $\mathbf{R}_{p,ro}^c$, only the acyclic route is considered

for this study. The parameters of those TSs are presented in Figure 4.7 and Table 4.5. The
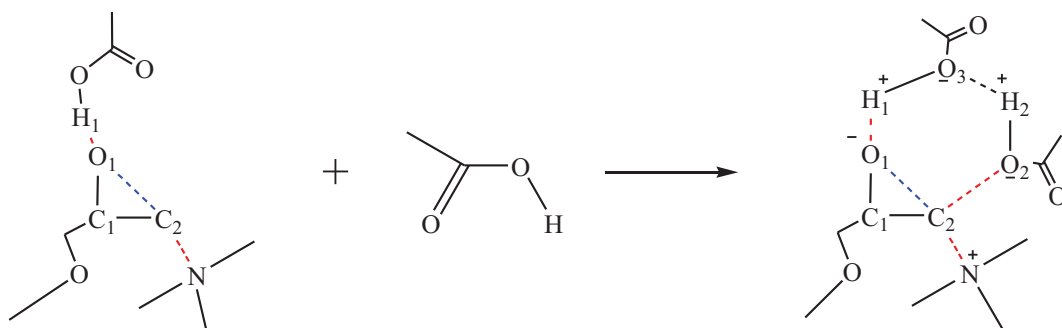
Figure 4.6. Process via the second step of the $R_{p,ro}^c$.
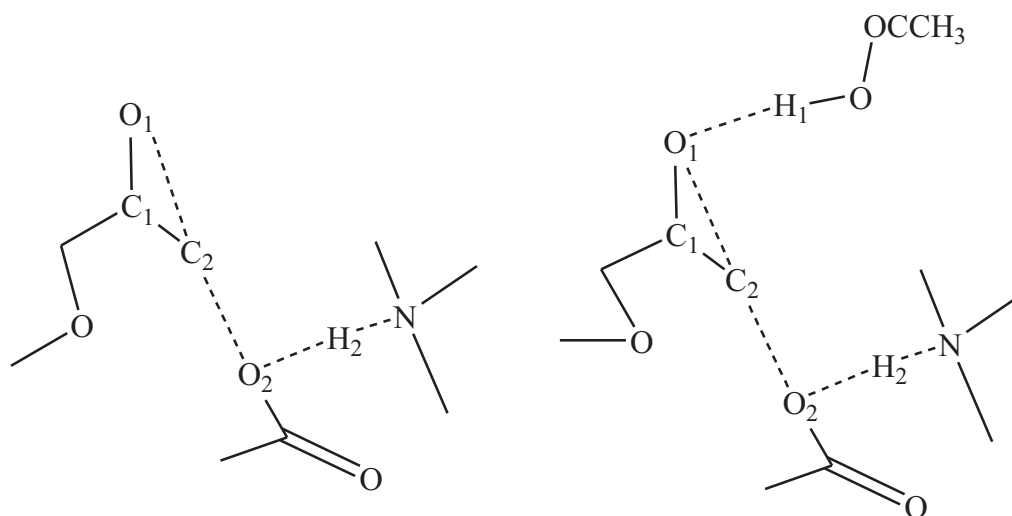
Figure 4.7. Transition state geometries of $R_{i,ro}^c$ and $R_{p,ro}^c$ respectively from left to right.

Table 4.5. Parameters of the $TS_{i,hb}^c$ and $TS_{p,hb}^c$.

Parameters	$TS_{i,hb}^c$	$TS_{p,hb}^c$
$\nu^{\neq}$ ($i.cm^{-1}$)	330.4	436.2
d(O2-C2) (Å)	1.714	1.920
d(C2-O1) (Å)	2.111	1.934
d(H1-O1) (Å)		1.395
d(C1-O1) (Å)	1.336	1.398
d(C1-C2) (Å)	1.512	1.474
d(O2-H2) (Å)	1.598	1.505
d(H2-N) (Å)	1.074	1.094
$\angle$ (O1-C1-C2) (deg)	95.5	84.6
$\angle$ (C1-C2-H2) (deg)	118.2	114.4
$\Delta V_a^{\neq G}$ (kJ/mol)	166	90

hydrogen bonding of the epoxy and the acid promoter O1-H1 in this case accounts for the lower energy barrier by 76 kJ/mol.

4.4   Discussion

Table 4.1 presents all energetic parameters in both the gas phase and the condensed phase. Values in the condensed phase are used for the following discussion. Energy barriers are first examined and they follow the order: $TS_{i,hb}^{c}$ (166 kJ/mol) > TS_i (125 kJ/mol) > $TS_{i,ro}^{c1}$ (122 kJ/mol) > TS_p (114 kJ/mol) > $TS_{p,hb}^{c}$ (90 kJ/mol) > $TS_{p,ro}^{c1}$ (58 kJ/mol). Note that for a two step reaction, the energy barrier of the rate-determining step accounts for the comparison with that of the other one step reactions. This trend is divided into two groups: 1) a group that does not contain the stabilization of a hydrogen bond between an acid promoter and epoxy ($TS_{i,hb}^{c}$, TS_i , $TS_{i,ro}^{c1}$) and 2) A group that contains this stabilization (TS_p , $TS_{p,hb}^{c}$, $TS_{p,ro}^{c1}$). The first group obtains an energy barrier higher than the second by 50 kJ/mol on average.

The comparison of energy barriers between two corresponding pathways whose transition states differ by a hydrogen bond between an epoxy and an acid promoter yields a similar result. The transition states containing this hydrogen bond always render a lower energy barrier than the others. For instance, a lowering of the energy barrier by 11 kJ/mol is obtained when TS_p is compared to TS_i , 64 kJ/mol when $TS_{p,ro}^{c1}$ is compared to $TS_{i,ro}^{c1}$, and 76 kJ/mol when $TS_{i,hb}^{c}$ is compared to $TS_{p,hb}^{c}$ (Table 4.1). This leads to speculation that the acid always plays a dual role as a curing agent and as an accelerator by forming a hydrogen bond complex with epoxy to stabilize the transition state.

A similar comparison is applied for two corresponding pathways that differ by a tertiary amine molecule. As the tertiary amine participates in the curing as a ring opener, its catalytic property is indicated by the decrease in energy barriers, e.g. $TS_i > TS_{i,ro}^{c1}$ (in group 1) and $TS_p > TS_{p,ro}^{c1}$ (in group 2). However, as the tertiary amine forms a hydrogen bonded complex with an acid curing agent, the result is opposite in the first group, i.e., $TS_{i,hb}^c$ obtains a higher energy barrier than TS_i by 41 kJ/mol. Meanwhile, hydrogen bond formation between an acid curing agent and a NR_3 catalyst is supposed to strengthen the nucleophilicity of the acid curing agent, resulting in a decrease in the energy barrier.

Since a carboxylic acid cures the epoxy by heat, both the energy barriers and heat consumption are compared. The potential energy of epoxy-acid in the gas phase is plotted in Figure 4.8. Assume that the reference point is a point at which the epoxy, the acid and the tertiary amine are separated infinitely.

In some pathways, the hydrogen bonding complex C2 and/or C3 participates in the curing process and releases heat. This leads to the order of energy consumption as follows: $\mathbf{R_i}$ (125 kJ/mol) > $\mathbf{R_{i,ro}^c}$ (122 kJ/mol) > $\mathbf{R_{i,hb}^c}$ (114 kJ/mol) > $\mathbf{R_p}$ (73 kJ/mol) > $\mathbf{R_{p,ro}^c}$ (17 kJ/mol) > $\mathbf{R_{p,hb}^c}$ (-3 kJ/mol). This trend of energy consumption agrees well with the trend of energy barriers: pathways in which the transition states are stabilized by a hydrogen bond of the epoxy and an acid promoter result in ower energy consumptions than the others by over 91 kJ/mol on average.

$\mathbf{R_{p,hb}^c}$ is the most dominant curing epoxy-acid because it has the smallest heat consumption. Heat consumption of the $\mathbf{R_i}$, $\mathbf{R_{i,ro}^c}$, and $\mathbf{R_{i,hb}^c}$ pathways is over one hundred
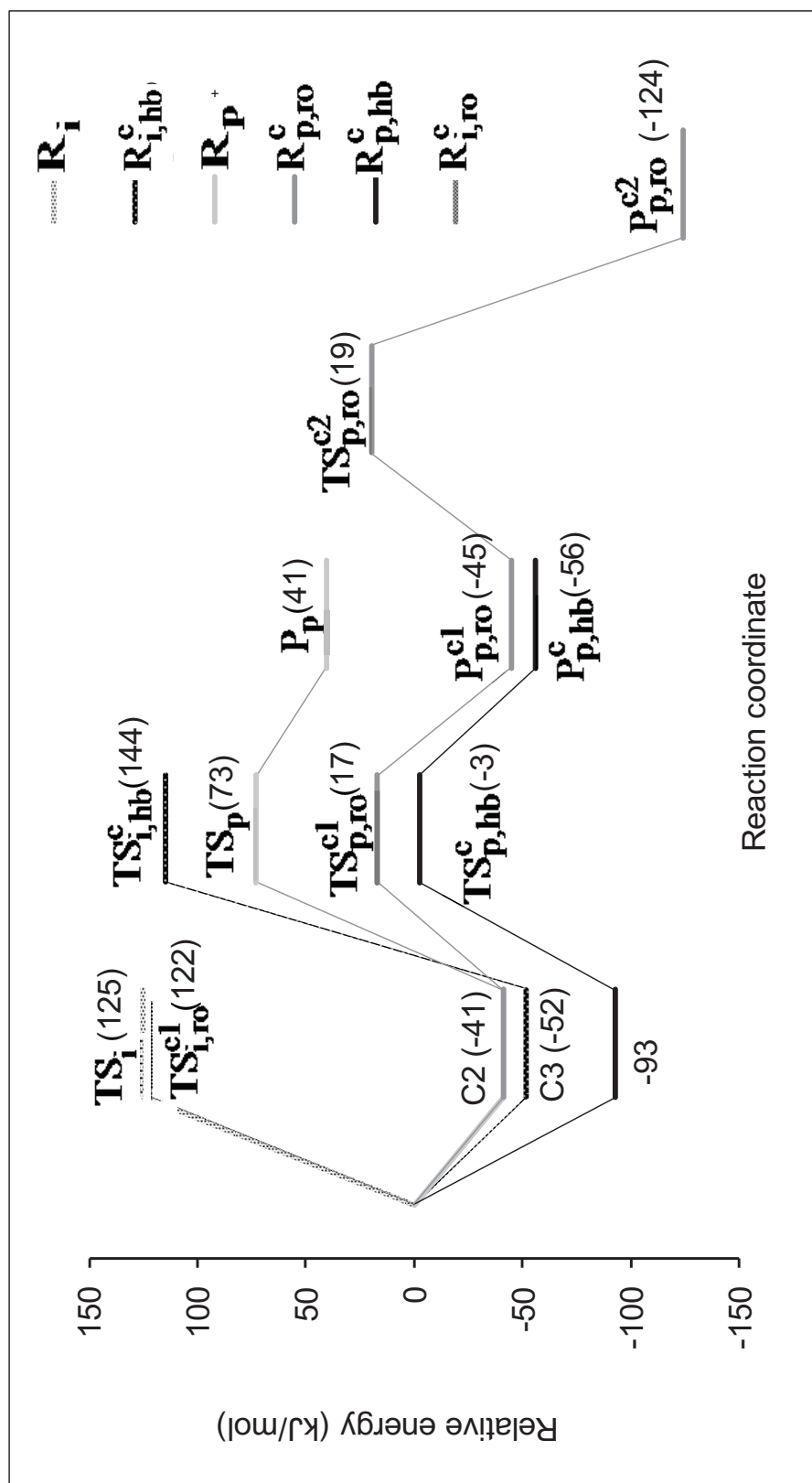
Figure 4.8. Potential energy for epoxy-acid curing in the gas phase.

times higher than the smallest heat consumption of the $\mathbf{R}^c_{p,hb}$ pathway. Therefore, these pathways might not participate in the curing between the epoxy and the acid and the epoxy-acid curing is likely always promoted by acid curing agents.

Hydroxyl products can accelerate the curing by formation of a hydrogen bond with the epoxy in the same way acid curing agents can. Due to steric effects, those products might not combine with an epoxy by a hydrogen bond or they may require a very high energy consumption to react with an epoxy. Thus, these processes can be ignored in the epoxy-acid curing reactions or be supposed to be more difficult than the curing by acid.

There exist three pathways in the epoxy-acid curing reaction that are: $\mathbf{R}_p$, $\mathbf{R}^c_{p,ro}$ and $\mathbf{R}^c_{p,hb}$. This curing is mimicked in acetic acid solution by calculating the single point energy of the optimized system in the gas phase. The potential energies of these pathways in both the gas and the condensed phases are presented in Figure 4.9. The hydrogen bonded complexes and the transition states are solvated similarly. The transition states are less solvated than the products in each pathway (see Table 4.1), and the potential energy seems litle changed in the acetic acid solution but it might be more changed in other solutions. In the most dominant pathway, $\mathbf{R}^c_{p,hb}$, the product is more stable in solution than in the gas phase, although the reaction is still predicted to be endothermic. The comparison is opposite to the order of heat consumption, that is self-promoted < ring opening of tertiary amine < hydrogen bonding catalyzed pathway in both phases.

A tertiary amine can participate in two catalytic roles: 1) It attacks epoxy to form a zwitterion and then this zwitterion reacts with an acid, resulting in a lower energy barrier as well as heat consumption by 56 kJ/mol and 2) it forms a hydrogen bonded complex with the acid curing agent to lower the energy barrier by 24 kJ/mol and heat consumption by 76
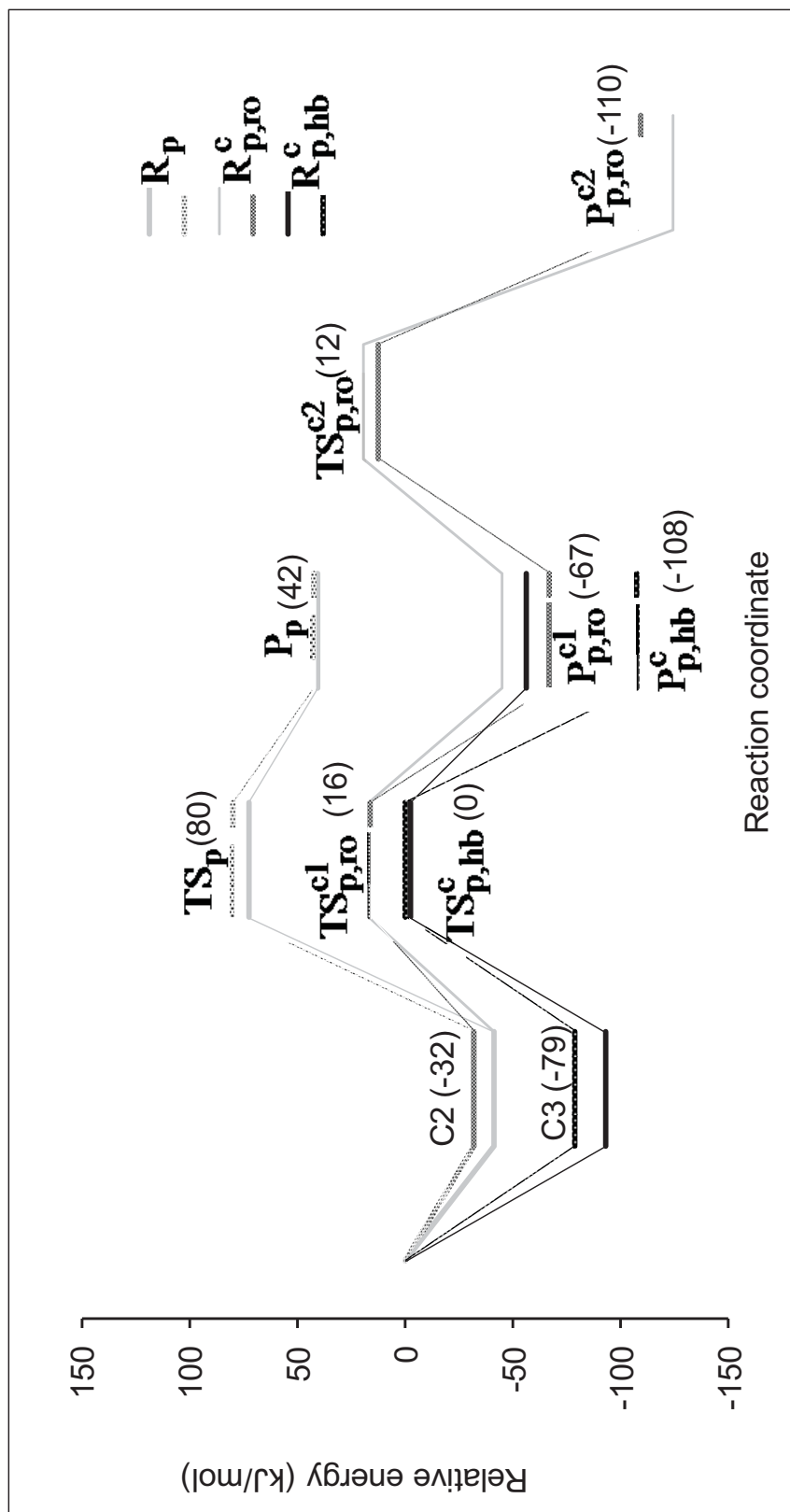
Figure 4.9. Potential energy for epoxy- acid curing reaction both in the gas phase (solid lines) and in the condensed phase (dashed lines). Energetic values are in the condensed phase.

kJ/mol, compared with the corresponding values in the uncatalyzed pathway ($\mathbf{R_p}$). Due to the commercial epoxies having greater steric effects compared with carboxylic acids that could lead to the more difficult attachment of a tertiary amine to the epoxy than to an acid to form a hydrogen bonding complex. In addition, the potential energies in Figures 4.8 and 4.9 demonstrate that the second role leads its pathway having the smallest energy consumption. This confirms that in the epoxy-acid curing, the tertiary amine catalysts' main function is to form a hydrogen bond with the acid curing agent, rather than opening the epoxy ring.

Although there are no experimental data for the same model to compare with our results, some still can be used as validation. Batog et al.[65] reported that curing reactions of 3-cyclohexene-1-carboxylic acid, 2-oxiranylmethyl ester ($C_{10}H_{14}O_3$) and peracetic acid (PAA, CH_3CO_3H) required activation energies of 47.76 kJ/mol whereas the activation energies of the curing between oxirane, 2-[(3-cyclohexen-1-ylmethoxy)methyl] ($C_{10}H_{16}O_2$) and PAA is 65.01 kJ/mol. The authors also cited the average activation energy for aliphatic-cycloaliphatic epoxy compounds (ACECs) and PAA as being about 50-72 kJ/mol. Rafizadeh[80] reported that the activation energy for the curing between DGEBA and methacrylic acid with triphenylphosphine is 80 kJ/mol at 95-100^{0}C. The activation energy for the curing of methyl glycidyl ether and acetic acid catalyzed by trimethylamine in our calculation is 79 kJ/mol. So our calculated value is comparable with other reports within an order of magnitude and consequently can be a reference point for the estimation of other epoxy-acid curing systems.

4.5   Conclusions

In this study, possible pathways in the epoxy-acid curing reaction were examined using the quantum chemistry density functional theory. Both gas and condensed phase

results suggest that the acid has dual roles as hardener and as self-promoter. In the second role, the acid combines with the epoxy by a hydrogen bond that stabilizes the transition states, leading to a lower barrier energy by 50 kJ/mol and to a decrease of heat consumption by 91 kJ/mol on average.

Tertiary amines assume two catalytic roles. The first role is to lower the energy barrier of the reaction by 56 kJ/mol by opening the epoxy ring to form a zwitterion before an acid attaches to an epoxy. The second is to stabilize the transition state by hydrogen bonding with an acid curing agent as well as to strengthen the nucleophilicity of the acid curing agent, leading to decreases in the energy barrier by 24 kJ/mol and the heat of consumption by 76 kJ/mol. Due to its having the smallest heat of consumption as well as the greatest stabilization in $\mathbf{R}^{c}_{p,hb}$, a tertiary amine is supposed to be a promoter of acid curing by forming a hydrogen bond complex.

As with the epoxy-amine curing,[8] epoxy-acid curing belongs to the S_N2-type II process, and the acyclic TS pathway is preferred as compared to the cyclic TS pathway. The mechanism of this curing follows the order: self-promoted < ring opening of tertiary amine catalyzed < hydrogen bonding catalyzed. Without the catalyst, an acid cures epoxy slowly because of a high energy barrier of about 114 kJ/mol. With the assistance of a catalyst, the barrier energy and heat consumption decrease, leading to a faster curing that agrees well with experimental observation.

The resulting mechanism of the epoxy-acid curing performs predictive and functional-design capabilities. Its reactants, transition states, and products can be applied to the development of other systems by changing substituents on the epoxy, carboxylic acids, and even catalysts.

CHAPTER 5

# MECHANISMS OF THE EPOXY-ANHYDRIDE

CURING REACTIONS

5.1 Introduction

Anhydrides are among the first epoxy curing agents to have been used. Epoxy-anhydride systems exhibit low viscosity, long pot life, low exothermic heats of reaction, and little shrinkage when cured at elevated temperatures. Due to their unique low exothermic heats of reaction, these systems can be used in large scale applications.[7]

Epoxy-anhydride curing involves two steps, initiation and propagation. In the initiation step, an anhydride attaches to an epoxy ring to form an internal salt. In the propagation step, this internal salt attacks another anhydride to create another internal salt that contains an anionic carboxylate group. This anionic carboxylate group might react with an epoxy. This curing, shown in Scheme 5.1, is considered as an uncatalyzed reaction without hydroxyl groups in the backbone of epoxy resins ($\mathbf{R''}$) but has not been mentioned as established mechanism.

A well accepted mechanism for the uncatalyzed reactions involves the attachment of hydroxyl groups in the epoxy resins to the anhydride molecules to form an ester linkage and a carboxyl group. The latter then reacts with the epoxy ring to yield a diester and a new secondary hydroxyl group, thus perpetuating the mechanism (Scheme 5.2).[7, 81-83] However, such a mechanism cannot apply to a system without an available hydroxyl group in the

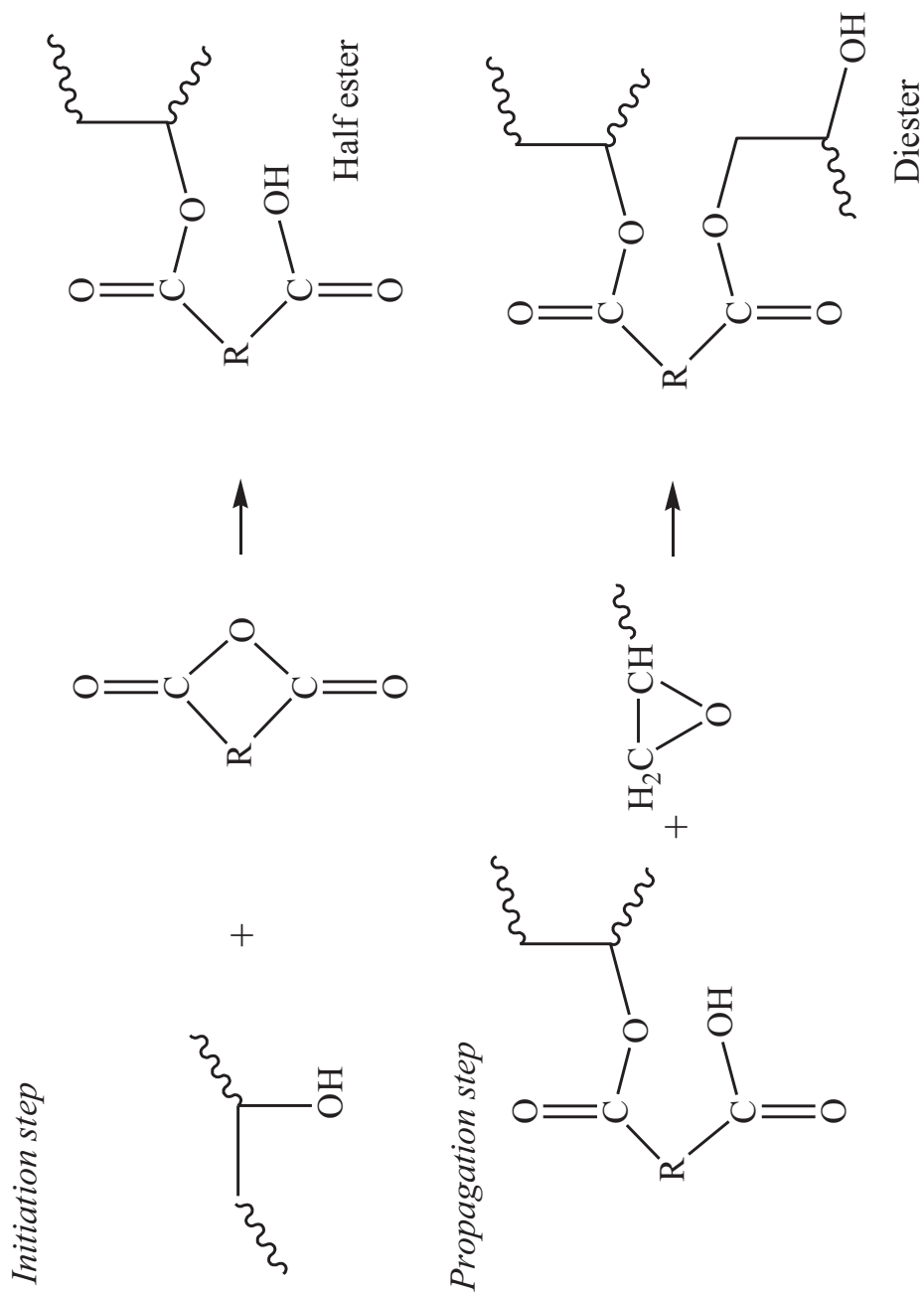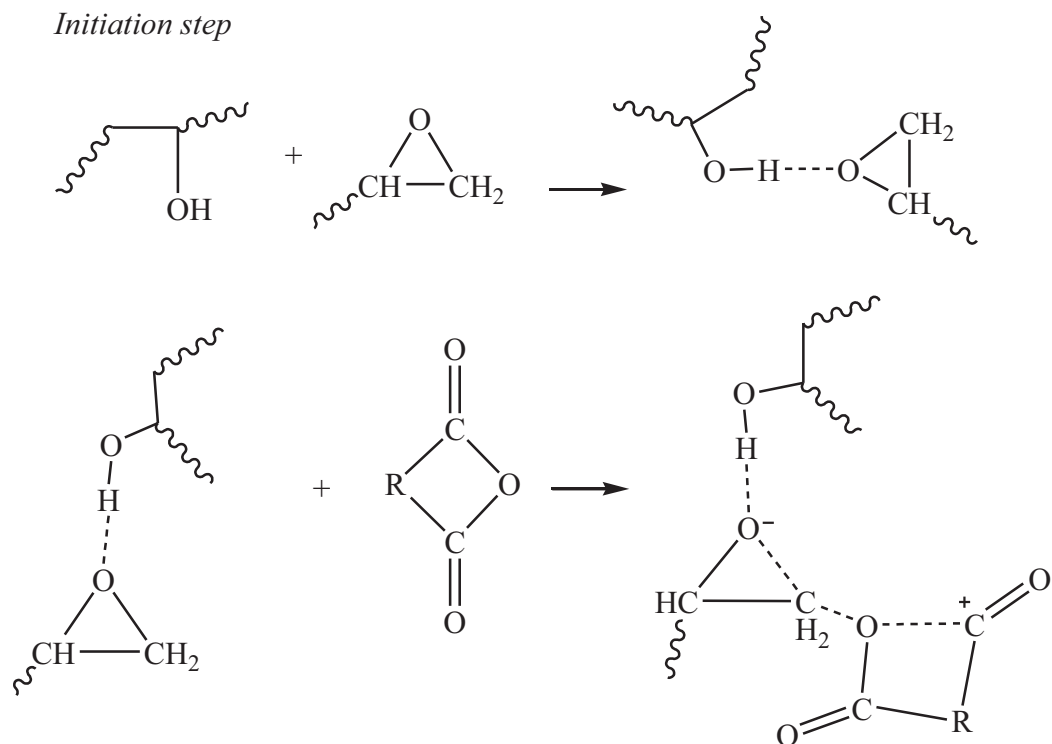*Initiation step:*
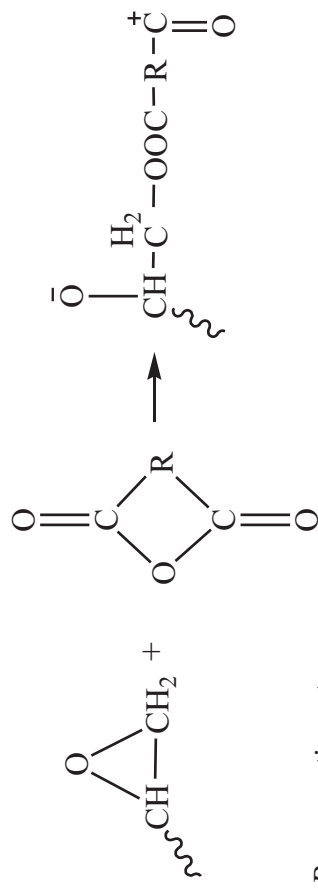
Propagation step:
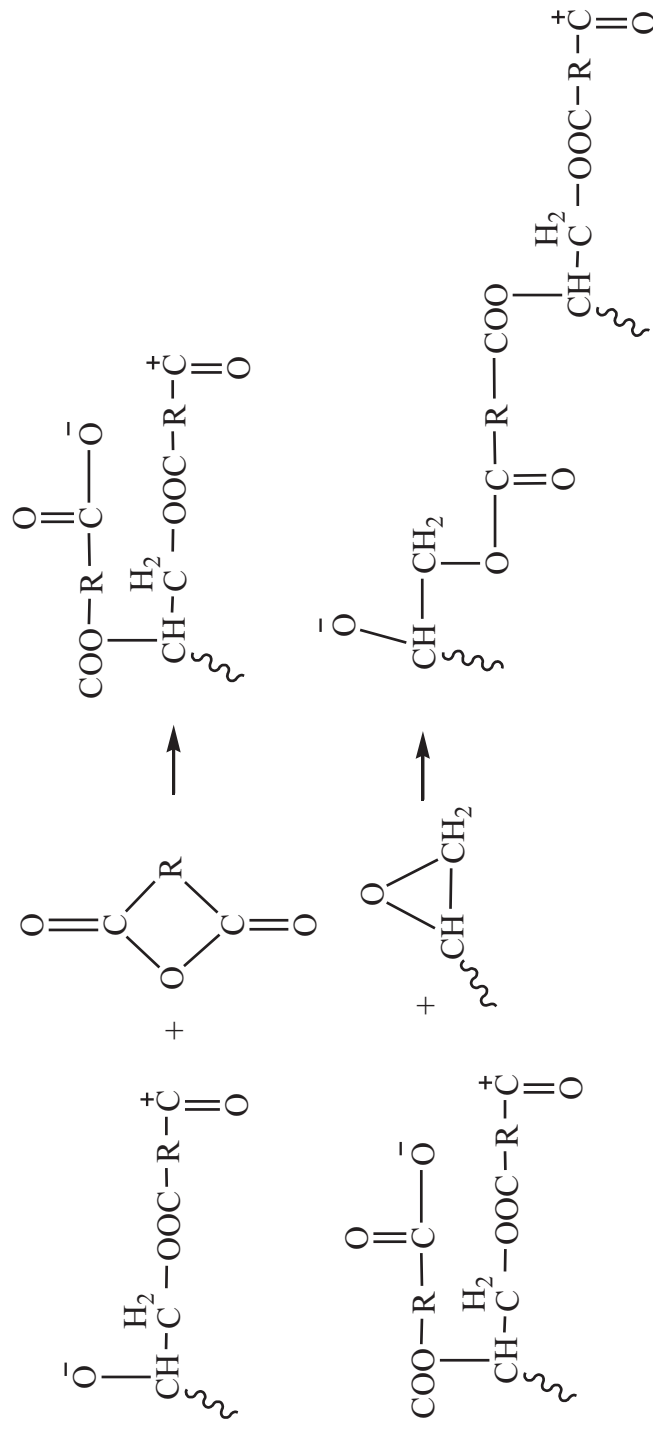
**Scheme 5.1**. Uncatalyzed reaction without hydroxyl groups (**R"**).

Scheme 5.2. Uncatalyzed reaction with a hydroxyl group attacking an anhydride ($\mathbf{R}^{u}_{A,OH}$).

epoxy backbone and it is only the mechanism for the uncatalyzed reaction having a hydroxyl group in the epoxy backbone that attacks an anhydride ($\mathbf{R}_{A,OH}^{u}$). This means that the uncatalyzed reaction with an attachment of a hydroxyl group in the epoxy backbone to another epoxy ring ($\mathbf{R}_{E,OH}^{u}$) has not been examined. In this reaction, the hydroxyl groups attack the epoxy ring to form a hydrogen bonded complex that then reacts with an anhydride similar to the initiation step in $\mathbf{R}^{u}$ (cf. Scheme 5.3). Up to the present time, at least two reactions, $\mathbf{R}^{u}$ and $\mathbf{R}_{E,OH}^{u}$, that might be in the uncatalyzed reaction class are not known.Since uncatalyzed reactions of epoxy resins and anhydrides proceed slowly even at 200^{0}C, the anhydride curing system is often catalyzed by a strong base such as a tertiary amine.[7, 81] Similar to uncatalyzed reactions, the tertiary amine catalyzed reactions are divided into classes with or without hydroxyl groups in the epoxy backbone. Only the catalyzed reactions without hydrogen groups have been mentioned for the anhydride curing systems. These reactions differ in that the tertiary amine catalyst attaches either to the epoxy or to the anhydride moieties in the initiation step.

In $\mathbf{R}_{E}^{c}$, which was suggested by Okaya and Takana,[27] the tertiary amine attacks the epoxide to form a zwitterion which then reacts with an anhydride molecule to form a new zwitterion with an anionic carboxylate group. The carboxylate group then reacts with the epoxide to propagate the reaction (see Scheme 5.4). In $\mathbf{R}_{A,}^{c}$, Fischer[26, 84] proposed that the tertiary amine attacks the anhydride molecule first to form a different type of zwitterion that has a carboxylate group. The carboxylate group then attacks the epoxy ring to form a diester and an oxygen anion which can propagate similar to the uncatalyzed mechanism (see Scheme 5.5).

Initiation step

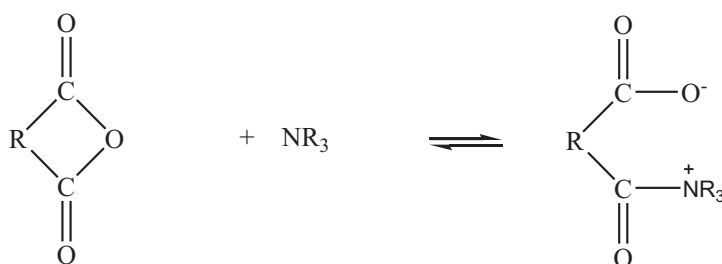

Scheme 5.3. Uncatalyzed reaction with a hydroxyl group attacking an epoxy ($R^u_{E,OH}$).
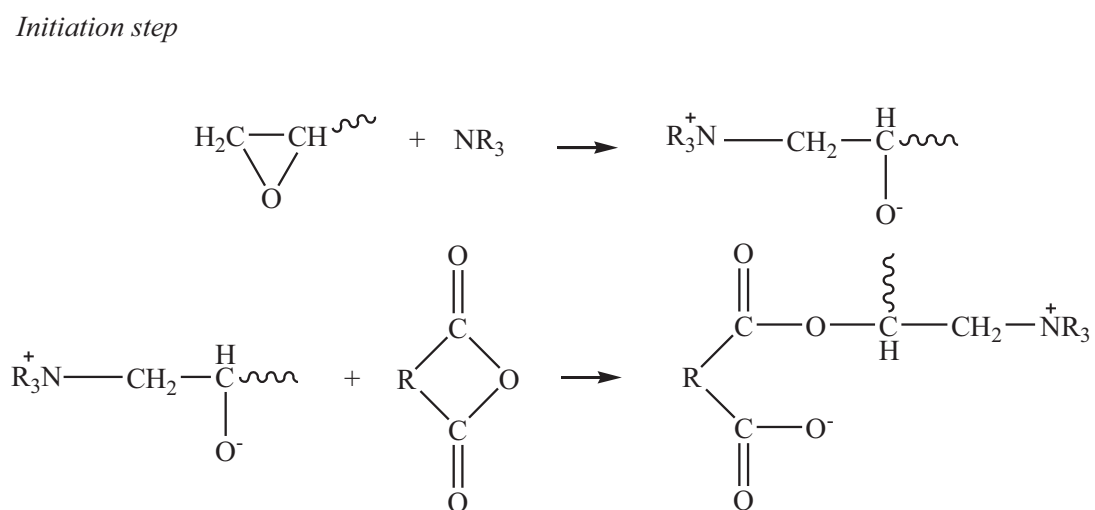
Initiation step

Scheme 5.4. Okaya & Takana's mechanism for a catalyzed reaction in which a tertiary amine attacks the epoxy ($R^c_{E,}$).

Initiation step

Propagation step
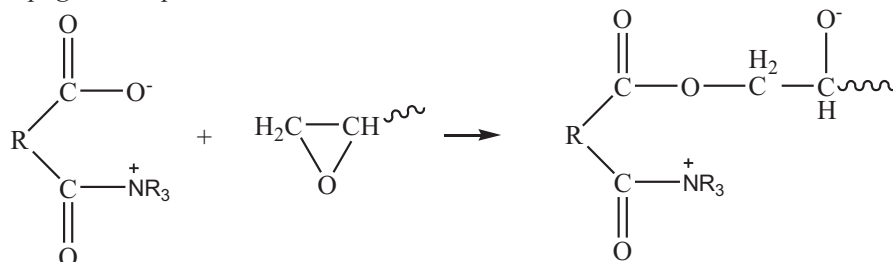
Scheme 5.5. Fischer's mechanism for a catalyzed reaction in which a tertiary amine attacks the anhydride ($\mathbf{R}_{\mathbf{A}}^{\mathbf{c}}$).

Additionally, Sorokin[70, 85] suggested a catalytic mechanism wherein a tertiary amine catalyzes the reaction of a secondary alcohol with the anhydride to form a carboxylic acid, which then follows the same mechanism for acid curing (Scheme 5.6). Note that this secondary alcohol is a co-catalyst with the tertiary amine.

For the tertiary amine catalyzed reactions with a hydroxyl group on the epoxy chain, these cases can be considered as reactions of two catalysts (tertiary amines and hydroxyl groups) and two moieties, epoxy and anhydride. As the initiation of the curing reactions starts from the attack of a tertiary amine (TA) on the epoxy and the anhydride moieties, we have $\mathbf{R}_{\mathbf{TA\text{-}E,OH}}^{\mathbf{c}}$ and $\mathbf{R}_{\mathbf{TA\text{-}A,OH}}^{\mathbf{c}}$ respectively in Schemes 5.7 and 5.8. Note that the hydrogen bonded complex of the epoxy-hydroxyl group is assumed to exist in this case. Similarly, in the initiation step of $\mathbf{R}_{\mathbf{OH\text{-}E,OH}}^{\mathbf{c}}$ and $\mathbf{R}_{\mathbf{OH\text{-}A,OH}}^{\mathbf{c}}$, the hydroxyl group attacks the epoxy ring and

Initiation step
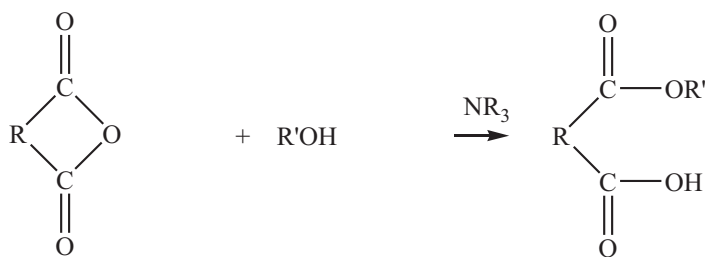
Propagation step
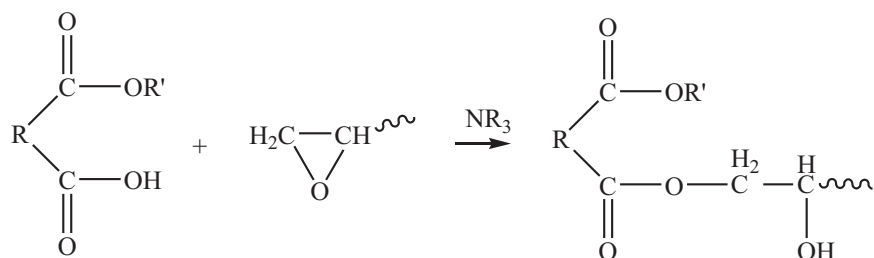
Scheme 5.6. Sorokin's mechanism of catalyzed epoxy-anhydride curing ($\mathbf{R}_{\mathbf{OH\text{-}A,OH}}^{\mathbf{c}}$).

Initiation step
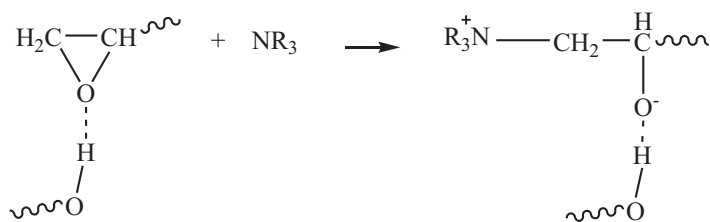
Propagation step
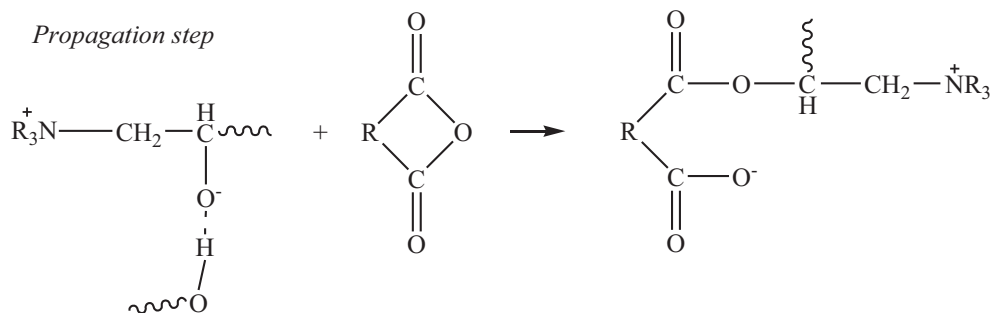
Scheme 5.7. Catalyzed reaction in which a tertiary amine attacks an epoxy with hydroxyl groups in the system ($\mathbf{R}_{\mathbf{TA\text{-}E,OH}}^{\mathbf{c}}$).

Initiation step

Propagation step
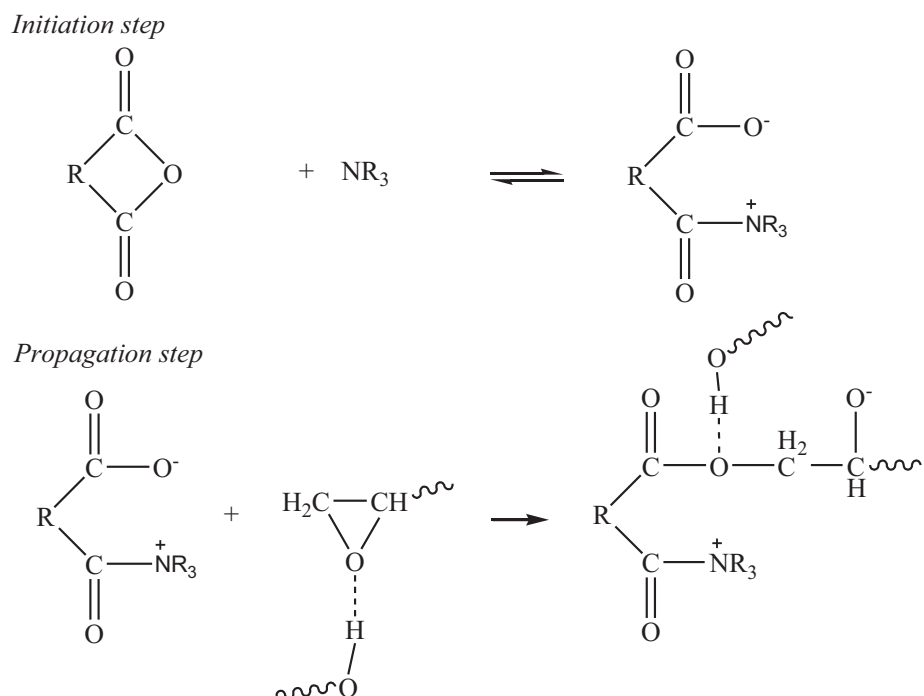
Scheme 5.8. Catalyzed in which a tertiary amine attacks an anhydride with hydroxyl groups in the system ($\mathbf{R^c_{TA\text{-}A,OH}}$).

the anhydride respectively. The former is presented in Scheme 5.9 and the latter is in Scheme 5.6.

Epoxy-anhydride curing reactions face the same difficulties as curings by amines, phenols or acids in that they remain incomplete mechanisms. As these incomplete mechanisms are applied to the kinetic model, they might lead to physically meaningless values. In addition, the currently known mechanisms for a particular epoxy-anhydride curing process cannot be used to extrapolate other curings, making it difficult to improve or design products. Thus, it is necessary to develop a systematic mechanism for the epoxy-anhydride system.

The objective of this study is to have a molecular-modeling mechanism that performs a predictive function for the anhydride curing systems. All possible pathways of these curing systems were examined in both gas and condensed phase during Density Functional

Initiation step
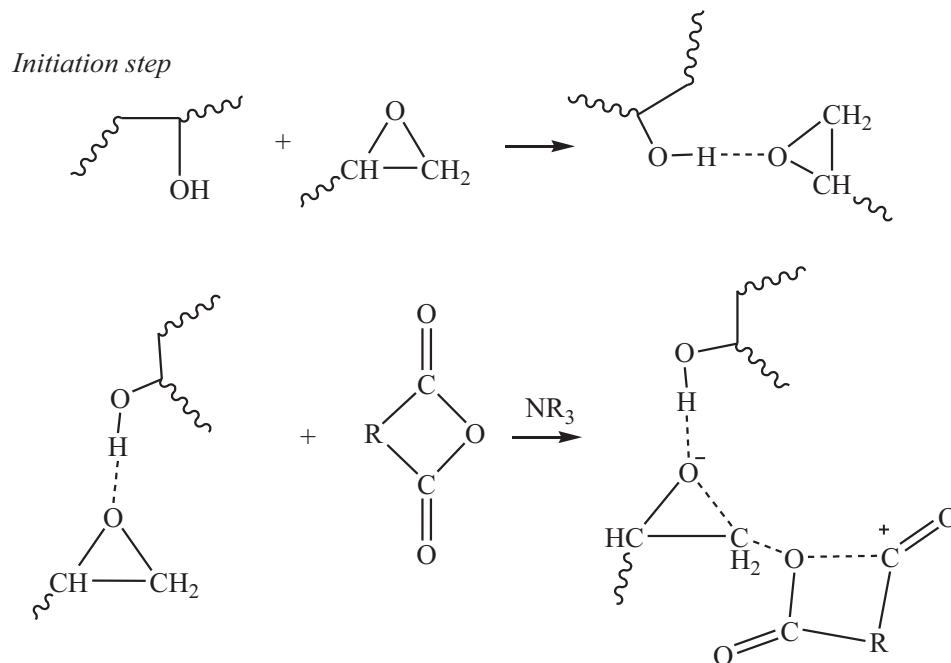
Scheme 5.9. Catalyzed reaction in which a hydroxyl group attacks an epoxy with hydroxyl groups in the system ($\mathbf{R}^{\mathbf{c}}_{\mathbf{OH\text{-}E,OH}}$).

Theory (DFT), and energetic information is used to evaluate competing mechanisms.

5.2   Computational details

5.2.1   Physical models

Commercial epoxies and anhydride curing agents are large and complicated structures. Therefore, it is necessary to choose physical models that can fairly represent these commercial reactants but are small enough to be computationally feasible. Methyl glycidyl ether was chosen to be a model for commercial epoxies. Succinic acid anhydride (SAA) was chosen as an anhydride model, and trimethylamine was chosen for the catalysts. Additionally, 2-propanol represents either a secondary alcohol in the epoxy backbone or an alcohol catalyst.

5.2.2 Computational models

Electronic structure calculations were carried out using the Gaussian 03 program package.[42] A hybrid nonlocal density functional theory B3LYP level of theory[43] with the 6-31G(d, p) basis set was used for locating all stationary points, namely reactants, transition states, intermediates, and products. Stationary points were characterized by normal mode analyses. To confirm the transition state for each reaction pathway, the minimum energy paths (MEPs) from the transition state to both the reactants and products were calculated using the Gonzalez-Schlegel steepest descent path method[44, 45] in mass weight Cartesian coordinates with the step size of 0.01 $(amu)^{1/2}$ Bohr.

Single point solvation calculations were performed with Gaussian 09[77] on the optimized DFT geometries using a polarizable continuum model (PCM)[46, 62] with an acetic acid solvent ($\varepsilon = 6.25$) to mimic the reactions in solutions. It has been shown that solvation free energies obtained from single point PCM calculations with gas phase geometries from DFT calculations are in reasonable agreement with the values from full geometry optimizations.[63, 64] All solvation calculations used the UFF (Universal Force Field) radii model, which places a sphere around each solute atom, with the radii scaled by a factor of 1.1 parameters.

5.3 Results

All possible reactions of the epoxy-anhydride curing as mentioned above were examined in both the gas and condensed phases. Because of the limited ability of Gaussian to mimic the anhydride solution, acetic acid was chosen as the solution for the epoxy-anhydride curing reactions. Single point energy calculations at the optimized structures of all stationary points were done using the polarizable continuum model (PCM). The

activation energies, approximated to be equal to the corrected energy barriers in the condensed phase, are used to compare with experimental data. Both these activation energies and the zero-point energy corrected barriers $\Delta V_a^{\neq G}$ in the gas phase are presented in Table 5.1.

The model system is divided into four main classes, which are: 1) an uncatalyzed reaction without a hydroxyl group in the system, 2) an uncatalyzed reaction with hydroxyl groups 3) a catalyzed reaction without a hydroxyl group and 4) a catalyzed reaction with hydroxyl groups. Note that in our model, hydroxyl groups represent both hydroxyl groups in the epoxy backbone and the alcohol catalyst. In each class, the reaction whose initiation step requires the lowest barrier energy is considered to be the representative reaction for the class.

Table 5.1. Energetic values (kJ/mol) of possible reactions in the anhydride curing systems. (* is noted for propagation steps)

Reaction		$\Delta V_a^{\neq G}$	E_a	Location
1)	Uncatalyzed reaction without a hydroxyl group			
R^u	$E + A \rightarrow [TS]^{\neq} \rightarrow I^u$	291	261	Fig 5.1- T 5.2
2)	Uncatalyzed reaction with a hydroxyl group			
$R^u_{E,OH}$	$E...HOR + A \rightarrow [TS]^{\neq} \rightarrow I^u_{E,OH}$	> 240		
$R^u_{A,OH}$	$A + ROH \rightarrow [TS]^{\neq} \rightarrow I^u_{E,OH}$ (RCOOH)	130	130	Fig 5.2- T 5.1
*	$RCOOH + E \rightarrow [TS]^{\neq} \rightarrow$ Diester	114	112	
3)	Catalyzed reaction without a hydroxyl group			
R^c_E	$E + NR_3 \rightarrow [TS]^{\neq} \rightarrow I^u_{E,OH}$	122		
*	$I^u_{E,OH} + A \rightarrow [TS]^{\neq} \rightarrow P^u_{E,OH}$			No TS
R^c_A	$A + NR_3 + E \rightarrow [TS]^{\neq} \rightarrow I^c_A$	269	262	Fig 5.3- T 5.2
4)	Catalyzed reaction with a hydroxyl group			
$R^c_{TA-E,OH}$	$E...HOR + NR_3 \rightarrow [TS]^{\neq} \rightarrow I^c_A$	64		
*	$I^c_A + A \rightarrow [TS]^{\neq} \rightarrow P^c_A$			No TS
$R^c_{TA-A,OH}$	$(A + NR_3) + E...HOR \rightarrow [TS]^{\neq} \rightarrow I^c_{TA-A,OH}$	216	178	Fig 5.4- T 5.2
$R^c_{OH-E,OH}$	$E...HOR + A \xrightarrow{NR_3} [TS]^{\neq} \rightarrow I^c_{OH-E,OH}$	216	178	Fig 5.4- T 5.2
$R^c_{OH-A,OH}$	$A + ROH \xrightarrow{NR_3} [TS]^{\neq} \rightarrow I^c_{OH-A,OH}$	111	115	Fig 5.5- T 5.1
*	$I^c_{OH-A,OH} + E \xrightarrow{NR_3} [TS]^{\neq} \rightarrow$ Diester	90	79	

5.3.1 Uncatalyzed reactions without a hydroxyl group (R^u)

The transition state for the initiation step (TS^u) is depicted in Figure 5.1. Its parameters and the energy barrier of 291 kJ/mol are shown in Table 5.2.

5.3.2 Uncatalyzed reaction with a hydroxyl group ($R^u_{A,OH}$ and $R^u_{E,OH}$)

Note that the mechanism of the epoxy-anhydride curing in this case can include R^u.

In $R^u_{A,OH}$, Scheme 5.2, 2-propanol (ROH), which represents the secondary alcohol in the
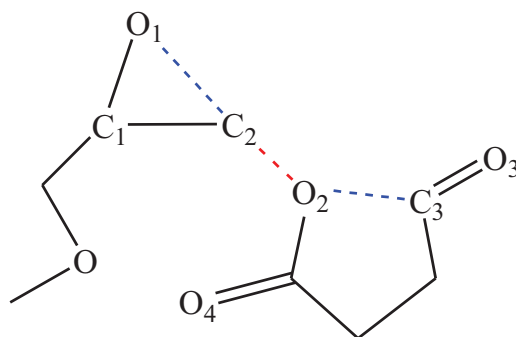
Figure 5.1 Transition state of the initiation step in the R^u.

Table 5.2. Parameters of the TS^u in Figure 5.1, TS^c_A in Figure 5.3, and $TS^c_{TA-A,OH}$/ $TS^c_{OH-E,OH}$ in Figure 5.4.

Parameters	TS^u	TS^c_A	$TS^c_{TA-A,OH}$
$v^{\neq}$ ($i \cdot cm^{-1}$)	376	396	384
d(H1-O1) (Å)			1.636
d(O1-C1) (Å)	1.330	1.381	1.383
d(C1-C2) (Å)	1.511	1.470	1.490
d(O1-C2) (Å)	2.210	2.136	2.022
d(C2-O2) (Å)	1.625	2.157	1.826
d(O2-C3) (Å)	1.356	1.307	1.316
d(O2-C4) (Å)	1.924	2.193	1.217
d(C4-N) (Å)		1.617	1.641
$\angle$ (O1-C1-C2) (deg)	101.91	97.02	89.39
$\angle$ (C1-C2-O2) (deg)	111.76	43.31	117.60
$\angle$ (C3-O2-C4-O4) (deg)	-133	92.39	123.78
$\Delta V_a^{\neq G}$ (kJ/mol)	291	269	216
E_a (kJ/mol)	261	262	178

epoxy backbone, attacks SAA to form a half ester. In the transition state of the initiation step, the breaking C2-O1 bond in SAA is lengthened to 2.084 Å, the forming bond of hydrogen H1 of the hydroxyl group and the ether oxygen O1 of SAA is shortened to 1.451 Å, and the forming C2-O2 bond in the ester group is 1.712 Å (Figure 5.2- Table 5.3). The formation of a half ester is revealed by the imaginary vibration of -484 cm^{-1}, and its energy barrier is 130 kJ/mol.

This half ester possesses a carboxyl group that exhibits an attachment to an epoxy to form a diester. This step is the same as that for the uncatalyzed reaction in the epoxy-acid curing. That is, it was examined as the self-promoted catalyzed pathway of acid curing systems and its energy barrier is 114 kJ/mol in the model study.

In the attachment of a hydroxyl group to an epoxy of $\mathbf{R}^{u}_{E,OH}$, Scheme 5.3, the binding energy of the hydrogen bonding complex is -27 kJ/mol and the length of the hydrogen bond formed between the hydrogen of the hydroxyl group and the epoxy oxygen is 1.94 Å. The transition state of the reaction between this hydrogen bonded complex and an anhydride ($\mathrm{TS}^{u}_{E,OH}$) is not converted in the DFT calculation.
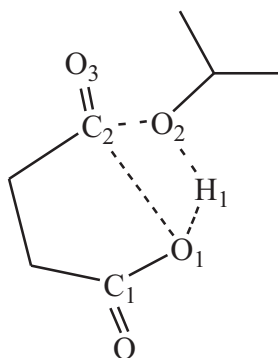
Figure 5.2. The transition state of the initiation step in $\mathbf{R}^{u}_{A,OH}$.

Table 5.3. Parameters of transition state geometries in the initiation step of $R^u_{A,OH}$ and $R^c_{OH-A,OH}$.

Parameters	$TS^u_{A,OH}$	$TS^c_{OH-A,OH}$
Catalyst	-	NR_3
$v^{\neq}$ ($i \cdot cm^{-1}$)	484	455
d(O1-C2) (Å)	2.084	2.158
d(H1-O1) (Å)	1.451	1.531
d(H1-O2) (Å)	1.053	1.045
d(O2-C2) (Å)	1.712	1.613
d(H1-N) (Å)		2.609
$\angle$ (C1-O1-C2-O3) (deg)	-50.85	-46.03
$\Delta V^{\neq G}_a$ (kJ/mol)	130	111
E_a (kJ/mol)	130	115

In the epoxy-phenol and epoxy-carboxylic acid curing reactions, the hydrogen bond between the acidic hydrogen and the epoxy oxygen atoms accounts for an average decrease of the energy barriers by 56 and 51 kJ/mol, respectively. Compared to phenol and acid curing agents, hydroxyl groups in the epoxy backbone might be more sterically able to reach the epoxy and form a hydrogen bonded complex. Thus, the hydrogen bond between a hydroxyl group on the epoxy backbone and an epoxy, which is the difference of the transition state in $\mathbf{R}^u$ and $\mathbf{R}^u_{E,OH}$, might decrease the energy barrier by less than these values. Consequently, the energy barrier of the $TS^u_{E,OH}$ might be larger than 240 kJ/mol, compared to a 291 kJ/mol energy barrier of TS^u. Comparing $\mathbf{R}^u_{A,OH}$ and $\mathbf{R}^u_{E,OH}$ in the initiation step, $\mathbf{R}^u_{A,OH}$ is preferred because of its lower energy barrier, and thus it dominates the uncatalyzed reactions with a hydrogen group in the system.

5.3.3   Catalyzed reactions

5.3.3.1   Catalyzed reactions without a hydroxyl group

in the system ($\mathbf{R}_E^c$ and $\mathbf{R}_A^c$)

In the initiation step of $\mathbf{R}_E^c$, Scheme 5.4, the tertiary amine attacks the epoxy to form a zwitterion that was calculated in both the epoxy-phenol and the epoxy-acid curing systems as encountering an energy barrier of 122 kJ/mol in the gas phase. The intermediate zwitterion is unstable in the gas phase but stable in the condensed phase. For instance, in acetic acid solution the energy barrier is 76 kJ/mol and the enthalpy of reaction is 64 kJ/mol at 0 K. The transition state in the propagation step is not found by DFT calculation in the gas phase, however, it might exist in the condensed phase.

In the initiation step of $\mathbf{R}_A^c$, Scheme 5.5, the tertiary amine attacks the anhydride to form an internal salt. In the propagation step, the carboxylate anion reacts with the epoxy group, generating an alkoxide. The alkoxide then further reacts with another anhydride, propagating the cycle by generating another carboxylate which reacts with another epoxy group. The end product is the formation of polyester-type linkages.[7] In our calculation, the transition states performing the initiation and propagation steps do not occur separately as shown in Scheme 5.5 but simultaneously. The energy barrier of this reaction is 269 kJ/mol (see Figure 5.3 and Table 5.2).

In the curing process, which is catalyzed by a tertiary amine and does not contain a hydroxyl group in the epoxy backbone, the energy barrier of $\mathbf{R}_E^c$ is smaller than that of $\mathbf{R}_A^c$ by 147 kJ/mol. Thus, $\mathbf{R}_E^c$ dominates the curing and, consequently, its energy barrier of 122 kJ/mol should be chosen to be the energy barrier for this curing class. However, since the
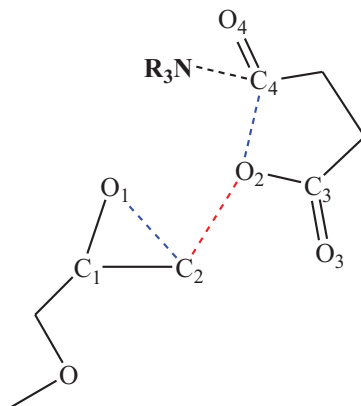
Figure 5.3. The transition state of the $\mathbf{R}_A^c$.

product of the initiation step in $\mathbf{R}_E^c$ is unstable and the fact that the transition state of the

propagation step could not be found in our calculations, $\mathbf{R}_E^c$ cannot be chosen to be a

representative reaction. Thus, the curing prefers to happen via $\mathbf{R}_A^c$ instead of $\mathbf{R}_E^c$. That

means if there is no hydroxyl group in the epoxy backbone, the attachment of the tertiary

amine catalyst on the anhydride, as well as attack of this anhydride to the epoxy ring, happen

at the same time, and the energy barrier is 269 kJ/mol.

5.3.3.2   Catalyzed reactions with a hydroxyl

 group in the epoxy backbone

Note that the epoxy-alcohol complex is assumed to exist in this case. The initiation

step for $\mathbf{R}_{TA\text{-}E,OH}^c$ is the reaction of an epoxy-alcohol complex and a tertiary amine to form

an intermediate zwitterion. This zwitterion is unstable in the gas phase but stable in the

condensed phase, similar to the zwitterions in $\mathbf{R}_E^c$. The energy barriers are 62 kJ/mol and 51

kJ/mol, respectively, in the gas and condensed phases. However, the transition state of the

propagation step is not found in the DFT calculation.

In $\mathbf{R}_{TA\text{-}A,OH}^c$, the initiation and propagation steps occur simultaneously in our result

and require an energy barrier of 216 kJ/mol (see Figure 5.4 and Table 5.2).

In $R^c_{OH-E,OH}$, the attachment of an alcohol on the epoxy forms a hydrogen bonded complex and the reaction of the hydrogen bonded complex with an anhydride occurs simultaneously as same as in the $R^c_{TA-A,OH}$, illustrated in Figure 5.4 and Table 5.2.

In $R^c_{OH-A,OH}$, the initiation step is a reaction of 2-propanol and SAA that is catalyzed by trimethylamine and requires an energy barrier of 111 kJ/mol. Its transition state is depicted in Figure 5.5 and Table 5.3. The product of this reaction, a half ester, possesses a carboxylic acid group that then cures an epoxy to form a diester in the propagation step. This step is the same as the tertiary amine catalyzed epoxy-acid curing reaction that requires an energy barrier of 79 kJ/mol.

In the system involving the hydroxyl group either in the epoxy backbone or from the co-catalyst with a tertiary amine, the $R^c_{OH-E,OH}$ is most favorable among $R^c_{TA-E,OH}$, $R^c_{TA-A,OH}$, $R^c_{OH-E,OH}$ and $R^c_{OH-A,OH}$ because it involves the smallest energy barrier in the initiation step. However, the product of its initiation step is unstable and the transition state of the propagation step has not been found. The $R^c_{OH-A,OH}$ process dominates the curing instead of $R^c_{OH-E,OH}$, resulting in the energy barrier of 111 kJ/mol in the gas phase.

5.4   Discussion and validation

Table 5.1 summarizes all energetic values of the possible reactions in the anhydride curing systems in both gas and condensed phases. In the uncatalyzed reaction, when the epoxy resins do not have any hydroxyl group in the backbone, the curing of epoxy and anhydride requires 291 kJ/mol (R'') in the gas phase. In case the epoxy resins contain
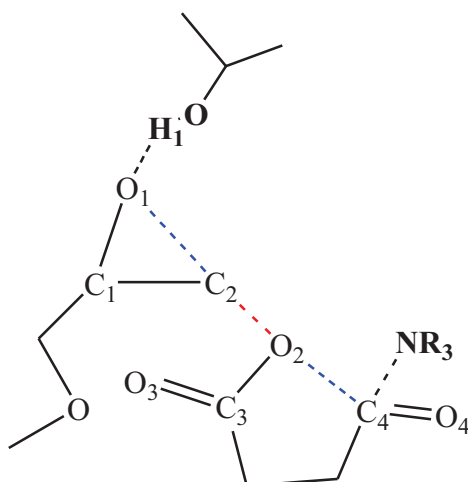
Figure 5.4. The transition state of $R^c_{TA-A,OH}$.
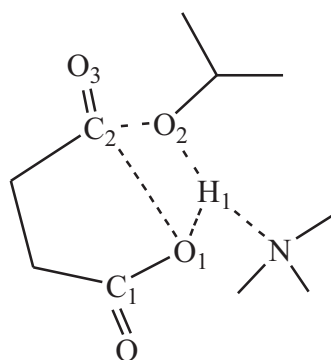
Figure 5.5. The transition state of the $R^c_{OH-A,OH}$.

hydroxyl groups, the initiation step of the curing reaction preferably happens via the attack

of these hydroxyl groups to open the anhydride ring at the energy barrier of 130 kJ/mol

($R^u_{A,OH}$). However, the curing might still be slow because of the difficulty of arranging the

hydroxyl group in the epoxy backbone to attach to the anhydride to form a half ester.

In the reaction catalyzed by a tertiary amine, when the epoxy resins do not have any

hydroxyl group in the backbone, the curing between the epoxy and anhydride is accelerated

by the attachment of a tertiary amine catalyst to the anhydride that happens simultaneously

with the curing. The energy barrier of this curing is 269 kJ/mol (R^c_A). In case the epoxy

resins contain hydroxyl groups or the system is added to an alcohol co-catalyst with tertiary

amine, the anhydride is first attacked by the hydroxyl group and the energy barrier lowers to 111 kJ/mol and ($\mathbf{R}^{c}_{OH-A,OH}$).

The priority curing of the epoxy-anhydride systems follows the order: $\mathbf{R}^{u} < \mathbf{R}^{c}_{A} < \mathbf{R}^{u}_{A,OH} < \mathbf{R}^{c}_{OH-A,OH}$, which is opposite of their energy barriers in both gas and condensed phases. This indicates that the hydroxyl group might be more crucial than the tertiary amine catalyst for accelerating the curing of the epoxy by anhydride. With or without a tertiary amine catalyst, the energy barrier of the system containing hydroxyl groups in the epoxy backbone decreases the energy barrier of the system without hydroxyl groups by more than half. Meanwhile, the tertiary amine catalytic role decreases the energy barrier by 25 kJ/mol on average (comparing $\mathbf{R}^{u}$ to $\mathbf{R}^{c}_{A}$ and comparing $\mathbf{R}^{u}_{A,OH}$ to $\mathbf{R}^{c}_{OH-A,OH}$).

As hydroxyl groups originate only from the epoxy backbone, even though the energy barrier is decreased by half, the curing might still consume more energy in bringing about a rearranggament the hydroxyl groups to reach and attack the anhydride. Therefore, the epoxy-anhydride curing might need alcohol which is a co-catalyst of the tertiary amine.

In some previous studies, an alcohol together with or without added acid was used as a co-catalyst with a tertiary amine.[81, 86-88] In Peyser and Bascom's study of diglycidyl ether bisphenol A (DGEBA) and hexahydrophthalic anhydride (HHPA) catalyzed by N,N'-dimethylbenzylamine (BDMA), acid and alcohol,[86] the activation energy of this curing is 104.60 kJ/mol. The kinetics of the curing reaction for a system of o-cresol formaldehyde epoxy resin/succinic anhydride (SA) and BDMA as a catalyst was investigated with a differential scanning calorimeter.[89] Among experimental materials of this study, ethyl alcohol was listed but was not mentioned to be a co-catalyst with the tertiary amine. This system required the activation energy of 109 kJ/mol for the initiation step. Thus, those

values agreed well with the activation energy of 115 kJ/mol in our model study of the tertiary amine catalyzed reaction that contained hydroxyl groups either in the epoxy backbone or from an alcohol co-catalyst.

Although not mentioned as using a co-catalyst, some experimental studies showed activation energies that were within an order of magnitude of our results. The activation energy of the curing between DGEBA and HHPA at 125^0C with a catalyst is 92 kJ/mol.[7] With the BDMA catalyst, the activation energy of the DGEBA and meleic anhydride (MA) curing is 60.16-87.80 kJ/mol, that of the DGEBA and methyl tetrahydrophthalic anhydride (MTHPA) curing is 78.93 kJ/mol at 110^0C in Sun and co-author's study,[90] and the corresponding value of isophthalic diglycidyl ester (IPDGE) and HHPA curing is 68.9-75.2 kJ/mol in Khanna and Chanda's study. [91] Thus, these values demonstrate that our mechanism model is comparable with experience.

5.5 Conclusions

In this study, an epoxy-anhydride model system was examined through four classes of reactions. They are tertiary amine uncatalyzed and catalyzed reactions with or without hydroxyl groups in the system. Hydroxyl groups are not distinguished whether they are on the epoxy backbone or in an alcohol catalyst. The results show that with and without a tertiary amine catalyst, the energy barriers of the curing system without a hydroxyl group are as high as 269 kJ/mol and 291 kJ/mol respectively. In the curing systems with or without a tertiary amine catalyst, the hydroxyl group accounts for a decrease in the energy barrier by more than half, to 111 kJ/mol and 130 kJ/mol in the gas phase. The result in the condensed phase is similar to that in the gas phase.

Alcohol is suggested to be a co-catalyst with tertiary amine, decreasing the energy barriers in the initiation step of the epoxy-anhydride curing. The role of tertiary amine is recognized to lead to an acceleration of the initiation step of the anhydride opening of a hydroxyl group either in an epoxy backbone or from an alcohol catalyst. Additionally, the tertiary amine is a catalyst for the propagation step of the epoxy-acid curing. Thus, tertiary amine in the anhydride curing systems is reformed.

CHAPTER 6

FIRST-PRINCIPLES BASED KINETIC MODEL FOR THE

EPOXY-AMINE CURING REACTION

6.1   Introduction

A fundamental understanding of the mechanisms and kinetics of epoxy-amine curing reactions is crucial for its use in functional-design of new polymer materials for composites, adhesives, lacquers, coatings, paints, and electronic-related products[3, 92, 93].   Despite numerous studies since the pioneering work of Shechter[10] and Smith[12], detailed knowledge of the mechanism of such reaction is far from complete. Existing kinetic models of epoxy-amine reactions nearly all rely on experimental thermometric measurements of the whole process and fitting proposed mechanisms to experimental results.[13-18, 35, 94, 95] From these studies, one could only speculate on the nature of the transition states or important reaction pathways, and a number of such speculations have been found to be incorrect or contradictory.

It is well accepted that the general amine curing reaction occurs via a nucleophilic attack of the amine nitrogen atom on the terminal carbon atom of the epoxy function. The mechanism has been known to be a S_N2-type II and thus the reaction rate obeys second-order kinetics as shown in Scheme 6.1.[8] The reaction may involve both primary and secondary amines as well as hydrogen bonding catalysts and promoters which can be shown to have a considerable effect on the energy barrier of the curing reactions.[8]
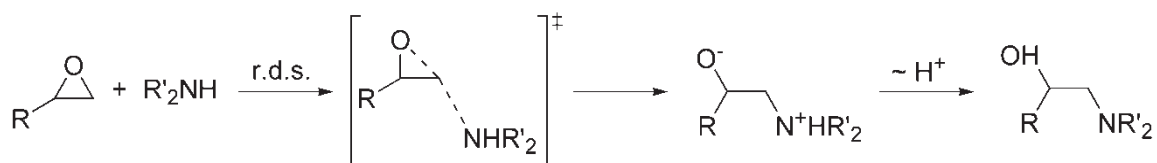
Scheme 6.1. General mechanism for epoxy-amine curing

A number of possible reaction pathways that probably occur during the curing process have been suggested and evaluated according to their importance by Chapman and his coworkers since 1959.[96] They were known to be catalyzed by hydroxyl groups[10] or by catalytic impurities.[12] Mijovic and coworkers[13] suggested a possible concerted mechanism that involves acyclic hydrogen bonded complexes with amine molecules. Three different types of hydrogen bonded complexes were suggested, i.e., epoxy-amine, epoxy-hydroxyl and amine-hydroxyl. However, only the epoxy-hydroxyl complexes were used in actual kinetic modeling, such as in the recent Riccardi,[14] Blanco[15] and Mounif[16] models. These models have been used, refined or slightly altered or extended, especially the Horie's model.[8, 15, 97] Other approaches were also employed,[98] particularly using kinetic modeling combined with experimental measurements. In such cases, a kinetic model was used involving a set of elementary reactions whose rate parameters were determined by fitting to experimental data from rate equation thermometric measurements conducted with the aid of differential scanning calorimetry (DSC).[19, 20] It is important to point out that such fitting does not guarantee that the kinetic and/or thermodynamic parameters are physically realistic. For example, the fitting for the hydrogen bonded complex formation between an epoxy and a hydroxyl group in Blanco et al. kinetic model leads to an activation energy of 58.2 kJ.mol^{-1}. Meanwhile, the hydrogen bonded complex formation is known to have an activation energy of less than 5 kJ.mol^{-1} because of the loss of the reactant translational and rotational motions upon forming the complex. Although the existing kinetic models were shown to fit well with

experimental results in the individual epoxy-amine reaction, they still have two main problems, specifically: 1) there is no guarantee for the completeness of the mechanism and 2) kinetic and thermodynamic properties were used as adjustable parameters and thus they can hide the incompleteness of the mechanism. These models have had limited success to date and cannot be extrapolated to new initial reaction conditions. More importantly, they do not have predictive and functional-design capabilities.

The primary objective of this study is to develop and validate a detailed kinetic model for the epoxy curing process by amines derived from first principles quantum chemistry calculations. For simplicity in the discussion below, we label this kinetic model as the Pham-Truong (PT) model. The PT kinetic model is constructed from quantum chemistry calculations of different possible reaction pathways that can take place in the epoxy-amine curing process. Validation is performed by direct comparisons with experimental observations with simulations of conversion versus time profiles. This is the first step in achieving the long-term vision, namely the predictive and functional-design capabilities for the epoxy curing process with the goal of creating a computational workflow that can bridge first-principles quantum chemistry calculations to simulations of macroscopic polymer properties. Such a workflow would enable a bench chemist to pose a question: 'if we use this particular curing agent, or epoxy resin, or change the reaction condition, what would the mechanical properties of the resulting polymer be?'

6.2 Pham-Truong (PT) kinetic model development

6.2.1 Reaction mechanism

From quantum chemistry calculations in a previous study of our group,[8] we found that the epoxy-amine curing process can proceed via three separate pathways: 1) uncatalyze;

2) amine-self promoted and 3) alcohol-accelerated pathways and these can be illustrated in Scheme 6.2 for the initial stage of the polymerization process.

The above scheme helps to elucidate the relative importance of the different pathways. First, from quantum chemistry calculations, the NH group from the amine or OH group from the product or added accelerator can stabilize the transition state and thus lowers the reaction barrier. This is consistent with the well-known practice of adding a small amount of alcohol as an accelerator for speeding up the curing process. However, it is important to point out that although the activation energies for both the alcohol-accelerated and the self-promoted reactions are lower than that of the uncatalyzed pathway, the formation constants K_c for the hydrogen precursor complexes for these pathways must also be taken into account. For instance, complex HB_RNH$_2$-E, which leads to the transition state complex TS_RNH$_2$-E-H$_2$NR is less likely to form than complex HB_ROH-E by almost two orders of magnitude (estimated from the difference in the calculated binding energies from our quantum chemistry calculations).[8] From these arguments, it is possible that the
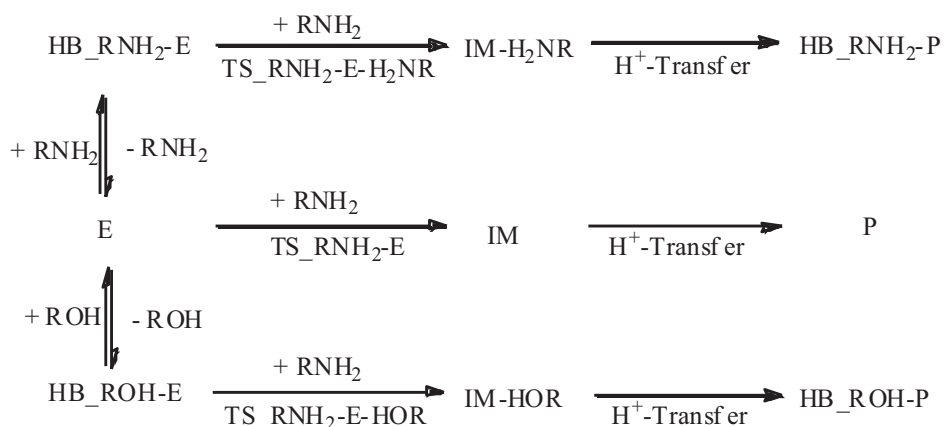
Scheme 6.2. Schematic illustration of the mechanism of the initial stage of the epoxy-amine polymerization.

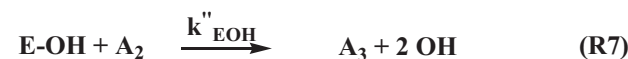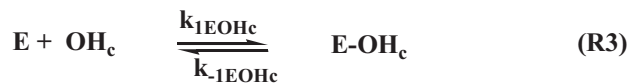uncatalyzed pathway (via TS_RNH$_2$-E) and the self-promoted pathway (the top pathway on Scheme 6.2) are competing in the absence of any added alcohol accelerators. Meanwhile the alcohol-accelerated pathway (the bottom pathway on Scheme 6.2) is supposed to be the most probable pathway whenever an external alcohol is added or the product alcohol species can participate in the reaction. Detailed analysis of the results from kinetic modeling will help to confirm this hypothesis.

From the above scheme, the mechanism of the epoxy-amine curing process can be written as below (Scheme 6.3). E denotes the epoxy group, OH denotes the hydroxyl groups of the epoxy chain and OH$_c$ denotes the externally added alcohol. E-OH represents a complex between the epoxy and the hydroxyl groups of the epoxy chain and E-OH$_c$ represents the complex between the epoxy and the alcohol. E-A represents the complex between the epoxy and the amine and A$_1$, A$_2$, and A$_3$ represent primary, secondary and tertiary amines, respectively.

The first three reactions are hydrogen bonded complex formations with 1) the epoxy-OH group adjacent to the oxygen atom of the epoxy group; 2) the primary amine curing agent; and 3) the epoxy-OH of the external alcohol accelerator, respectively. The fourth and fifth reactions are the uncatalyzed epoxy curings by primary and secondary amines, respectively. The sixth and seventh reactions are the alcohol-accelerated reactions via the epoxy-alcohol hydrogen bond complex with primary and secondary amines, respectively. The eighth and ninth are the self-promoted epoxy curings by primary and secondary amines, respectively. The last two, involving external alcohol-accelerated reactions, were added to distinguish from reactions involving epoxy OH groups. We found that it was necessary necessary to distinguish the epoxy OH groups from those with the

$$E + OH \xrightleftharpoons[k_{-1EOH}]{k_{1EOH}} E\text{-}OH \qquad (R1)$$

$$E + A_1 \xrightleftharpoons[k_{-1EA}]{k_{1EA}} E\text{-}A_1 \qquad (R2)$$

$$E + OH_c \xrightleftharpoons[k_{-1EOHc}]{k_{1EOHc}} E\text{-}OH_c \qquad (R3)$$

$$E + A_1 \xrightarrow{k_1} A_2 + OH \qquad (R4)$$

$$E + A_2 \xrightarrow{k_2} A_3 + OH \qquad (R5)$$

$$E\text{-}OH + A_1 \xrightarrow{k'_{EOH}} A_2 + 2\,OH \qquad (R6)$$

$$E\text{-}OH + A_2 \xrightarrow{k''_{EOH}} A_3 + 2\,OH \qquad (R7)$$

$$E\text{-}A_1 + A_1 \xrightarrow{k'_{EA}} A_2 + OH + A_1 \qquad (R8)$$

$$E\text{-}A_1 + A_2 \xrightarrow{k''_{EA}} A_3 + OH + A_1 \qquad (R9)$$

$$E\text{-}OH_c + A_1 \xrightarrow{k'_{EOHc}} A_2 + OH + OH_c \qquad (R10)$$

$$E\text{-}OH_c + A_2 \xrightarrow{k''_{EOHc}} A_3 + OH + OH_c \qquad (R11)$$
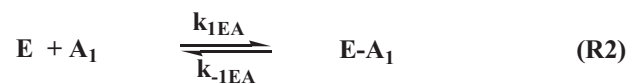
Scheme 6.3. Mechanism of the epoxy-amine curing process with specific denoted rate constants

externally added accelerators. The external alcohol is often smaller in size compared to the epoxy species so its OH group would be able to get closer to the epoxy oxygen atom than the OH in the epoxy chain. Thus, this would lead to optimal stabilization effects. Meanwhile the OH groups of the epoxy require additional energy for rearrangement to have configurations for hydrogen-bond complex formation and thus would not be able to get close to the oxygen atom of the epoxy for favorable hydrogen-bond interaction. For this reason, one expects the activation energy for R10 to be lower than that of R6.

6.2.2 Computational detail

6.2.2.1 Reaction model

For the first three reactions, the simplest reactants of epoxy, amine and alcohol were used to model hydrogen bond complex formations reactions. We used ethylene oxide to model epoxy, methylamine for primary amine, and methanol for alcohol. The structures are shown in Figure 6.1.

For the remaining reactions (R4-R11), complex reactants of epoxy and amine were used to facilitate comparison with available experimental data. In particular, we used methyl glycidyl ether to model epoxy, aniline for primary amine, and methyl aniline for secondary amine. The structures are shown in Figure 6.2.

All electronic structure calculations were carried out using the Gaussian 03 program package.[42] A hybrid nonlocal density functional theory B3LYP level of theory[43] with the 6-31G(d,p) basis set has been used for locating all stationary points, namely for reactants, transition states, intermediates, and products. Normal analyses were performed to verify the nature of these stationary points. To confirm the transition state for each reaction pathway,
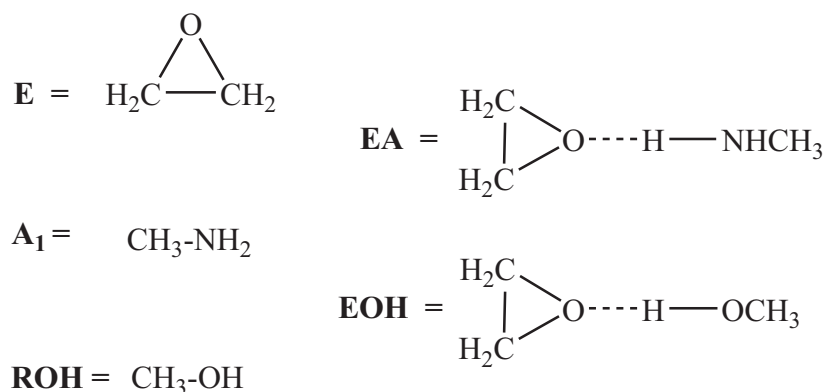

Figure 6.1. Structures of reactants and products were used to model the hydrogen bond complex formation reactions (R1-R3)
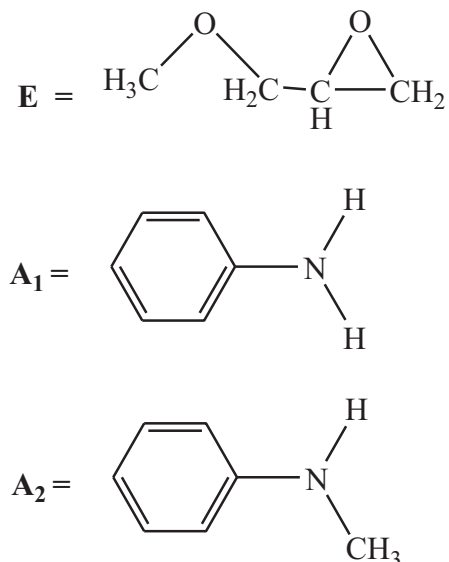
Figure 6.2. Structures of reactants are used to model R4-R11 reactions

the minimum energy paths (MEPs) from the transition state to both the reactants and products was calculated using the Gonzalez-Schlegel steepest descent path method[45] in mass weight Cartesian coordinates with the step size of 0.01 $(amu)^{1/2}$ Bohr.

6.2.2.2 Calculation of kinetic rate parameters

To determine the kinetic parameters of the PT models, we have performed first-principles calculations using the transition state theory with potential energy surface information taken from accurate quantum chemistry calculations for a model system. Note that the use of the model system is necessary to make the quantum chemistry calculations feasible. The thermal rate constants for the R1-R9 reactions were carried out at the transition state theory (TST) level with the TheRate program, employing the kinetic module of the web-based Computational Science and Engineering Online (CSE-Online) environment.[99] These values of the rate constants are expressed as a function of temperature in terms of an Arrhenius equation (6.1)

$$\ln k = \ln A - (\frac{E_a}{R})(\frac{1}{T}) \tag{6.1}$$

Since quantum chemistry calculations cannot precisely predict condensed phase effects by using a dielectric continuum model, specific hydrogen bond interactions beyond those explicitly considered in the model are approximated. In addition, the uncertainty for quantum chemistry calculations is on the order of 5-8 kJ/mol for hydrogen bond energies and of 15-35 kJ/mol for activation energies. To correct for these deficiencies in the modeling, we adjusted three activation energies to get better agreement with experimental observations. In particular, the reverse barrier for the hydrogen-bond complex formation between the epoxy and the OH group (the reverse direction of R1) is increased by 8 kJ/mol and that of epoxy and the amine group (the reverse direction of R2) is increased by 1.45 kJ/mol. The activation energy of the alcohol-accelerated reaction (R6) is lowered by 33.70 kJ/mol from quantum chemistry results. These adjustments are within the uncertainty of the calculations. The other parameters are shifted relatively using results from our quantum chemistry calculations.

6.2.3 Chemical kinetic simulations

From Scheme 6.3, the general equation for the rate of disappearance of epoxy groups can be written:

$$-\frac{d[E]}{dt} = k_{1\,EOH}[E][OH] - k_{-1\,EOH}[E\text{-}OH] + k_{1\,EA}[E][A_1] - k_{-1\,EA}[E\text{-}A_1]$$
$$+ k_{1\,EOH_c}[E][OH_c] - k_{-1\,EOH_c}[E\text{-}OH_c] + k_1[E][A_1] + k_2[E][A_2] \tag{6.2}$$

Let x be the epoxy conversion and [E], [OH], [OH$_c$], [E-OH], [E-OH$_c$], [E-A$_1$], [A$_1$], [A$_2$] and [A$_3$] are the corresponding molar concentrations of the different groups, made dimensionless by dividing by the initial molar concentration of epoxy groups ([E]$_0$). The conversion at any time t is calculated as:

$$x = 1 - [E]_t - [E\text{-}OH]_t - [E\text{-}OH_c]_t - [E\text{-}A_1]_t \tag{6.3}$$

The Chemical Kinetic Simulator (CKS) program[100] was used to simulate the time conversion profiles at different isothermal and dynamic conditions that mimic differential scanning calorimetry (DSC) experiments.

6.3   Validation

To validate the PT model, a number of chemical kinetics simulations were performed using the same reaction conditions of some recently available experimental data. One set of experimental data is from the study of Blanco, Corcuera, Riccardi and Mondragon,[15] denoted in this report as the BCRM model. BCRM data apply for the case in which no alcohol accelerator is added. The other set is from the work of Perrin, Nguyen, and Vernet,[17, 18, 95] denoted in this report as the PNV model, for the case wherein an external alcohol accelerator is added. In detail, since the BCRM does not include the effect of external alcohol catalysts, its model includes five reactions, i.e., R1 and R4-7. Since the PT model includes the effect of an epoxy-amine complex, when applied and compared to BCRM's work, it has three more reactions, i.e., reactions forming the epoxy-amine complex (R2) and those of this complex with amines (R8 and R9). When applied for PNV which contains the effect of an external alcohol catalyst, the PT model includes all 11 reactions, adding reactions R3, R10 and R11. The kinetic parameters for PT's model of the BCRM and PNV experimental systems are

summarized in Table 6.1. The three bold parameters for each experimental system are adjusted to reproduce experimental observations, and other parameters are shifted accordingly by using quantum chemistry results.

6.3.1   Validation of the PT kinetic model

with the uncatalyzed system

The epoxy monomer and monoamine used in BCRM model are diglycidyl ether of bisphenol A (DGEBA) and p-toluidine with a stoichiometric ratio r (Figure 6.3). It is assumed that the initial hydroxyl chain/epoxy ratio for the kinetic simulation is 0.015 as used previously in BCRM and PNV models when fitting to experimental data. The BCRM's

Table 6.1. Calculated kinetic rate parameters for PT reaction model. (QC is noted for quantum calculation values).

| Reaction No	Rate constants	ln (A)	E_a (kJ/mol)			r^2
			QC	BCRM	PNV	
1	$k_{1E\text{-}OH}$	20.38	4.34	4.34	4.34	0.99
1	$k_{-1E\text{-}OH}$	29.50	24.81	**32.81**	**32.81**	1.00
2	$k_{1E\text{-}A}$	21.42	4.53	4.53	4.53	0.99
2	$k_{-1E\text{-}A}$	29.35	13.75	**15.20**	**15.20**	1.00
3	$k_{1E\text{-}OHc}$	20.38	------	------	4.34	0.99
3	$k_{-1E\text{-}OHc}$	29.50	------	------	**22.81**	1.00
4	k_1	18.59	131.69	97.99	94.49	1.00
5	k_2	18.16	129.64	95.94	92.44	1.00
6	$k'_{E\text{-}OH}$	15.00	88.97	**55.27**	**51.77**	1.00
7	$k''_{E\text{-}OH}$	14.11	88.22	54.52	51.02	1.00
8	$k'_{E\text{-}A}$	14.93	95.60	61.90	58.40	1.00
9	$k''_{E\text{-}A}$	14.32	95.01	61.31	57.81	1.00
10	$k'_{E\text{-}OHc}$	15.00	------	------	**41.77**	1.00
11	$k''_{E\text{-}OHc}$	14.11	------	------	41.02	1.00

Diglycidyl ether of bisphenol A

p-Toluidine
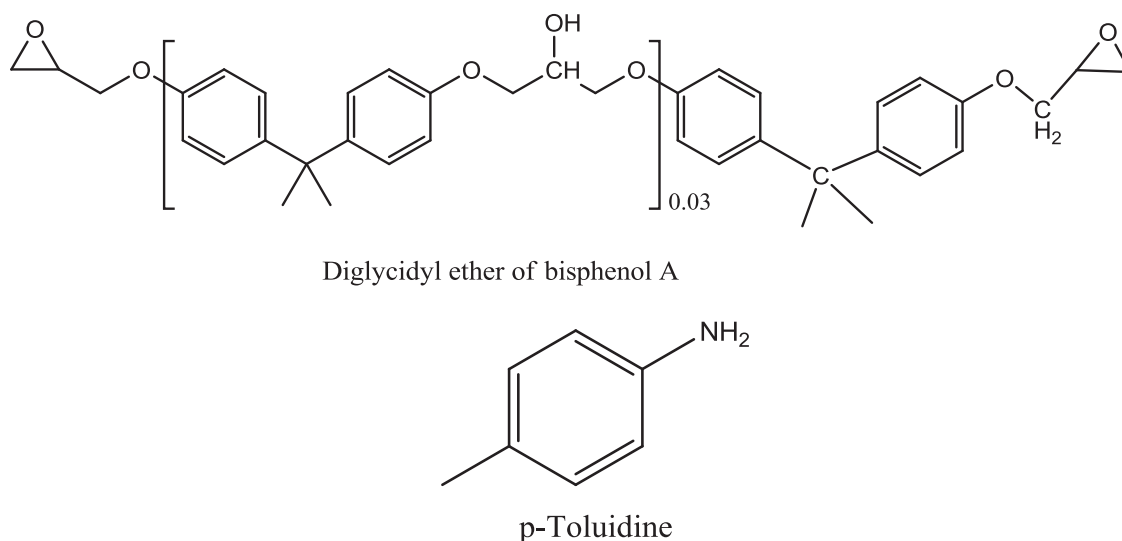
Figure 6.3. Epoxy and amine structures in BCRM.

reaction conditions and rate parameters are summarized in Table 6.2 and Table 6.3. Since the

BCRM kinetic model does not include the self-promoted reaction pathway, it is interesting to

gauge the relative importance of this pathway and to validate the PT model by calculating

the isothermal conversion and dynamic conversions at BCRM's reaction conditions but with

different rate parameters and kinetic models. In particular, for Figures 6.4-6.7, the BCRM

model denotes the use of the BCRM kinetic model with its original parameters, which

include five reactions, R1 and R4 – R7. The BPT model uses the BCRM kinetic model with

PT's parameters and the PT model uses the PT kinetic model with its own parameters. The

PT model applied for the BCRM paper does not include the effect of an alcohol catalyst,

which means excluding reactions R3, R10 and R11.

Comparing Figures 6.4a to 6.4c, the PT and BPT data show better agreement with

experimental observations than the BCRM data. This indicates that the PT model is more

complete. The relative importance of the self-promoted pathway can be seen by the

Table 6.2: BCRM's reaction conditions

Ratio (eq/eq)	Initial concentrations									Temp. (°C)	Heating rate (°C/min)
	Experimental data					Kinetic model					
	(eq/l)		(mol/l)			(mol/l)					
E/N-H	[E]	[N-H]	[E]	[A₁]	[OH]	[E]	[A₁]	[OH]		(°C)	(°C/min)
1	5.01	5.01	2.505	2.505	0.075	5.01	2.505	0.075		80 - 110	10
0.75	4.62	6.16	2.310	3.080	0.069	4.62	3.080	0.069			
0.5	3.99	7.98	1.995	3.990	0.060	3.99	3.990	0.060			

Table 6.3: BCRM's rate parameters

Ratio	A	Equilibrium reaction		Non-catalytic reaction		Catalytic reaction	
		k_{1EOH}	k_{-1EOH}	k_1	k_2	k'_{EOH}	k''_{EOH}
1	(L/eq min)	9.61 E+06	2.37 E+07	4.27 E+05	4.27E+05	2.33 E+04	2.33E +04
	(L/mol min)	**9.61 E+06**	**2.37 E+07**	**2.135 E+05**	**4.27E+05**	**1.165 E+04**	**2.33E +04**
0.75	(L/eq min)	1.42 E+07	1.63 E+07	4.44 E+05	4.44 E+05	1.83 E+04	1.83 E+04
	(L/mol min)	**1.42 E+07**	**1.63 E+07**	**2.22 E+05**	**4.44 E+05**	**0.915 E+04**	**1.83 E+04**
0.5	(L/eq min)	2.01 E+07	6.75 E+06	9.75 E+05	9.75 E+05	1.52 E+04	1.52E +04
	(L/mol min)	**2.01 E+07**	**6.75 E+06**	**4.875 E+05**	**9.75 E+05**	**0.76 E+04**	**1.52E +04**
E_a	(kJ/mol)	**58.2**	**77.9**	**64.9**	**64.9**	**41.4**	**41.4**
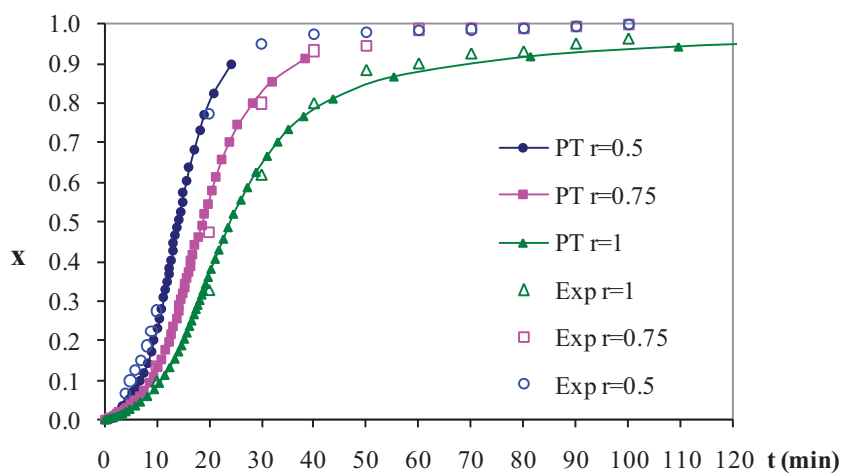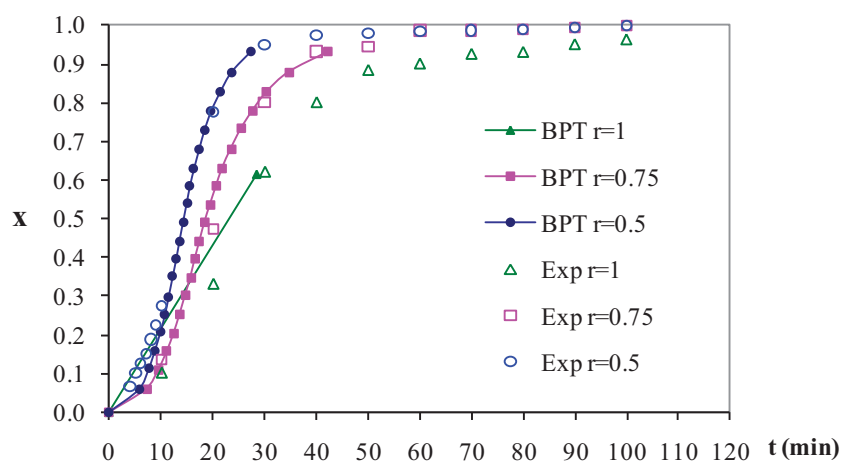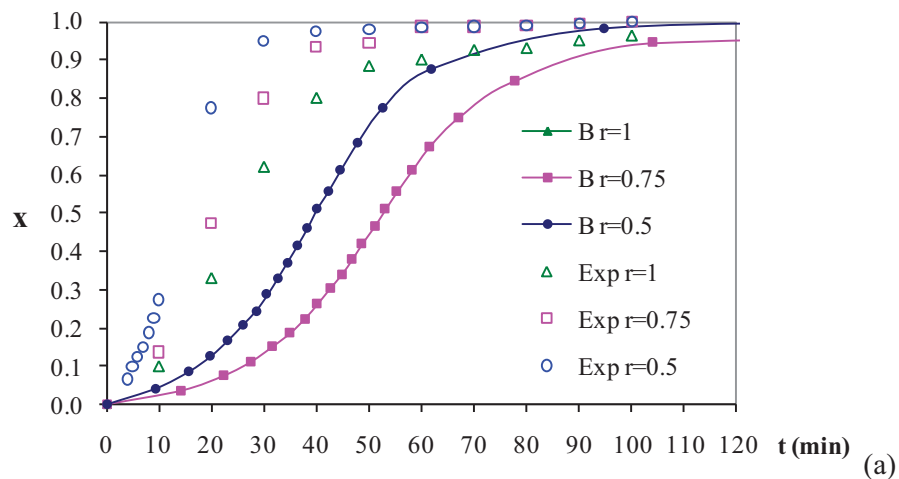
Figure 6.4. Predicted isothermal conversion versus time profiles at 110°C for different epoxy/amine ratios: r = 1, r = 0. 75 and r =0.5 (excess amine) compared again experimental data.[15] The lines represent calculated data from a) BCRM model, b) BPT model and c) PT model.

Figure 6.5. Isothermal conversion versus time profiles for epoxy/amine stoichiometric ratio (r = 1) at different temperatures. The lines represent the calculated data from a) BCRM model, b) BPT model and c) PT model.

Figure 6.6. Isothermal conversion versus time profiles for epoxy/amine stoichiometric ratio (r = 0.75) at different temperatures. The lines represent the calculated data from a) BCRM model, b) BPT model and c) PT model.
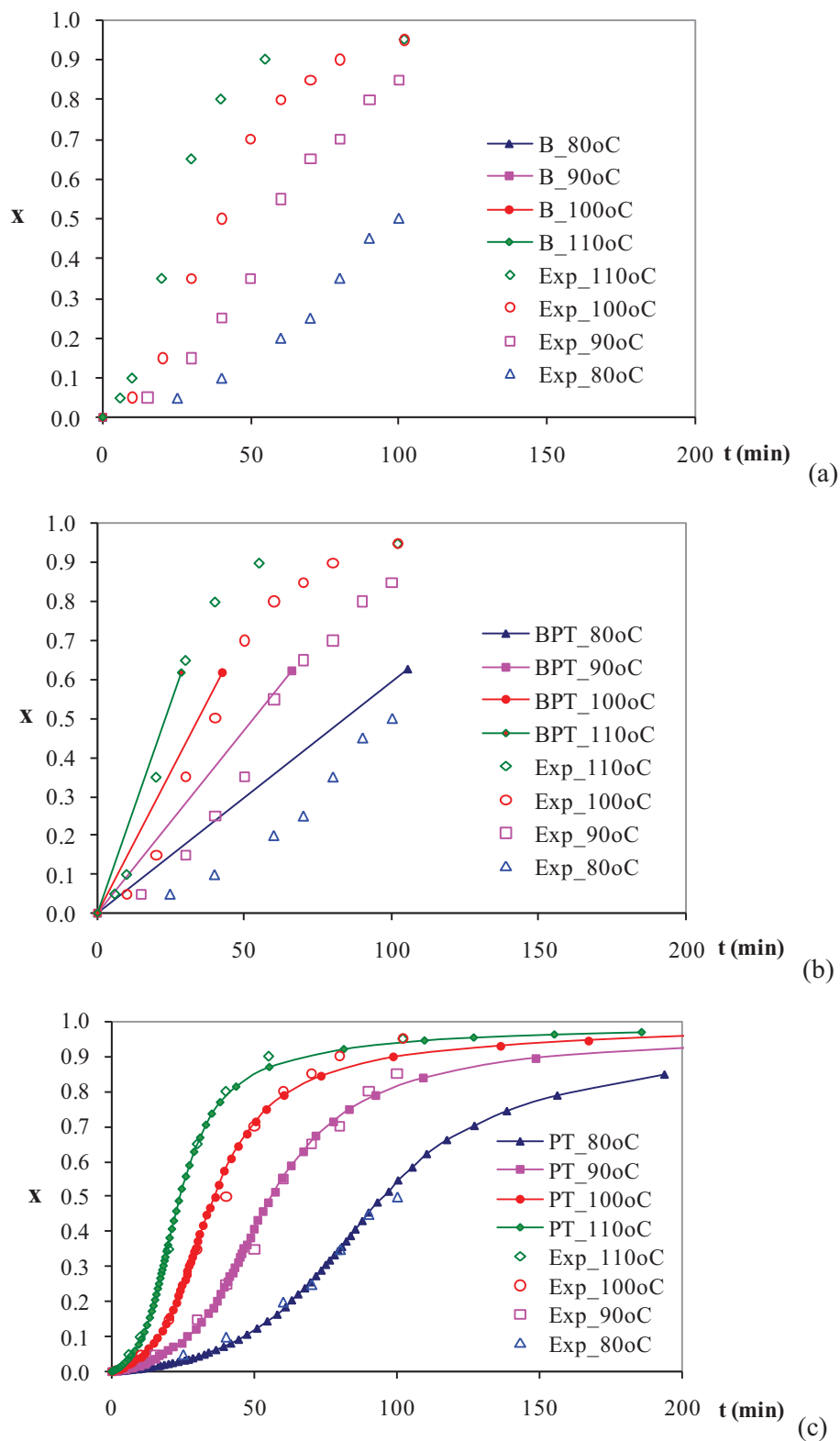
Figure 6.7. Isothermal conversion versus time profiles for epoxy/amine stoichiometric ratio (r = 0.5) at different temperatures The lines represent the calculated data from a) BCRM model, b) BPT model and c) PT model.
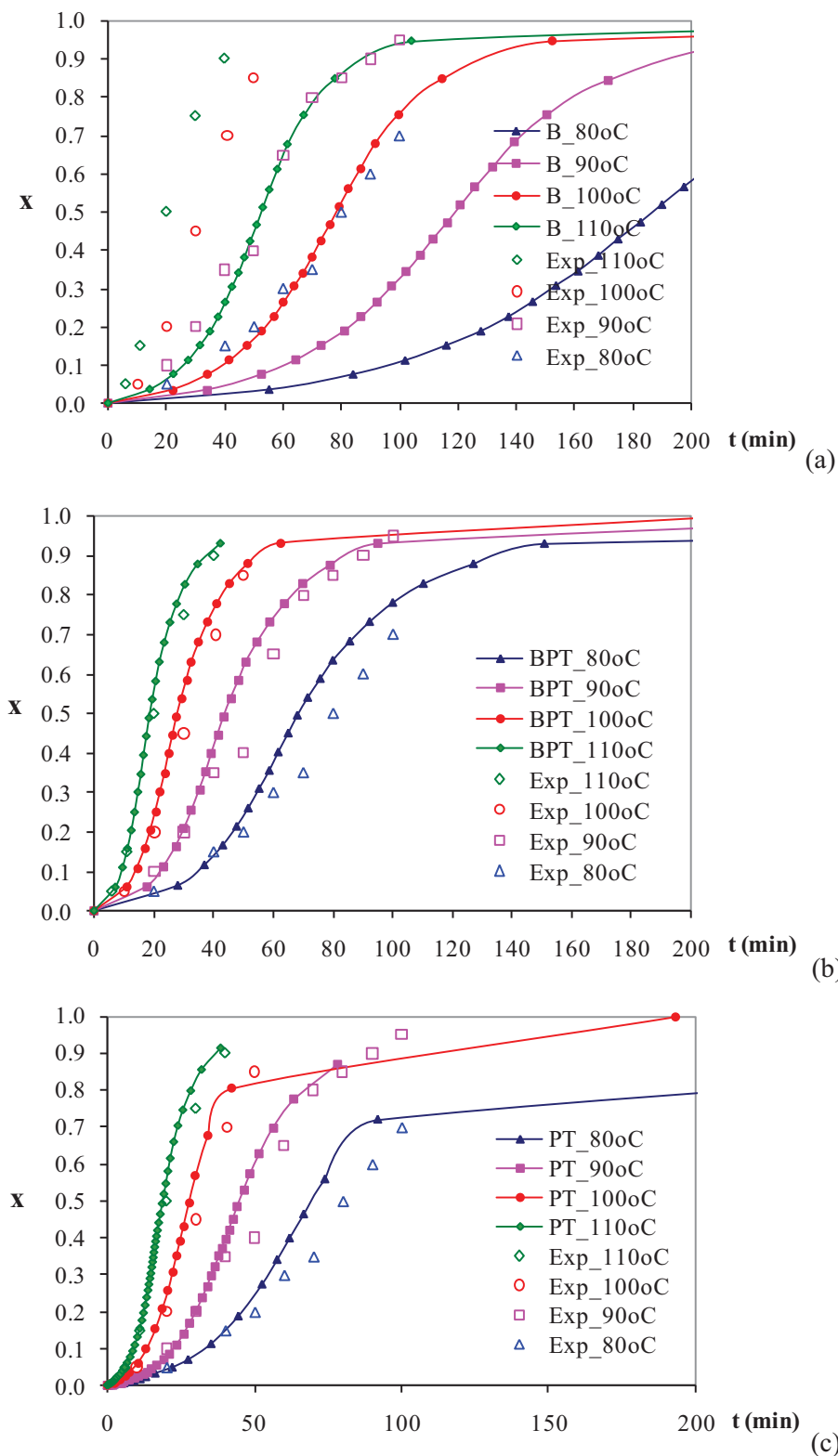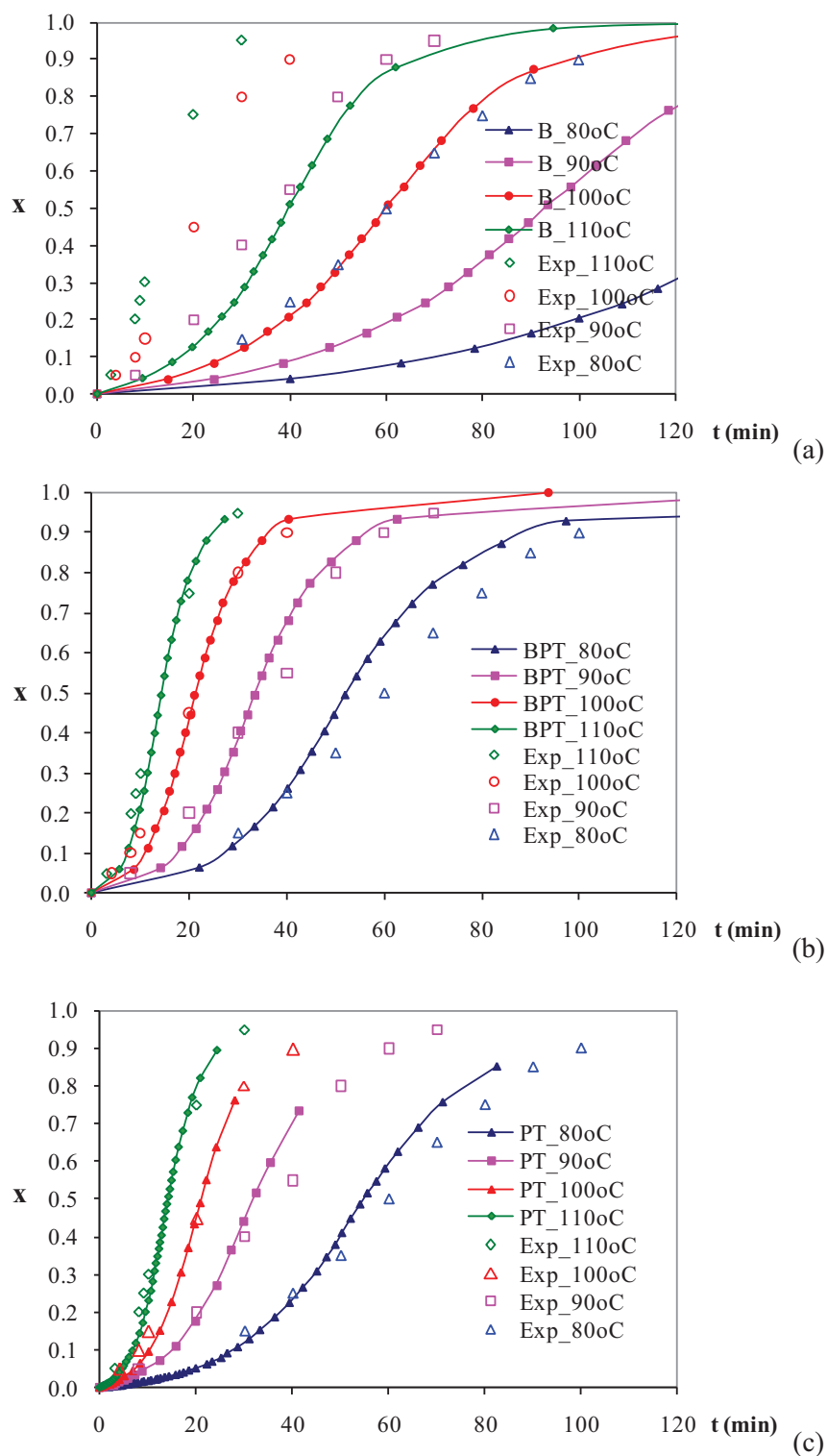
differences between Figures. 6.4b and 6.4c. For larger epoxy/amine ratios, the BPT data, which do not include the contribution from the self-promoted pathway, noticeably underestimate the conversion profile. When such a pathway is included in the PT model, better agreement with experimental observations is achieved. Figures 6.5-6.7 show the calculated isothermal conversion profiles at different temperatures and epoxy/amine ratios. It is noted that in Figure 6.5a, there is no line for the BCRM model. This is because in this period of time, no reaction happens in the simulation or it takes too long to react when the ratio of epoxy/amine is equal to 1.

Figures 6.4-6.7 further support the conclusion made earlier regarding the performance of the PT model and the roles of the self-promoted pathway particularly in the excess amine condition. Figure 6.8 shows the dynamic conversion profiles at the heating rate of 10^0C/min. The conversion increases with the decrease of epoxy/amine ratios.

Both calculated isothermal and dynamic conversion profiles show that the PT model can reproduce the experimental DSC results better than the BCRM or BPT models. In addition, better agreement with experimental observation is obtained for dynamic conversion profiles than for isothermal ones. It is recognized that dynamical conversion profiles are reliable since it is easier to control heating rate than to maintain the system's temperature.

Table 6.4 and Figure 6.9 show the results of varying the predicted concentration of species against reaction time at 110^0C when the epoxy/amine ratio is 1, using the PT model. Over all reactions, we can see that the epoxy group [E] is consumed faster than the concentration of primary amine [A_1]. The formation of epoxy-hydroxyl complex is more significant compared to the formation of epoxy-amine and affects the formation of the products.
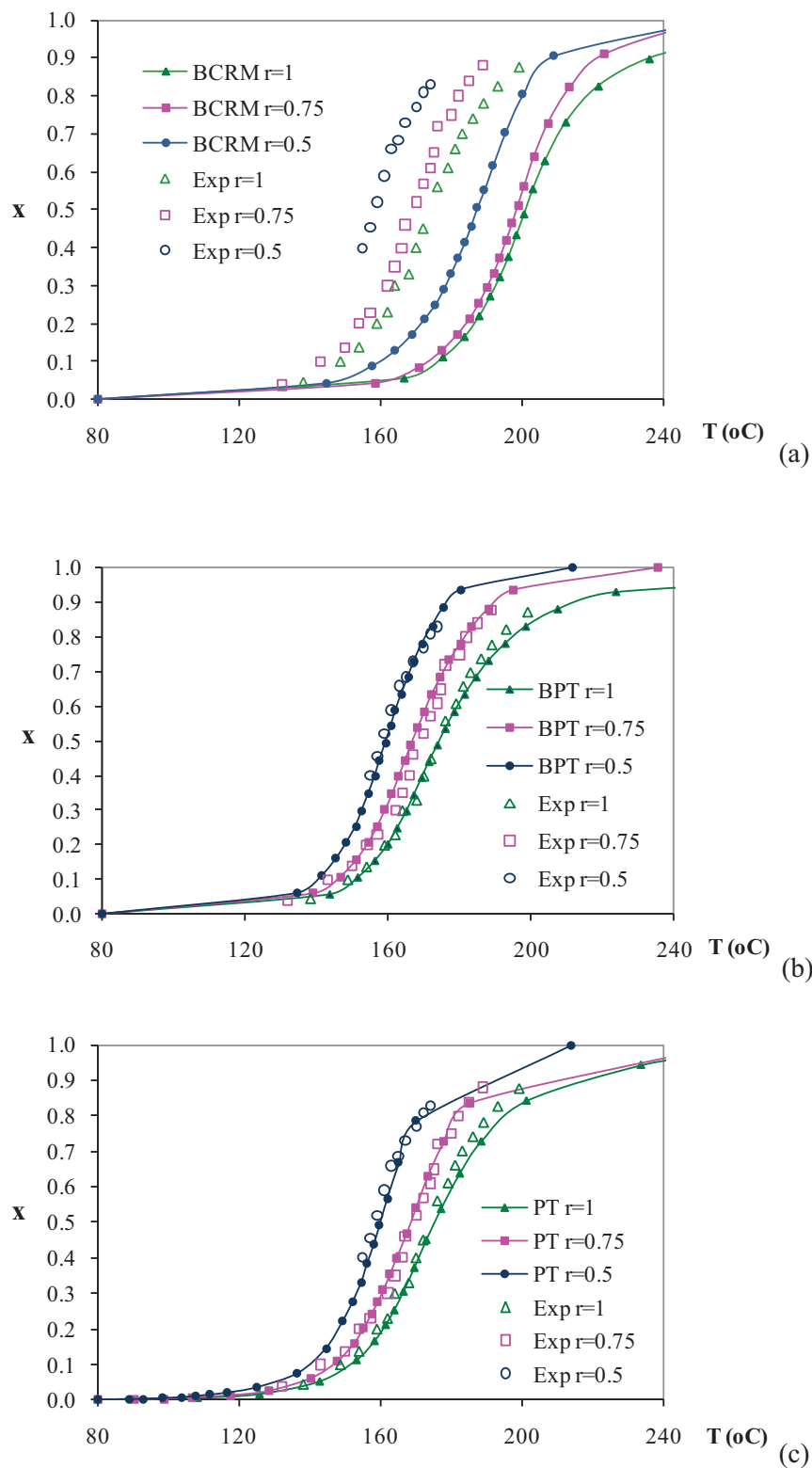
Figure 6.8. Dynamic conversion versus temperature profile compared again experimental data in BCRM study.[15] The lines represent calculated data from: a) BCRM model, b) BPT model and c) PT model.

Table 6.4. Concentration profiles (mol/L) as functions of the reaction time (min) at 110°C and r = 1.

| Time	A1	A2	A3	E	E-A1	E-OH	OH
min	mol/l	mol/l	mol/l	mol/l	mol/l	mol/l	mol/l
0	2.505	0.000	0.000	5.010	0.000	0.000	0.075
2	2.327	0.046	0.000	4.736	0.132	0.096	0.024
4	2.285	0.101	0.001	4.651	0.118	0.139	0.039
6	2.223	0.170	0.003	4.544	0.109	0.182	0.069
8	2.134	0.278	0.009	4.360	0.083	0.271	0.100
10	2.000	0.409	0.027	4.089	0.068	0.389	0.150
15	1.613	0.739	0.101	3.292	0.052	0.726	0.290
20	1.020	1.135	0.337	2.024	0.013	1.164	0.720
25	0.578	1.224	0.694	1.084	0.009	1.306	1.380
31	0.281	1.099	1.123	0.577	0.002	1.086	2.335
38	0.134	0.889	1.481	0.295	0.001	0.864	3.062
44	0.092	0.752	1.661	0.229	0.000	0.707	3.441
55	0.046	0.563	1.895	0.154	0.000	0.502	3.926
81	0.020	0.358	2.126	0.087	0.000	0.313	4.373
110	0.006	0.263	2.235	0.050	0.000	0.226	4.583
127	0.005	0.225	2.276	0.048	0.000	0.187	4.664
155	0.004	0.182	2.319	0.031	0.000	0.159	4.736
186	0.003	0.151	2.351	0.035	0.000	0.123	4.805
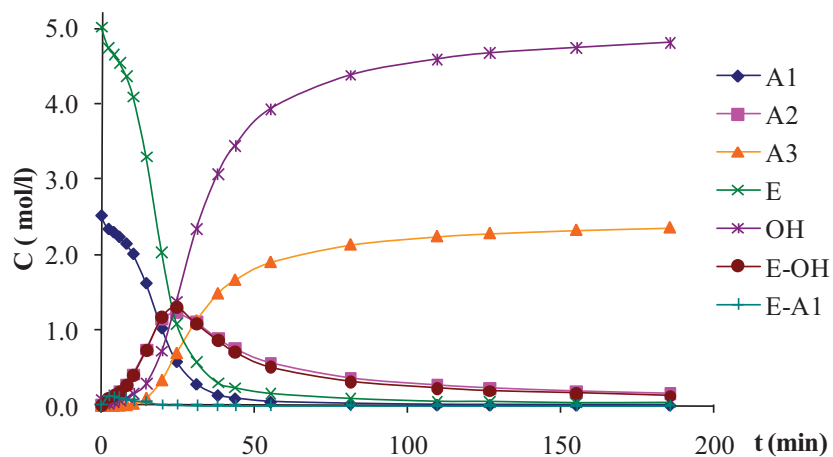
Figure 6.9. Calculated concentration profiles for different species versus time at 110°C and r =1.

In the first 20 min., $[A_2]$ is excessive compared to $[A_3]$ and their ratio is over 10. At 25 min., [E-OH] and $[A_2]$ reach their maximum values. From this point, the ratio of $[A_2]$ and $[A_3]$ also changes inversely, decreasing from about 2 to less than 0.1. This confirms the effect of R5, R7 and R9 wherein not only the epoxy but also the E-OH and E-A_1 complexes react with A_2 to form A_3 and the hydroxyl product in the PT model. [E-A_1] seems too small in the whole process. However, its approximate equilibrium with [E-OH] at the initial time (first 6 min.) confirms its presence in the curing process, especially when $[A_1]$ is too large compared to a small amount of formed [OH]. The longer initial time is obtained to maintain this equilibrium at lower reaction temperatures. The [E-OH] will control the process when [OH] is sufficient to form this complex. It confirms our hypothesis that the uncatalyzed and the self-promoted pathway may be competing in the absence of any epoxy-hydroxyl complex.

6.3.2 Validation of the PT kinetic model for systems

with adding alcohol accelerator

The reactants used in the PNV experimental studies[17, 18, 95] consist of a mixture of diglycidyl ether of bisphenol A and F (DGEBA/DGEBF), aliphatic amine and bisphenol A as an external accelerator (Figuge 6.10). The reaction conditions of this system are summarized in Table 6.5 and Table 6.6. Here we also assume the initial hydroxyl chain/epoxy ratio for the kinetic simulation is 0.015.

To model this system, the parameters for the PT kinetic model must be modified for the following reasons: 1) this epoxy-amine curing system uses an aliphatic amine while the previous case used an aromatic amine; 2) this system has two different types of OH

oxypropylene diamine

diethylenetriamine

bisphenol A
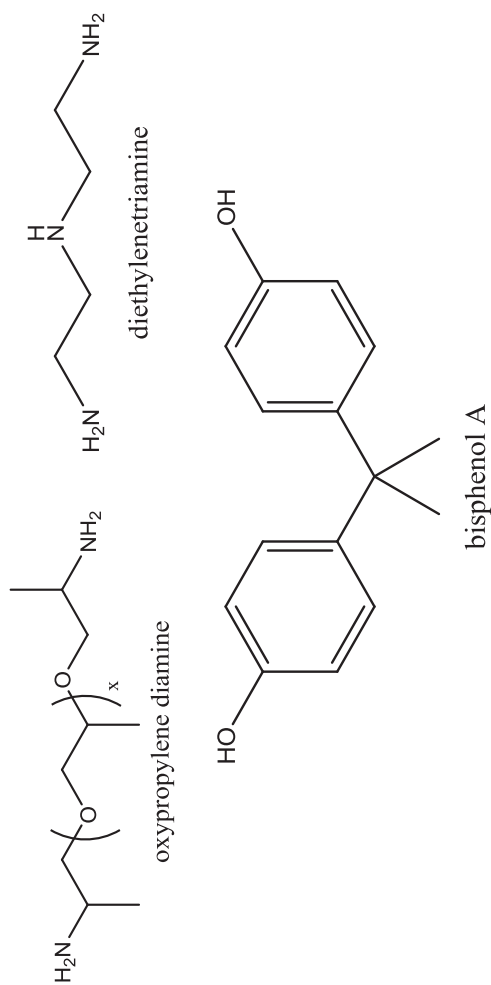
Figure 6.10. Amine structures in PNV (left to right: JEFF, DETA and BPA)

Table 6.5 Intial concentrations of PNV reaction conditions.

Ratio	Experimental data				Kinetic model				Temp	Heating rate
(wt/wt)	(eq/l)				(mol/l)				(°C)	(°C/min)
$[OH]_c/[N-H]$	[E]	[N-H]	[OH]	$[OH]_c$	[E]	$[A_1]$	[OH]	$[OH]_c$		
3%	5.019	5.02	0.075	0.08	5.019	2.51	0.075	0.08	40 - 80	5, 10, 15, 20, 25
7%	5.019	5.02	0.075	0.187	5.019	2.51	0.075	0.187		

Table 6.6. Initial values of amines, [N-H] and $[OH]_c$ of PNV reaction conditions.

$[OH]_c/[N-H] = 3\%$	n (mol)	M (g/mol)	% (wt)
JEFF	1.175	234 ± 3	93.4
DETA	0.1	103	3.5
BPA	0.04	228	3.1
$[OH]_c$	0.08		
[N-H]	5.20		

species, one from the epoxy and the other from the added alcohol. First, it is known from quantum chemistry calculations that the activation energy for the alcohol-catalyzed step is lower by 16-20 kJ/mol for the aliphatic amines as compared to those of aromatic amines. Hence, we assign the activation energy for the external alcohol catalyzed step of R10 to be 41.77 kJ/mol, 13.5 kJ/mol lower than that of the previous case (R6, 55.27 kJ/mol). Second, we treat the interactions between OH from epoxy and OH from external alcohol with epoxy differently by allowing the activation energies for the dissociation of the hydrogen bond complexes to be different by 10 kJ/mol. Thus, if the activation energy for the reverse reaction of R3 is adjusted to 22.81 kJ/mol and that of R6 is adjusted to 51.77 kJ/mol, excellent agreement with experimental observations is obtained. The values of ln(A) for R3, R10 and R11 are gotten from those of the similar reactions, R1, R6 and R7. Namely, it is necessary to have the quantum calculated values for eight reactions, R1-2 and R4-9.

Overall for the whole PT kinetic model, we have four adjustable parameters while all others are shifted accordingly using results from quantum chemistry calculations. In detail, 41.77 kJ/mol is the energy barrier for R10, 32.81 kJ/mol for the reverse reaction of R1, 15.2 kJ/mol for that of R2 and 22.81 kJ/mol for R3 (Table 6.7).

Table 6.7. Modified rate parameters for the added alcohol accelerator case. The bold parameter is a corrected value.

Reaction No	Rate constants	ln(A)	E_a (kJ/mol)			r^2
			QC	BCRM	PNV	
1	$k_{-1E\text{-}OH}$	29.50	24.81	32.81	32.81	1.00
2	$k_{-1E\text{-}A}$	29.35	13.75	15.20	15.20	1.00
3	$k_{-1E\text{-}OHc}$	29.50	------	------	22.81	1.00
6	$k^{'}_{E\text{-}OH}$	15.00	88.97	55.27	51.77	1.00
7	$k^{''}_{E\text{-}OH}$	14.11	88.22	54.52	51.02	1.00
10	$k^{'}_{E\text{-}OHc}$	15.00	------	------	**41.77**	1.00
11	$k^{''}_{E\text{-}OHc}$	14.11	------	------	41.02	1.00

Table 6.8 and Figure 6.11 show the calculated concentration profiles of species at 80 ^{0}C and 3% BPA. The epoxy group [E] is consumed faster than the primary amine [A_1] due to the hydrogen bond complex formation between the epoxy and alcohol OH groups. As expected, the OH_c group from external alcohol plays the role of an accelerator or catalyst, thus the concentrations of [E-OH_c] and [OH_c] reach steady state.

The calculated isothermal conversion time profiles at different temperatures using the

Table 6.8. Conversion (x) and isothermal concentration profiles (mol/l) at 80 ^{0}C and 3% BPA.

| Time	A1	E	E-A1	E-OH	E-OH$_c$	OH	OH$_c$	x
min	mol/l	mol/l	mol/l	mol/l	mol/l	mol/l	mol/l	mol/l
0	2.510	5.019	0.000	0.000	0.000	0.075	0.080	0.000
1	2.303	4.676	0.151	0.119	0.017	0.013	0.063	0.011
2	2.191	4.415	0.106	0.263	0.016	0.032	0.064	0.044
6	1.657	3.277	0.065	0.793	0.016	0.150	0.064	0.173
8	1.435	2.780	0.061	1.020	0.012	0.201	0.068	0.228
9	1.225	2.294	0.050	1.216	0.008	0.310	0.072	0.289
11	1.053	1.845	0.027	1.391	0.005	0.436	0.075	0.349
12	0.887	1.434	0.018	1.525	0.005	0.586	0.075	0.406
15	0.642	0.876	0.011	1.608	0.008	0.984	0.072	0.501
22	0.290	0.364	0.001	1.328	0.001	2.073	0.079	0.663
59	0.035	0.065	0.000	0.499	0.000	4.032	0.080	0.888
265	0.001	0.015	0.000	0.087	0.001	4.906	0.079	0.980
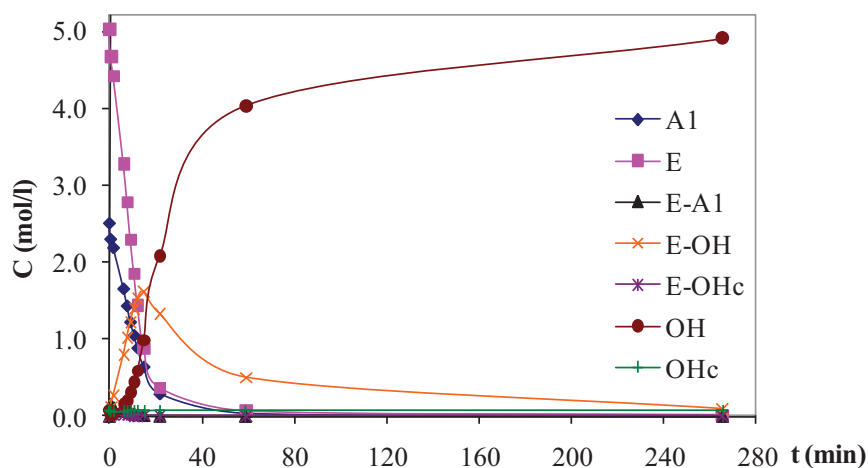
Figure 6.11. Predicted concentration profiles versus time at 80°C and 3% BPA using PT model.

PT model are shown in Figure 6.12. The calculation reproduces the experimental temperature dependent behaviors much better at high temperatures, but poorly at lower temperatures (40-60 ^{0}C). Since the reactions of the epoxy complexes with amines (R6-R11) might dominate the curing process, the concentration of epoxy complexes should be considered. The concentration profiles at low temperatures (40-60 ^{0}C compared again 70-80 ^{0}C) show that the concentration of epoxy complexes increases slowly, resulting in slow reactions of the epoxy complexes with amines.

Figure 6.13 shows the dynamic conversion profiles as functions of the heating rates. The agreement with experimental data is better than those of isothermal conversion profiles.

The dynamic conversion profiles as a function of temperature for different external alcohol content shown in Figure 6.14 are in excellent agreement with the observed data. The
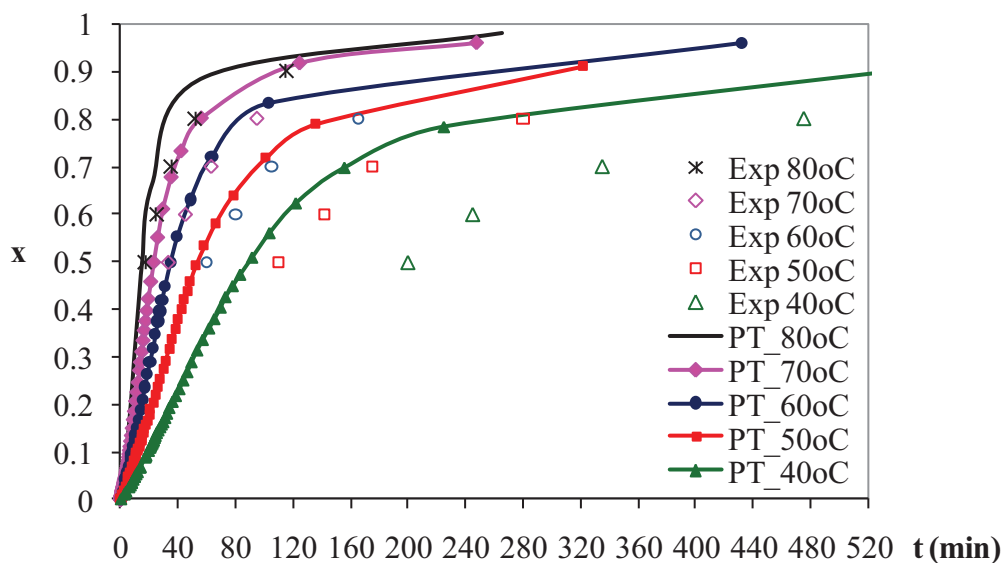

Figure 6.12. Calculated isothermal conversion time profiles at various temperatures as compared to PNV experimental data.[18] The solid lines represent the calculated data using the PT model
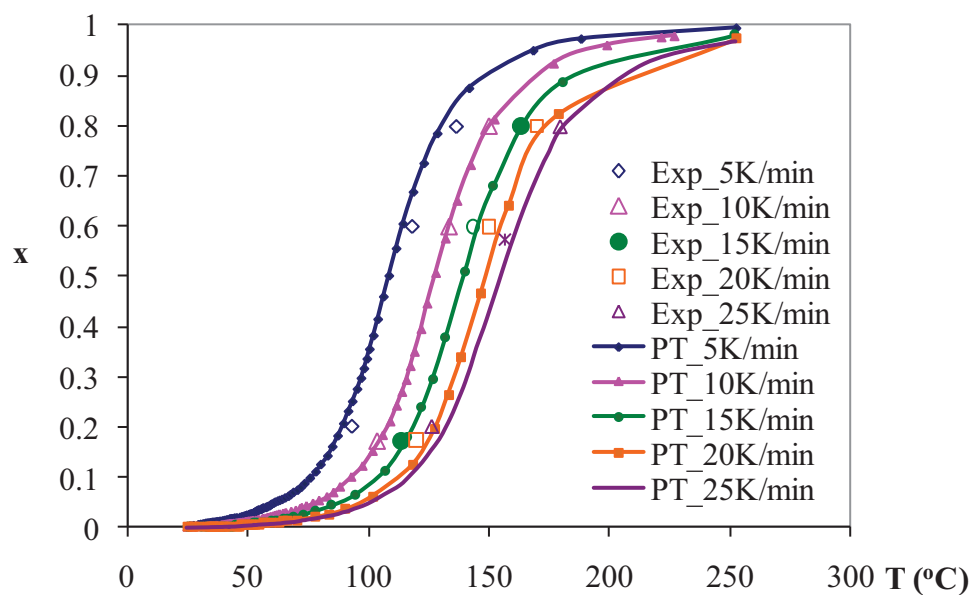
Figure 6.13. Calculated DSC conversion profiles at different heating rates as compared to PNV experimental data [17] The solid lines represent the calculated data using the PT model
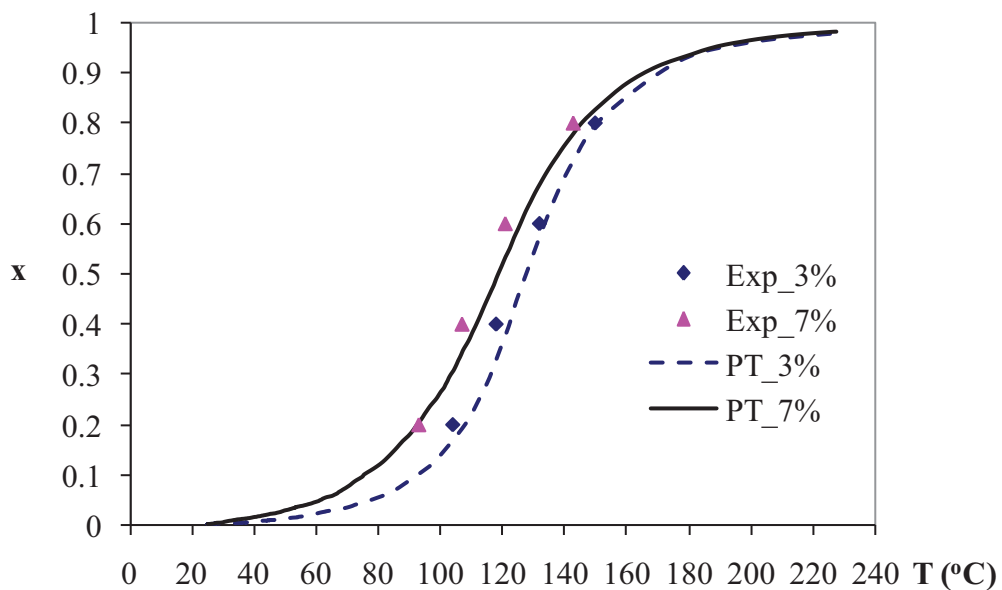

Figure 6.14. Calculated dynamic conversion versus temperature profile with different alcohol content (wt. -% relative to amine hardener) using PT model compared with experimental values.[17]

calculated concentration profiles of the hydrogen bond complex between the epoxy and the OH from the epoxy chain as a function of the conversion at different temperatures shown in Figure 6.15 also agree well with experimental observations. The orange line in Figure 6.15 represents the correlation of the [E-OH] (column 5 – Table 6.8) and the conversion (x) (column 9 – Table 6.8) at 80 ^{0}C. These results validate treating the interactions of different OH species in the system differently.

Finally, the calculated equilibrium constants of the E-OH hydrogen bond complex formation with OH from the epoxy chain as a function of temperature are shown in Figure 6.16. These results are calculated from the isothermal conversion profiles (80, 90, 100 and 110 ^{0}C and r=1) of the PT model with the BCRM reaction condition. Since the reaction system and conditions used here are the same as that of Flammersheim's[94] experimental work, a comparison can be made. Our calculated value for K varies from 1.7 to 0.8 as the temperature increases from 80 to 110 ^{0}C for the aromatic amine curing system. This can
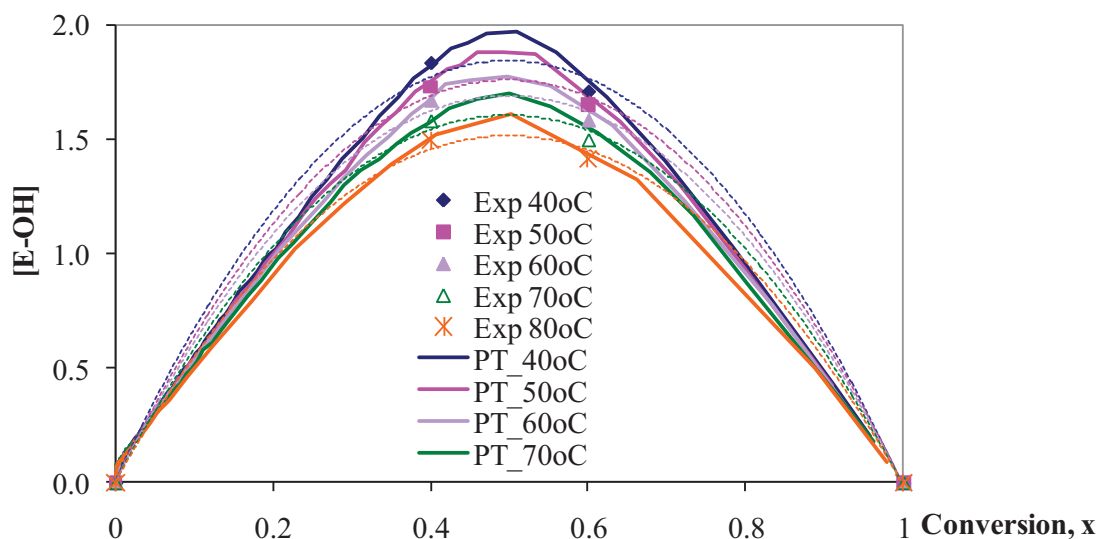

Figure 6.15. Solid lines represent the calculated concentrations of the epoxy-hydroxyl complexes (OH from epoxy chain) as functions of conversion at different temperature using PT model. Symbols and dotted lines represent experimental data.[17]
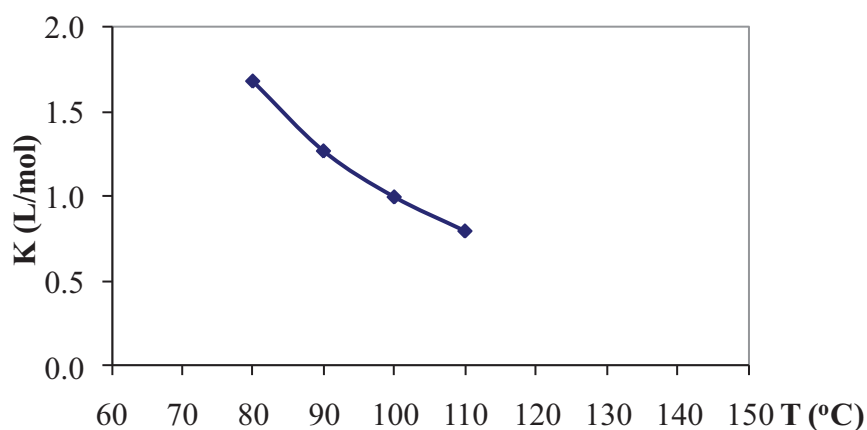
Figure 6.16. Equilibrium constant for the formation of the E-OH complex (OH from epoxy chain), K (L/mol), as a function of temperature.

compared with the averaged K of 0.7 L/mol in the 70-150 ^{0}C range for the DGEBA/aniline system.[94] It confirms the reliability of the PT model as well as the importance of the E-OH hydrogen bonded complex formed from the epoxy chain.

6.3.3 The poor fitting of isothermal conversion profiles

The poor fitting of isothermal conversion in Figure 6.12 at low temperatures and the improved fitting for the correlation of epoxy-hydroxyl complex concentration with conversion in Figure 6.15 might support the proposal that the experimental data generate a contradiction. The following calculated results nicely confirm this hypothesis.

As mentioned above, the PT model reproduced imperfectly the isothermal conversions at low temperatures. It agrees well with experimental values if its reaction rate is slower. The reversible formation of the epoxy-hydroxyl complex plays an important role in the reactions' shift. The easier the reverse is, the slower the conversion is. Table 6.9 shows four tests of different values compared with the original PT model's parameters, especially the activation energies of reversible reactions. Figures 6.17 and 6.18 reproduce

Table 6.9. Activation energies of PT model at different tests.

E_a	PT	Test 1	Test 2	Test 3	Test 4
1	4.34	4.34	4.34	4.34	4.34
1'	32.81	30.81	28.81	29.81	28.81
2	4.53	4.53	4.53	4.53	4.53
2'	15.20	13.75	13.75	15.20	15.20
3	4.34	4.34	4.34	4.34	4.34
3'	22.81	20.81	18.81	19.81	17.81
4	94.49	94.49	94.49	94.49	94.49
5	92.44	92.44	92.44	92.44	92.44
6	51.77	51.77	51.77	51.77	51.77
7	51.02	51.02	51.02	51.02	51.02
8	58.40	58.40	58.40	58.40	58.40
9	57.81	57.81	57.81	57.81	57.81
10	41.77	41.77	41.77	41.77	40.77
11	41.02	41.02	41.02	41.02	40.02
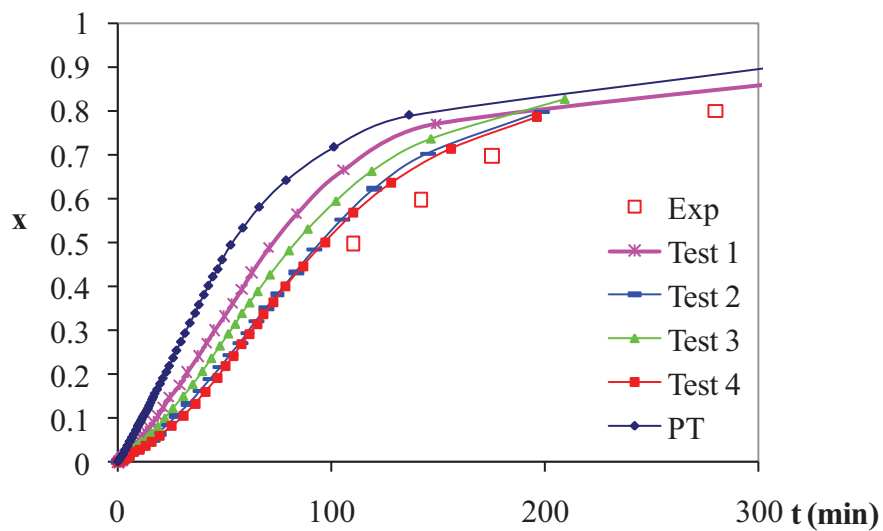
Figure 6.17. Isothermal conversion profiles at 50 ^{0}C and 3% BPA by using different PT model's paramenters.
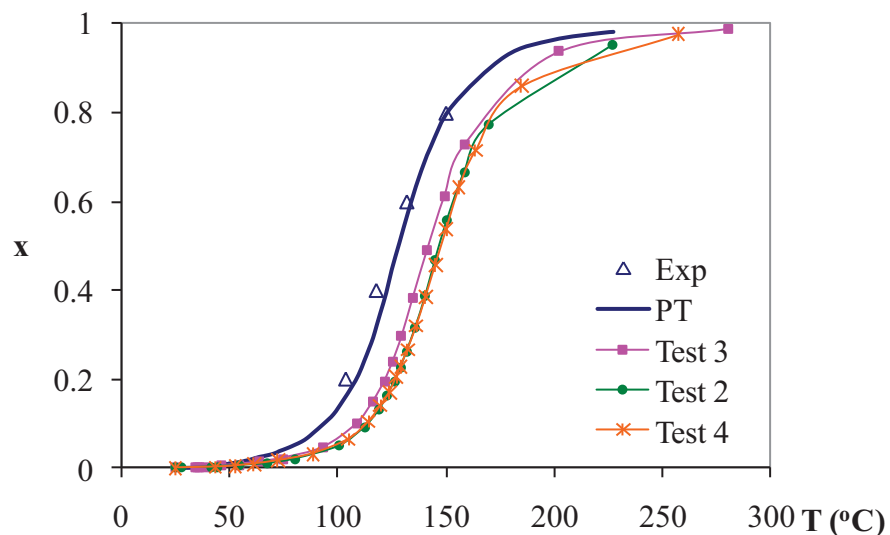
Figure 6.18. Dynamic conversion profiles of 3% BPA by using different PT model's paramenters.

respectively the isothermal and dynamic conversions for four tested parameter models. In Figure 6.17, isothermal conversion at 50 ^{0}C is chosen to provide the validation. Both conversions shift consistently forward lower rates from Test 1 to Test 4. Although this shift in isothermal conversion gradually agrees well to experiments, the shift in dynamic conversion disagrees. It is not possible to find a better PT model's parameters than the original.

In addition, the contradiction of experimental data is confirmed in Figures 6.19, 6.20 and 6.21. Among four testing sets, Test 4 shows the best experimental agreement for isothermal conversion at 50 ^{0}C. Thus, it is chosen to reproduce the isothermal conversion profiles at different temperatures, 40-80 ^{0}C, as shown in Figure 6.19. There are two reasons to propose that the correlation of epoxy-hydroxyl complex concentration with the conversion might be reproduced perfectly by Test 4's parameters, shown in Figure 6.20. First, Figure 6.19 shows better experimental agreement than Figure 6.12. Second, both Figures 6.12 and 6.15 are from the same isothermal conversion profiles and Figure 6.15 agrees well with experimental data. Similarly, Figures 6.19 and 6.21 are from the same isothermal
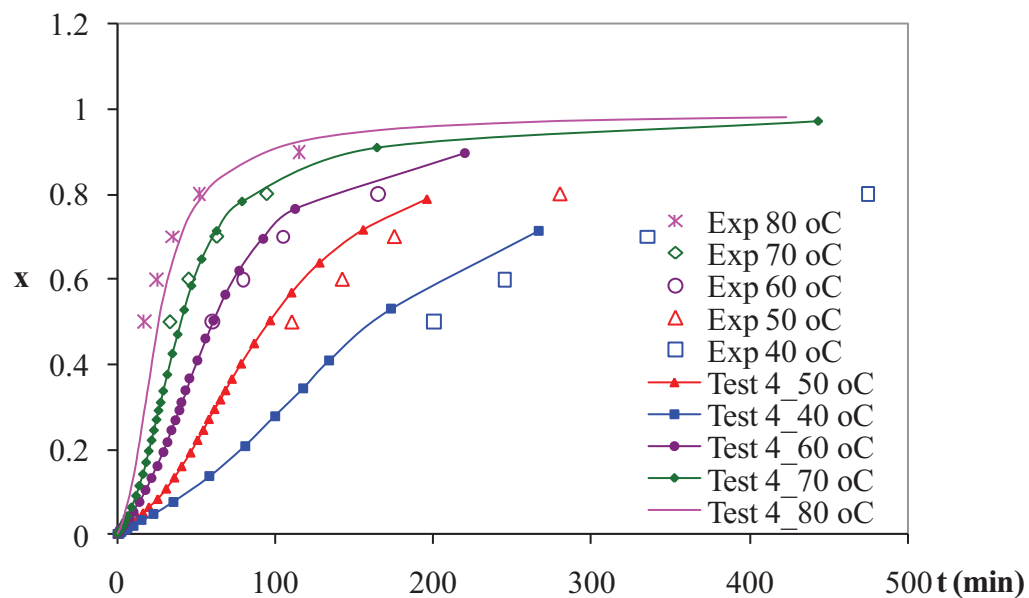
Figure 6.19. Isothermic conversion profiles of different temperatures at Test 4's paramenters compared with experimental data.[18]
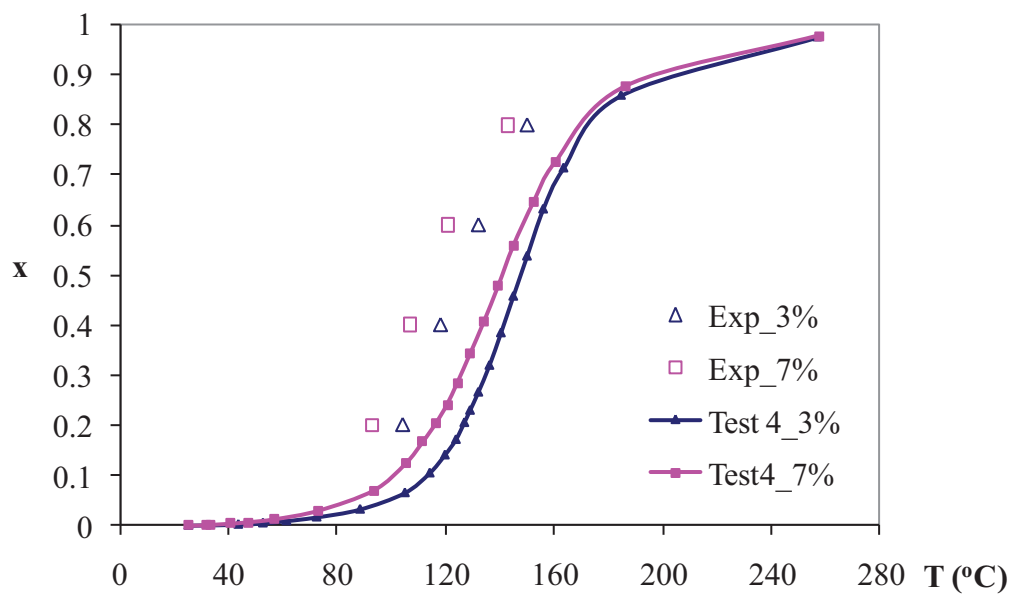

Figure 6.20. Calculated dynamic conversion versus temperature profile with different alcohol content (wt. -% relative to amine hardener) at Test 4's paramenters compared again the experimental data.[17]
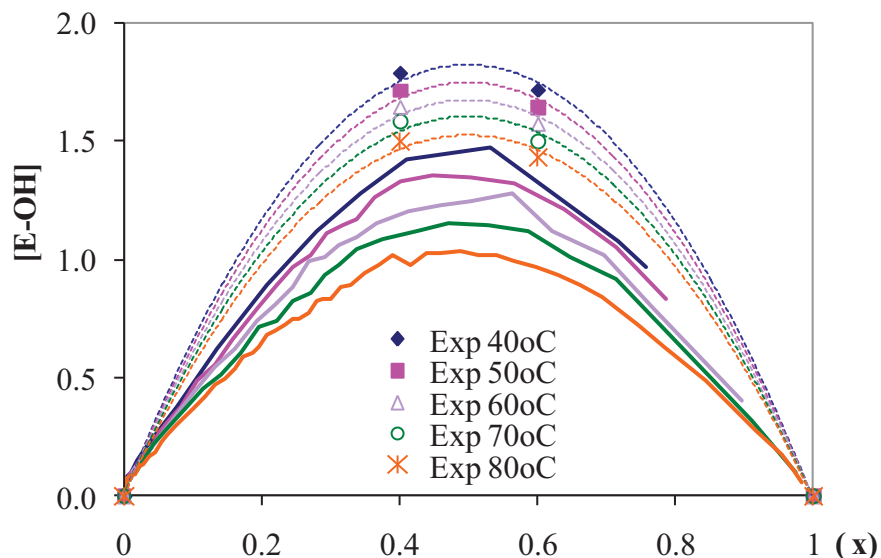
Figure 6.21. Solid lines represent the calculated concentrations of the epoxy-hydroxyl complexes (OH from epoxy chain) as functions of conversion at different temperature. Symbols and dotted lines represent experimental data taken from reference 17. PT model's parameters are in Test 4 column of Table 6.8.

conversion. However, it is too abnormal to get the poor reproduction of experimental correlations of [E-OH] concentrations and conversions at different temperatures. Moreover, the dynamic conversions of Test 4's parameters are a bad reproduction as shown in Figure 6.20. Meanwhile, except for the poor fitting of isothermal conversion at low temperatures in Figure 6.12, the original PT model reproduces well the dynamic conversion at both different alcohol catalyst percentages (Figure 6.14) and different heating rates (Figure 6.13). It also repeats well the functions of [E-OH] concentrations and conversions (Figure 6.15). Nevertheless, the separate publication of experiments in Figure 6.12 in reference 18 and the others in Figure 6.13, 6.14 and 6.15 in reference 17 are a curiosity. Such things make the PT model believable though it cannot reproduce well the isothermal conversions at low temperatures for PNV's experiments.

6.4   Conclusion

We have developed a new kinetic model for the epoxy-amine curing system guided by quantum chemistry calculations. This allows the use of only three adjustable rate parameters to compensate for the uncertainties in the calculations and limitations of the chemical models in representing the real systems. Excellent agreement in all measurable properties from different experiments for two different curing systems validates the completeness of the kinetic model and its accuracy. This kinetic model can be extended to other systems by adjusting the differences in the activation energies for the rate limiting step of the most favorable pathway, i.e., the alcohol catalyzed pathway for different amines and epoxies. Such differences can be derived from linear energy relationships that we propose to develop as the next step.

REFERENCES

1.   May, C. A., *Epoxy Resins: Chemistry and Technology*. 2 ed.; M. Dekker, New York, USA: 1988.

2.   Harper, C. A., *Handbook of Plastics, Elastomers and Composites*. 2 ed.; McGraw-Hill, New York, USA: 1992.

3.   Ellis, B., *Chemistry and Technology of Epoxy Resins*. Blackie Academic & Professional, London, England: 1993.

4.   Park, S. J.; Seo, M. K.; Lee, J. R.; Lee, D. R. *J. Korean Fiber Soc.* **1999,** 36, (10), 715-724.

5.   Han, S.; Yoon, H. G.; Suh, K. S.; Kim, W. G.; Moon, T. J. *Journal of Polymer Science,* **1999,** 37, (6), 713-720.

6.   Manzione, L. T., *Plastic Packaging of Microelectronic Devices; Van Nostrand Reinhold*. First Edition ed.; New York, 1990.

7.   Pham, H. Q.; Marks, M. J., Epoxy Resins. In *Ulmann's Encyclopedia of Industrial Chemistry*, WILEY-VCH Verlag GmbH & Co. KGaA: Weinheim, 2006.

8.   Ehlers, J.-E.; Rondan, N. G.; Huynh, L. K.; Pham, H.; Marks, M.; Truong, T. N. *Macromolecules* **2007,** 40, (12), 4370-4377.

9.   Horie, K.; Hiura, H.; Sawada, M.; Mita, I.; Kambe, H. *Journal of Polymer Science,* **1970,** 8, (6), 1357-72.

10.   Shechter, L.; Wynstra, J.; Kurkjy, R. P. *Journal of Industrial and Engineering Chemistry* **1956,** 48, 94-7.

11.   Shechter, L.; Wynstra, J.; Kurkjy, R. P. *Journal of Industrial and Engineering Chemistry* **1956,** 48, (1), 94-97.

12.   Smith, I. T. *Polymer* **1961,** 2, 95-108.

13.   Mijovic, J.; Fishbain, A.; Wijaya, J. *Macromolecules* **1992,** 25, (2), 979-85.

14.   Riccardi, C. C.; Fraga, F.; Dupuy, J.; Williams, R. J. J. *Journal of Applied Polymer Science* **2001,** 82, (9), 2319-2325.

15.   Blanco, M. C., M. Angeles; Riccardi, Carmen C.; Mondragon, Inaki *Polymer* **2005,** 46, (19), 7989-8000.

16.   Mounif, E.; V., B.; Tcharkhtchi, A. *Journal of Applied Polymer Science* **2008,** 108, (5), 2908-2916.

17.   François-Xavier Perrin, T. M. H. N., Jean-Louis Vernet,. *Macromolecular Chemistry and Physics* **2007,** 208, (1), 55-67.

18.   François-Xavier Perrin, T. M. H. N., Jean-Louis Vernet,. *Macromolecular Chemistry and Physics* **2007,** 208, (7), 718-729.

19.   Zvetkov, V. L. *Macromolecular Chemistry and Physics* **2002,** 203, (3), 467-476.

20.   Paz-Abuin, S.; Pellin, M. P.; Paz-Pazos, M. *Polymer* **1997,** 38, (15), 3795-3804.

21.   Rozenberg, B. A. *Springer-Verlag, Epoxy Resins and Composites. II.* **1986**, 113-165.

22.   Noyori, R.; Hashiguchi, S. *Accounts of Chemical Research* **1997,** 30, (2), 97-102.

23.   Meerwein, H.; Schmidt, R. *Ann.* **1925,** 444, 221-38.

24.   Ponndorf, W. *Angewandte Chemie* **1926,** 39, 138-43.

25.   Steinmann, B. *Polymer Bulletin* **1989,** 22, (5-6), 637-44.

26.   Fischer, R. F. *Journal of Polymer Science* **1960,** 44, 155-72.

27.   Okaya, T.; Tanaka, T.; Yuki, K. *Journal of Applied Polymer Science* **1993,** 50, (5), 745-751.

28.   Shechter, L.; Wynstra, J. *Journal of Industrial and Engineering Chemistry* **1956,** 48, 86-93.

29.   Sorokin, M. F.; Shode, L. G. *Zhurnal Organicheskoi Khimii* **1966,** 2, (8), 1463-8.

30.   Benioff, M. R. L., E.D.; Bajcsy, R.; Hannigan, W. J.;Jr., J.C.B.;Javitt, J.C.;Celis, P.; Klavans, J.L.; Evans, P.T.; Leighton, F.T.; Fernandez, M.A.;Fiallo, L.E.; Mortazavian, H.; Griffiths, J.-M.; Mott, R.D.; Neupert, P.M.; Noam, E.M.; Patterson, D.A.; Quintanilla, A.G.; Reed, D.A.; Spafford, E.H.; Staelin; D.H.; Tippett, P.S.; Yang, G.; Reed, D.A.; Bajcsy, R.; Fernandez, M.A.; Griffiths, J.-M.; Mott, R.D.; Dongarra, J.; Johnson, C.R. *Report to the President: Computational Science:*
Ensuring America's Competitiveness; June 2005.

31.   Liu, H. U., Alfred; Varley, Russell J.; Bannister, Michael K. *Journal of Polymer Science, Part A: Polymer Chemistry* **2004,** 42, (13), 3143-3156.

32.   Charlesworth, J. *Journal of Polymer Science,* **1980,** 18, (2), 621-8.

33.   Girard-Reydet, E.; Riccardi, C. C.; Sautereau, H.; Pascault, J. P. *Macromolecules* **1995,** 28, (23), 7599-7607.

34.   K. Duscaronek, M. B., S. Luňák,. *Journal of Polymer Science,* **1977,** 15, (10), 2393-2400.

35.   Mijovic, J.; Wijaya, J. *Macromolecules* **1994,** 27, (26), 7589-7600.

36.   Zhang, Y.; Vyazovkin, S. *The Journal of Physical Chemistry B* **2007,** 111, (25), 7098-7104.

37.   Pham, M.-P., In pKb = 3.36 for methylamine, pKb = 3.27 for of dimethylamine, pKb = 3.3 for cyclohecxylamine, pKb = 3.1 for cyclohecxylmethylamine, pKb = 9.4 for aniline, pKb = 9.16 for methylaniline.

38.   Sung, C. S. P.; Pyun, E.; Sun, H. L. *Macromolecules* **1986,** 19, (12), 2922-2932.

39.   Xiaorong Wang, J. K. G. *Journal of Applied Polymer Science* **1991,** 43, (12), 2267-2277.

40.   Min, B.-G.; Stachurski, Z. H.; Hodgkin, J. H. *Polymer* **1993,** 34, (21), 4488-4495.

41.   Burton, B. L. http://www.pcimag.com.

42.   Frisch, M. J.; Trucks, G. W.; Schlegel, H. B.; Scuseria, G. E.; Robb, M. A. C., J. R.; Montgomery, J. A., Jr.; Vreven T.; Kudin K .N.; Burant J. C.; Millam J. M.; Iyengar S. S.; Tomasi J.; Barone V.; Mennucci B.; Cossi M.; Scalmani G.; Rega N.; Petersson G.A.; Nakatsuji,H.; Hada M.; Ehara M.; Toyota, K.; Fukuda R.; Hasegawa, J.; Ishida, M.; Nakajima, T.; Honda, Y.; Kitao, O.; Nakai, H.; Klene, M.; Li X.; Knox, J. E.; Hratchian, H.P.; Cross, J.B.; Adamo, C.; Jaramillo, J.; Gomperts, R.; Stratmann, R.E.; Yazyev, O.; Austin, A.J.; Cammi, R.; Pomelli, C.; Ochterski, J.W.; Ayala, P.Y.; Morokuma, K.; Voth, G. A.; Salvador, P.; Dannenberg, J. J.; Zakrzewski, V. G.; Dapprich, S.; Daniels, A. D.; Strain, M. C.; Farkas, O.; Malick, D. K.; Rabuck, A. D.; Raghavachari, K.; Foresman, J. B.; Ortiz, J. V.; Cui, Q.; Baboul, A. G.; Clifford, S.; Cioslowski, J.; Stefanov, B. B.; Liu, G.; Liashenko, A.; Piskorz, P.; Komaromi, I.; Martin, R. L.; Fox, D. J.; Keith, T.; Al-Laham, M. A.; Peng, C. Y.; Nanayakkara, A.; Challacombe, M.; Gill, P. M. W.; Johnson, B.; Chen, W.; Wong, M. W.; Gonzalez, C.; Pople, J. A. *Gaussian 03, revision A.1*, Gaussian, Inc.: Pittsburgh, PA 2003.

43.   Becke, A. D. *J. Chem. Phys.* **1993,** 98, (7), 5648-52.

44.   Gonzalez, C.; Schlegel, H. B. *J. Chem. Phys.* **1989,** 90, (4), 2154-61.

45.   Gonzalez, C.; Schlegel, H. B. *J. Phys. Chem.* **1990,** 94, (14), 5523-7.

46.   Tomasi, J.; Persico, M. *Chemical Reviews* **1994,** 94, (7), 2027-94.

47.   Kamon, T.; Saito, K. *Kobunshi Ronbunshu* **1984,** 41, (5), 293-9.

48.   Johncock, P.; Porecha, L.; Tudgey, G. F. *Journal of Polymer Science:* **1985,** 23, (2), 291-301.

49.   Park, S.-J.; Seo, M.-K.; Lee, J.-R. *J. Polym. Sci., Part A: Polym. Chem.* **2000,** 38, (16), 2945-2956.

50.   Gagnebien, D.; Madec, P. J.; Maréchal, E. *European polymer Journal* **1985,** 21, (3), 289-299.

51.   Banthia, A. K.; McGrath, J. E. *Polym. Prepr., Am. Chem. Soc., Div. Polym. Chem.* **1979,** 20, (2), 629-33.

52.   Yoshizumi, A.; Hanyu, K.; Iketani, H.; Kihara, N. Epoxy resin compositions with phenolic and polycarbonate hardeners for sealing semiconductor devices. 88-12127301292025, 19880518., 1989.

53.   Bidulescu, G. D.; Popa, I. Environment friendly process for preparing a thermosetting epoxy resin varnish for producing heat-resistant, electric-insulating materials. 2005-200500772122149, 20050912., 2009.

54.   Naito, T.; Ando, M.; Asano, Y.; Kato, T.; Hayashida, N.; Tsujimura, T. Prepreg sheets for repair or/and reinforcement of concrete structures and method of using them. 94-26771008128209, 19941031., 1996.

55.   Nishida, S.; Yonetani, M. Epoxy acrylate fixing agent compositions for fixing anchor bolts in concrete or rocks. 97-16791911001664, 19970611., 1999.

56.   Sorokin, M. F.; Shode, L. G.; Gershanova, E. L.; Lipkina, S. I. *Lakokras. Mater. Ikh Primen.* **1967**, (6), 4-7.

57.   Tanaka, G.; Suzuki, H. Epoxy resin molding material for sealing semiconductors. 76-4879052132100, 19760428., 1977.

58.   Tanaka, G.; Suzuki, H. Carboxy-containing tertiary amines for use as hardening catalysts for thermosetting resins. 76-4136452125109, 19760414., 1977.

59.   Han, S.; Kim, W. G.; Yoon, H. G.; Moon, T. J. *Bull. Korean Chem. Soc.* **1997,** 18, (11), 1199-1203.

60.   Hale, A.; Macosko, C. W.; Bair, H. E. *J. Appl. Polym. Sci.* **1989,** 38, (7), 1253-69.

61.   Chen, Y.-C.; Chiu, W.-Y.; Lin, K.-F. *J. Polym. Sci., Part A: Polym. Chem.* **1999,** 37, (16), 3233-3242.

62.   Tomasi, J.; Mennucci, B.; Cammi, R. *Chem. Rev.* **2005,** 105, 2999-3093.

63.   Barone, V.; Cossi, M.; Tomasi, J. *J. Comput. Chem.* **1998,** 19, (4), 404-417.

64.   Mineva, T.; Russo, N.; Sicilia, E. *J. Comput. Chem.* **1998,** 19, (3), 290-299.

65.   Batog, A. E.; Pet'ko, I. P.; Penczek, P. *Advantages in Polymer Science* **1999,** 144, 49-113.

66.   Madec, P. J.; Marechal, E. *Adv. Polym. Sci.* **1985,** 71, (Anal./React./Morphol.), 153-228.

67.   Lebedev, N. N.; Gus'kov, K. A. *Kinet. Katal.* **1964,** 5, (3), 446-53.

68.   Sorokin, M. F.; Gershanova, E. L. *Kinet. Katal.* **1967,** 8, (3), 512-19.

69.   Rokaszewski, E. *Pol. J. Chem.* **1978,** 52, (7-8), 1487-94.

70.   Sorokin, M. F.; Shode, L. G.; Gershanova, E. L. *Chemicky Prumysl* **1967,** 17, (11), 590-4.

71.   Klebanov, M. S.; Kir'yazev, F. Y.; Chervinskii, A. Y.; Shologon, I. M. *Zh. Org. Khim.* **1984,** 20, (11), 2407-11.

72.   Alvey, F. B. *J. Appl. Polym. Sci.* **1969,** 13, (7), 1473-86.

73.   Dobinson, B.; Green, G. E. Bonding surfaces together using adhesive compositions. 73-32277303227, 19730514., 1974.

74.   Sorokin, M. F.; Shode, L. G.; Veslov, V. V.; Petrova, L. P. *Catalysis of the reaction of phenyl glycidyl ether with acetic acid and benzoic acids by aromatic tertiary amines*; Mosk. Khim.-Tekhnol. Inst., Moscow, USSR.: 1975; p 18 pp.

75.   Sorokin, M. F.; Shode, L. G.; Veslov, V. V.; Nogteva, S. I. *Catalytic activity of aliphatic amines in the reaction of phenyl glycidyl ether with acetic and benzoic acids*; Mosk. Khim.-Tekhnol. Inst., Moscow, USSR.: 1975; p 7 pp.

76.   Uejima, A. *Nippon Kagaku Kaishi* **1981**, (6), 974-9.

77.   Frisch, M. J.; Trucks, G. W.; Schlegel, H. B.; Scuseria, G. E. R., M. A.; Cheeseman, J. R.; Scalmani, G.; Barone, V.; Mennucci, B.; Petersson, G. A.; Nakatsuji, H.; Caricato, M.; Li, X.; Hratchian, H. P.; Izmaylov, A. F.; Bloino, J.; Zheng, G.; Sonnenberg, J. L.; Hada, M.; Ehara, M.; Toyota, K.; Fukuda, R.; Hasegawa, J.; Ishida, M.; Nakajima, T.; Honda, Y.;

Kitao, O.; Nakai, H.; Vreven, T.; Montgomery, Jr., J. A.; Peralta, J. E.; Ogliaro, F.; Bearpark, M.; Heyd, J. J.; Brothers, E.; Kudin, K. N.; Staroverov, V. N.; Kobayashi, R.; Normand, J.; Raghavachari, K.; Rendell, A.; Burant, J. C.; Iyengar, S. S.; Tomasi, J.; Cossi, M.; Rega, N.; Millam, N. J.; Klene, M.; Knox, J. E.; Cross, J. B.; Bakken, V.; Adamo, C.; Jaramillo, J.; Gomperts, R.; Stratmann, R. E.; Yazyev, O.; Austin, A. J.; Cammi, R.; Pomelli, C.; Ochterski, J. W.; Martin, R. L.; Morokuma, K.; Zakrzewski, V. G.; Voth, G. A.; Salvador, P.; Dannenberg, J. J.; Dapprich, S.; Daniels, A. D.; Farkas, Ö.; Foresman, J. B.; Ortiz, J. V.; Cioslowski, J.; Fox, D. J. *Gaussian 09*, Revision A.02; Gaussian, Inc.: Wallingford CT, 2009.

78.   Kakiuchi, H.; Tanaka, Y. *Kobunshi Kagaku* **1963,** 20, 619.

79.   Shvets, V. F.; Lebedev, N. N.; Tyukova, O. A. *Zh. Org. Khim.* **1971,** 7, 1851.

80.   Rafizadeh, M.; Ghasemi, H.; Haddadi-Asl, V. *Chinese Journal of Polymer Science* **2006,** 24, (6), 599-608.

81.   Antoon, M. K.; Koenig, J. L. *Journal of Polymer Science: Polymer Chemistry Edition* **1981,** 19, (2), 549-570.

82.   Fisch, W.; Hofmann, W.; Koskikallio, J. *J. Appl. Chem.* **1956,** 6, 429-41.

83.   O'Neill, L. A.; Cole, C. P. *J. Appl. Chem.* **1956,** 6, 356-64.

84.   Park, W. H.; Lee, J. K. *Journal of Applied Polymer Science* **1998,** 67, (6), 1101-1108.

85.   Pielichowski, K.; Czub, P.; Pielichowski, J. *Polymer* **2000,** 41, (12), 4381-4388.

86.   Peyser, P.; Bascom, W. D. *Journal of Applied Polymer Science* **1977,** 21, (9), 2359-2373.

87.   Tanaka, Y.; Kakiuchi, H. *J. Appl. Polym. Sci.* **1963,** 7, 1063-81.

88.   Tanaka, Y.; Kakiuchi, H. *J. Polym. Sci., Part A: Gen. Pap.* **1964,** 2, (8), 3405-30.

89.   Ma, Z.; Gao, J. *J. Phys. Chem. B* **2006,** 110, (25), 12380-12383.

90.   Sun, G.; Sun, H.; Liu, Y.; Zhao, B.; Zhu, N.; Hu, K. *Polymer* **2007,** 48, (1), 330-337.

91.   Khanna, U.; Chanda, M. *Journal of Applied Polymer Science* **1993,** 50, (9), 1635-44.

92.   Harper, C. A.; Editor, *Handbook of Plastics, Elastomers, and Composites, 2nd Edition*. 1992; p Unpaged.

93.   May, C. A., *Epoxy Resins Chemistry and Technology*. 2nd ed.; Marcel Dekker, New York: 1988.

94.   Flammersheim, H. J. *Thermochimica Acta* **1997,** 296, (1-2), 155-159.

95.   François-Xavier Perrin, T. M. H. N., Jean-Louis Vernet. *European polymer Journal* **2007,** 43, 5107.

96.   Chapman, N. B.; Isaacs, N. S.; Parker, R. E. *Journal of the Chemical Society* **1959**, 1925-34.

97.   Cole, K. C. *Macromolecules* **1991,** 24, (11), 3093-7.

98.   Vinnik, R. M.; Roznyatovsky, V. A. *Journal of Thermal Analysis and Calorimetry* **2003,** 73, (3), 807.817.

99.   Truong, T. N.; Nayak, M.; Huynh, H. H.; Cook, T.; Mahajan, P.; Tran, L. T.; Bharath, J.; Jain, S.; Pham, H. B.; Boonyasiriwat, C.; Nguyen, N.; Andersen, E.; Kim, Y.; Choe, S.; Choi, J.; Cheatham, T. E., III; Facelli, J. C. *Journal of Chemical Information and Modeling* **2006,** 46, (3), 971-984.

100.   Chian, W.; Timm, D. C. *Macromolecules* **2004,** 37, (21), 8098-8109.